



HAL
open science

Inflation in string cosmology

Emeline Cluzel

► **To cite this version:**

Emeline Cluzel. Inflation in string cosmology. High Energy Physics - Theory [hep-th]. Ecole Polytechnique X, 2011. English. NNT: . pastel-00653149

HAL Id: pastel-00653149

<https://pastel.hal.science/pastel-00653149>

Submitted on 18 Dec 2011

HAL is a multi-disciplinary open access archive for the deposit and dissemination of scientific research documents, whether they are published or not. The documents may come from teaching and research institutions in France or abroad, or from public or private research centers.

L'archive ouverte pluridisciplinaire **HAL**, est destinée au dépôt et à la diffusion de documents scientifiques de niveau recherche, publiés ou non, émanant des établissements d'enseignement et de recherche français ou étrangers, des laboratoires publics ou privés.

THÈSE DE DOCTORAT DE L'ÉCOLE POLYTECHNIQUE

Spécialité :



Physique théorique

Présentée par

Emeline CLUZEL



Pour obtenir le grade de Docteur de l'École Polytechnique

Inflation en cosmologie des cordes

Inflation in string cosmology

Soutenue le 22 septembre 2011

devant le jury composé de :

Philippe BRAX	Directeur de thèse
Carsten van de BRUCK	Rapporteur
Martin LEMOINE	Président du jury
Jérôme MARTIN	Co-directeur de thèse
Patrick PETER	Examineur
Danièle STEER	Rapporteur

Résumé

mots-clés : cosmologie (primordiale), inflation, k-inflation, inflation branaire, inflation DBI, fond diffus cosmologique ou CMB, théorie des perturbations, spectre de puissance de la perturbation de courbure, “feature” ou caractéristique, théorie tenseur-scalaire

L’inflation est responsable des fluctuations de densité primordiales qui sont à l’origine de la formation des grandes structures et qui sont reliées aux fluctuations de température du Fond Diffus Cosmologique (CMB en anglais). Dans cette thèse, nous nous intéressons à un modèle particulier d’inflation, de la classe des modèles avec terme cinétique modifié, l’inflation de Dirac-Born-Infeld (DBI) inspirée de la théorie des cordes. Dans ce scénario, l’inflation est générée par le mouvement d’une brane-test et des particules peuvent être créées pendant l’inflation si des branes piégées sont présentes le long de la vallée inflationnaire. On montrera qu’un tel couplage entre l’inflaton et les champs de matière peut conduire à des spécificités du spectre de puissance primordial, similaires à celles obtenues dans des modèles à la Starobinsky où le potentiel présente des discontinuités ou celles obtenues dans des théories scalaire-tenseur où la fonction de couplage inflaton-matière varie brusquement dans le temps. On insistera sur les conséquences observationnelles de telles théories.

Abstract

key-words : (primordial) cosmology, inflation, k-inflation, brane inflation, DBI inflation, Cosmic Microwave Background Radiation or CMB(R), perturbation theory, curvature perturbation power spectrum, feature, scalar-tensor theory

Cosmic inflation is responsible for the primordial density fluctuations which are the seeds of today's large-scale structures and which are observed through the temperature fluctuations of the Cosmic Microwave Background. In this thesis, we explore a particular model of inflation with modified kinetics : Dirac-Born-Infeld (DBI) inflation inspired by string theory. In this scenario, inflation is generated by the motion of a probe brane and particles can be created during inflation when trapped branes are present along the inflationary valley. We will show that such a coupling between the inflaton and matter fields leads to interesting features in the primordial power spectrum, similar to features à la Starobinsky sourced by the potential or scalar-tensor features sourced by a suddenly-varying inflaton-matter coupling function in k-inflation. We will insist on the possible observational consequences of our theories.

Remerciements

Je souhaite tout d'abord remercier ceux qui m'ont aidée à orienter mes études vers la cosmologie : Jérôme Perez, Roland Lehoucq, Rachel-Marie Pradeilles-Duval et Martin Lemoine. Je les remercie pour leur soutien, leurs conseils et leur amitié.

Je remercie mes deux tuteurs Philippe et Jérôme. Je remercie en particulier Philippe pour sa disponibilité, sa pédagogie et pour toutes les discussions que nous avons eues. Je remercie Jérôme pour sa rigueur et son goût pour le fortran 77.

Je remercie les autres membres de mon jury, en particulier les rapporteurs qui ont accepté cette tâche.

Je remercie aussi l'équipe de l'EDX qui rend les démarches administratives rapides et agréables !

J'exprime aussi mon amitié pour les thésards de l'IPhT et en particulier ceux de notre "promo" : Enrico, Francesco, Gaetan, Hélène, Jean-Marie et Sophie. Je remercie tous les participants au pot du jeudi soir au vieux chêne.

Je tiens aussi à dire merci à Jean-Yves et Olivier dans leur rôle de responsable des thésards et au secrétariat pour son aide et son efficacité. Je remercie aussi Henri pour ses bons mots et son amitié.

Je remercie Linda Guevel qui a été une interlocutrice de choix pour mon enseignement de tutorat à l'X.

Je remercie mes parents qui m'ont permis de sauver du temps pour ma thèse lors de ma deuxième année.

Et comme on garde toujours le meilleur pour la fin, je remercie Damien pour son incommensurable patience et pour tout le reste.

Résumé

La cosmologie moderne repose sur le principe cosmologique et la théorie de la relativité d'Einstein. Dans les années 20, Lemaître construit la théorie du “Big Bang” qui décrit l'univers et son évolution. Grâce à de nombreuses observations, nous possédons de précieuses informations sur notre univers. Il est plat (de courbure nulle avec une précision de plus d'un pourcent) et constitué à 70% d'une forme d'énergie dite énergie sombre qui “antigravite” et est responsable de l'accélération récente de l'expansion de l'univers. Dans les équations d'Einstein, qui relient la géométrie de l'univers à son contenu énergétique, elle apparaît sous la forme de la constante cosmologique. L'univers est également constitué de matière, principalement de matière invisible, la matière noire, qui n'interagit que gravitationnellement. Les preuves de l'existence de la matière noire sont solides mais indirectes et aucune particule de matière noire n'a encore été observée.

Le modèle du Big Bang est très satisfaisant car il permet de rendre compte de la plupart des observations. Néanmoins il a quelques limites : le problème de l'horizon, le problème de la platitude (et éventuellement le problème des reliques). Comme le stipule le principe cosmologique, l'univers est très homogène à grande échelle. C'est d'ailleurs ce qu'indiquent toutes les observations. Les galaxies sont réparties de façon homogène à grande échelle (cf. Sloan Digital Sky Survey). L'observation du fond diffus cosmologique, c'est-à-dire du rayonnement de corps noir des photons de la surface de dernière diffusion, nous montre que la température de l'univers est partout la même (2,725 K) à 10^{-5} près. Or il est impossible d'expliquer une telle homogénéité entre des régions causalement déconnectées puisqu'aucun processus de thermalisation n'a pu avoir lieu. C'est ce que l'on appelle le problème de l'horizon. Le problème de la platitude quant à lui souligne l'improbabilité que l'univers soit plat. Cela suppose un ajustement très fin des conditions initiales et cela semble donc marquer un manque de généralité dans la théorie du Big Bang.

Ces problèmes peuvent être résolus grâce au paradigme de l'inflation qui stipule l'existence d'une phase d'expansion accélérée de l'univers qui a eu lieu avant

l'ère dominée par la radiation. Le modèle le plus simple d'inflation, développé dans les années 80, est un modèle où l'univers est dominé par un champ scalaire (l'inflaton ϕ) en roulement lent le long de son potentiel. Ce modèle d'inflation en roulement lent, qui exige que le potentiel de l'inflaton soit très plat, est encore d'actualité puisqu'il satisfait toutes les contraintes observationnelles. Cela dit ce n'est pas un modèle très naturel car il ne donne aucune explication sur l'origine du champ scalaire. De plus, il présente deux problèmes majeurs : un problème de conditions initiales et le problème η . C'est pourquoi de nombreux autres modèles d'inflation ont été développés ces trente dernières années. On peut les classer en différentes catégories selon que ce sont des modèles à petits ou grands champs, à un ou plusieurs champs scalaires, à terme cinétique canonique ou non, etc. Il faut ensuite savoir distinguer ces modèles par leurs prédictions observationnelles. Et l'on peut espérer qu'avec les nouvelles données qui viendront du satellite Planck, il sera possible d'écarter certains modèles.

Non seulement la théorie de l'inflation permet de résoudre les problèmes du Big Bang mais en plus elle permet d'expliquer les légères fluctuations de température mesurées dans le rayonnement fossile du CMB et d'expliquer la formation des grandes structures. Les fluctuations quantiques de l'inflaton ont créé des fluctuations de densité et donc de température à la fin de l'inflation. Par instabilité gravitationnelle, les régions sur-denses se sont effondrées pour finalement donner naissance aux étoiles et galaxies.

L'inflation est sensible à la physique des hautes énergies. Il est donc naturel d'essayer de construire des théories inflationnaires à partir de théories plus fondamentales, par exemple de la théorie des cordes. En théorie des supercordes, il existe souvent des dizaines de moduli et l'on peut très bien imaginer que l'un d'eux est l'inflaton. L'inflaton peut par exemple être le dilaton ou bien un radion c'est-à-dire la distance entre un couple de brane et anti-brane.

Un tel modèle inflationnaire a pour la première fois été suggéré par Dvali et Tye et le célèbre article KKLMNT, du nom de ses auteurs, décrit un processus d'inflation généré par le mouvement relatif d'une brane D3 et d'une anti-brane $\overline{D3}$ à l'intérieur d'une gorge fortement voilée ("warped" en anglais). Une telle gorge peut apparaître localement dans les géométries compactifiées.

Dans le modèle d'inflation qui nous intéresse, l'inflation de Dirac-Born-Infeld, l'inflation est générée par le mouvement rapide d'une brane-test D3 à l'intérieur d'une gorge AdS de facteur de voilement $f(\phi) = \lambda/\phi^4$ où λ est le couplage de 't

Hooft et dépend du rayon de compactification. La brane-test est attirée vers le fond de la gorge où est fixée une anti-brane $\overline{D3}$. On parle d'inflation DBI du nom de l'action effective à 4 dimensions qui décrit le mouvement de la brane D3. C'est une action où le terme cinétique est fortement non linéaire. Il est caractérisé par le facteur γ qui est l'équivalent d'un facteur de Lorentz et une vitesse du son non triviale $c_s = 1/\gamma$. L'inflation DBI est efficace quand la brane-test est très rapide et se déplace à une vitesse proche de la vitesse limite. En cela l'inflation DBI est très différente de l'inflation standard en roulement lent. L'inflation a lieu même si le potentiel est très pentu. En première approximation on peut supposer que le potentiel est quadratique. Ce modèle d'inflation DBI se caractérise par un spectre de puissance scalaire très plat et des non-gaussianités assez grandes.

Nous étudions une généralisation de ce modèle en supposant la présence de branes piégées à l'intérieur de la gorge le long de la vallée inflationnaire. Pour simplifier on commence par étudier le cas où il n'existe qu'une seule brane piégée. On prend en compte le couplage entre des particules qui vivent sur cette brane et la brane inflationnaire. La masse effective des particules de matière est proportionnelle à la distance entre la brane piégée et la brane mobile de sorte que les particules vont être créées pendant l'inflation quand la brane inflationnaire croise la brane fixe.

On étudie les différents régimes de création de particules: par résonance paramétrique et par instabilité tachyonique. On prouve que le régime de création dépend de la constante $\xi = H^2/g|\dot{\phi}|$ qui dépend à son tour du taux de Hubble, de la constante de couplage et de la vitesse de la brane inflationnaire au passage. On calcule la densité d'énergie des particules qui correspond simplement à l'intégration sur tous les modes du nombre de particules créées avec un moment k multiplié par la quantité d'énergie $\hbar\omega$ comme pour tout oscillateur quantique. On trouve ainsi que la densité d'énergie est proportionnelle à la distance entre la brane-test et la brane piégée est qu'elle comporte un facteur de dilution en $1/a^3$. Cela signifie que la brane inflationnaire va subir une force de rappel vers la brane fixe mais que cette force ne peut se faire sentir que pendant quelques e-folds après la zone d'interaction.

Nous avons montré dans notre premier article que les branes inflationnaires qui satisfaisaient les conditions de normalisation de COBE n'étaient pas ralenties alors que celles qui ne les satisfaisaient pas étaient ralenties efficacement. Il existe ainsi un mécanisme de sélection selon l'efficacité du "brane bremsstrahlung". Pour les branes qui ont de l'importance pour nous, celles qui satisfont les conditions de normalisation de COBE, les particules de matière sont créées quasi-

instantanément par résonance paramétrique. Le mouvement de ces branes n'est pas affecté par la contre-réaction des particules tant que le nombre de branes piégées reste inférieur à un milliard.

Même si le fond n'est pas modifié, on ne peut rien dire sur ce qu'il se passe au niveau perturbatif. On souhaite savoir si le couplage à la matière va avoir des conséquences observationnelles, notamment dans le spectre de puissance scalaire du CMB. Une autre grosse partie de mes travaux de recherche de thèse a été de montrer qu'il existe une analogie entre mon modèle avec branes piégées et une théorie scalaire-tenseur en k -inflation couplée à la matière. J'ai étudié cette théorie scalaire-tenseur plus générale. J'ai étudié la théorie des perturbations en prenant en compte ce couplage à la matière et j'en ai déduit que des singularités pouvaient apparaître lorsque la fonction de couplage variait de façon abrupte. Ces singularités apparaissent sous forme de fonction de dirac dans l'équation des perturbations et sous forme de saut dans le spectre de puissance de la perturbation de courbure.

Le calcul des perturbations (c'est-à-dire des équations d'Einstein perturbées, de l'équation de continuité et de l'équation d'Euler) a été fait en toute généralité. Il pourrait donc très bien servir par la suite pour l'étude de toute théorie de k -inflation où il existe un couplage à la matière ou bien par exemple pour l'étude de la k -essence. Dans le cas qui nous préoccupe ici, comme la densité d'énergie de la matière reste toujours négligeable devant la densité d'énergie de l'inflaton, il est possible de simplifier grandement les équations des perturbations et de résoudre explicitement l'équation de Mukhanov et ainsi de prédire la forme du spectre et la valeur du saut entre petites et grandes échelles. Il est important de souligner que les fonctions de dirac viennent des dérivées secondes de la fonction de couplage soit via la renormalisation de la variable z qui relie la perturbation de courbure comobile et la variable de Mukhanov-Sasaki soit via la dérivée seconde du potentiel effectif. On note aussi que la variable z dépend de l'échelle k , ce qui est une nouveauté. Les résultats obtenus sont utilisés pour le cas des branes piégées où le lagrangien pour l'inflaton contient alors un terme cinétique type DBI et un terme potentiel effectif de type caméléonique et le spectre de puissance est calculé pour le cas d'une seule brane piégée mais aussi pour le cas d'un paquet dense de branes piégées afin d'obtenir un saut bien visible.

Brièvement, je dis aussi un mot sur un travail qui n'a pas encore eu le temps d'être entièrement achevé. Je me suis intéressée à ce qu'il se passe à l'intérieur de la zone d'interaction. On s'attend à ce que les effets de rediffusion modifient les perturbations et créent un taux important de non-gaussianités. Pour évaluer

cela, il est nécessaire de calculer l'action à l'ordre 3 et d'étudier les équations des perturbations au deuxième ordre. Le formalisme ADM se révèle alors fort utile.

Enfin, une autre partie de mon travail de thèse a été consacrée à l'étude de caractéristiques du spectre ayant une toute autre origine, les caractéristiques qui viennent directement du potentiel de l'inflaton. On s'est intéressé à un modèle très simple, celui de Starobinsky où le potentiel est linéaire mais avec un brusque changement de pente. Dans le cas de l'inflation canonique, Starobinsky a montré que le régime de roulement lent était violé au passage de la discontinuité, ce qui conduisait à des singularités dans le spectre de courbure scalaire.

Nous généralisons l'étude de ce modèle au cas de l'inflation DBI. Les choses sont assez similaires puisque les paramètres de "roulement lent DBI", sauf ϵ_1 , deviennent plus grands ou d'ordre un au passage de la brane piégée. Nous soulignons les difficultés que l'on a rencontrées dans l'étude analytique et les différences qu'il y a avec le cas standard. Dans le formalisme d'Hamilton-Jacobi, nous développons une méthode générale pour calculer la valeur du saut dans le spectre en fonction du potentiel et de ses dérivées. Nous avons aussi conduit une étude numérique de ce modèle.

Nous nous sommes rendus compte que les "features" obtenues dans le spectre, qu'elles soient de type Starobinsky ou de type scalaire-tenseur, avaient la même allure (saut et oscillations additionnelles) et nous pensons que la comparaison avec les "features" observées expérimentalement dans le spectre du fond diffus permettrait de contraindre les paramètres des modèles. Mais il serait sans doute *in fine* difficile de se prononcer sur l'origine physique d'une "feature" observée. Au cours de nos recherches, nous avons non seulement étudié en détail les "features" sourcées par un potentiel et celles sourcées par un couplage à la matière mais nous avons également montré que les "features" pouvaient aussi avoir comme origine un facteur de voilement et/ou une vitesse du son irréguliers.

Contents

Résumé	iii
Abstract	v
Remerciements	vii
Résumé	ix
Contents	1
List of Figures	4
I Prerequisites	7
1 Cosmology	9
1.1 Metric and Friedmann equation	10
1.2 Brief history of the universe	13
1.3 Observations and consequences	14
1.4 The Hot Big Bang limitations	15
1.4.1 The horizon problem	15
1.4.2 The flatness problem	19
1.4.3 The dark energy problem	19
1.4.4 Other puzzles	20
2 String Theory	21
2.1 Introduction	21
2.2 From the bosonic string to the superstring	22
2.3 D-branes	23
2.4 Compactification	25
2.5 Moduli stabilization	26
2.6 Gauge/gravity duality	27
2.7 String theory and cosmology	27

3	Inflation	29
3.1	The paradigm of inflation	29
3.2	Old and new inflation	31
3.2.1	Example of inflation with a quadratic potential	33
3.2.2	Preheating and reheating	33
3.2.3	Shortcomings of this model	33
3.3	The inflationary zoology	34
3.3.1	Small-field inflation	34
3.3.2	Large-field inflation	35
3.4	Multi-field inflation	35
3.4.1	Hybrid inflation	36
3.4.2	Curvaton scenario	36
3.5	K-inflation	36
3.6	Brane inflation	37
3.7	Tests for inflation	39
4	Perturbation theory	41
4.1	Basics on usual perturbation theory	41
4.2	Perturbations in k-inflation	45
4.2.1	Interesting quantities	49
4.2.2	Non-Gaussianities	50
5	The CMBR	53
5.1	History	54
5.2	Physics	55
6	DBI Inflation	59
6.1	Action	59
6.2	Dynamics	61
6.2.1	Hamilton-Jacobi formalism	62
6.2.2	Example of a quadratic potential	63
6.3	Perturbations	64
6.4	Characteristics, observational signatures	65
6.5	Brane annihilation and reheating	65
6.6	A word on multi-field DBI inflation	66
7	Scalar-tensor theories	67
7.1	Brans-Dicke theories, $f(R)$ theories and chameleons	67
II	PhD researches	71
8	Features	73
8.1	Starobinsky's model : background	73

8.2	Starobinsky's potential in DBI inflation	77
8.3	DBI perturbation equation	80
8.4	Starobinsky's perturbation equation	82
8.5	Evaluation of the dirac factor	83
8.6	Power spectrum and features in canonical inflation	85
8.7	Perturbation equation in DBI : challenges	87
8.8	Numerical analysis	89
8.9	About features	90
9	Coupling with matter	91
9.1	WKB approximation	91
9.2	Small ξ regime	93
9.3	Large ξ regime	94
9.4	Creation of particles	96
9.5	The modified potential	101
9.6	Discussion on the parameters	104
9.7	K-inflation coupled to matter	106
9.8	Abrupt change in the coupling function	109
9.9	Perturbations	110
9.10	Resolution of a perturbation equation with a dirac	114
9.11	Scalar-tensor features	115
9.12	Application	119
9.13	On other scales	121
9.14	Inside the interaction region	121
9.15	Non-Gaussianities from particle production	125
10	Prospects and conclusion	127
10.1	Conclusion	127
10.2	Open problems	128
Appendix A :		
	Matter radiation equality	129
Appendix B :		
	Perturbation computations in DBI Starobinsky model	131
Appendix C :		
	Perturbation equations with δ-singularities	133
Appendix D :		
	Perturbation equation with a δ and a δ' term	135
	Publications	137
	Bibliography	139

List of Figures

1.1	The bullet cluster	16
1.2	Hubble law	17
1.3	Observational constraints on Ω_K/Ω_Λ	17
1.4	Light elements abundances	18
2.1	Comic strip from XKCD	21
2.2	The different string theories	22
3.1	Comoving Hubble radius	30
3.2	Past light cone of an observer	30
4.1	Evolution of the quantum fluctuations to galaxies and planets	41
4.2	Evolution of perturbations in our universe	49
5.1	Anisotropies in the CMB temperature	53
5.2	Early Release Compact Source Catalog	54
5.3	CMB spectrum of anisotropies from WMAP5 and ACBAR	57
5.4	Joint constraints on the ratio r and spectral index n_s	58
6.1	DBI inflation	59
8.1	Slow-roll parameters in Starobinsky's model in canonical inflation	74
8.2	Comparison of the analytical and numerical solutions	76
8.3	Consistency of the approximation of a constant Hubble rate	77
8.4	Slow-roll parameters in DBI	78
8.5	Numerical DBI power spectrum	89
9.1	Configuration of the interaction zone in the complex plane	97
9.2	Computation of Bogoliubov coefficients around region I	97
9.3	Computation of Bogoliubov coefficients around region II	100
9.4	Features in power spectra from matter creation	120

Introduction

The Cosmic Microwave Background (CMB) experiments of the last twenty years have gathered evidence in favor of the inflationary scenario. The paradigm of inflation is now fully integrated in the Hot Big Bang Theory and accounts for the existence of stars and galaxies. The relation between inflation and fundamental physics is an active field of research. We will focus on an open string inflation model : Dirac-Born-Infeld (DBI) inflation where the inflaton is the position modulus of a mobile D-brane. We will study the effects of the coupling of the inflaton with matter during inflation and highlight the observational consequences. We will compare these observational features in the CMB spectra to other features such as Starobinsky's.

In the first part of this manuscript, we will only present well-known facts and calculations, which are necessary for a good understanding of the framework and motivations of this thesis. Chapter 8 and 9 sum up results from my three-year PhD researches, some of which have been published (see publication list at the end of the manuscript). In the first chapter we recall modern cosmology principles and shortcomings of the Hot Big Bang theory. In chapter 2, we give a brief introduction to string theory, the dynamics of D-branes and the challenges of compactification and moduli stabilization. In chapter 3, we depict some inflationary scenarios and show the large variety of viable models and origins for the inflaton field. In chapter 4, we give the basis for the computation of the CMB spectrum or bispectrum and in chapter 5 we explain how information on the inflationary era can be extracted from observations of the CMB. In chapter 6, we review the model of DBI inflation. In chapter 7, we introduce scalar-tensor theories because we later use an analogy between our DBI model with the presence of trapped branes and such theories with a suddenly varying coupling function. In chapter 8, we try to generalize Starobinsky's model of a piece-wise linear inflaton potential to DBI inflation. In chapter 9, we investigate the effect of trapped branes in the DBI scenario. We prove that particles become massless when the inflationary brane crosses the trapped brane and are easily created. We show that the particle production depends on the inflationary parameters. We analyze the backreaction of the particles on the inflaton field and its imprints on the observables.

Part I

Prerequisites

Cosmology

“Tant qu’un homme ne s’est pas expliqué le secret de l’univers, il n’a pas le droit d’être satisfait”, J. Renard

The study of our universe aims at finding out its past history as well as predicting its future. Primordial cosmology is the study of the very first moments of the universe, an era when atoms were not yet created. Primordial cosmology is a field concerned with high-energy physics. A major issue for cosmologists is the limitations on conducting experiments to confirm or rule out their theories. One of the only way out is numerical simulations. For the primordial cosmologist, solutions are even fewer. Very high energies can only be reached in super colliders. At the Large Hadron Collider (LHC), energies up to the TeV scale are reached. The most valuable tool for inflationary cosmology is the primordial power spectrum of the Cosmic Microwave Background (CMB) Radiation, that is to say the radiation from the photons of the surface of last scattering.

To understand what is the surface of last scattering, let’s try a simple thought experiment. Imagine you are falling backwards off a plane flying through very thick clouds. While falling, you cannot see much around you. But you soon get out of the clouds. You can see the surface of the lowest clouds above you. You keep falling. There is light and you can now see through thin air the mountain summits, then some birds, then some telephone lines and you can still see far above you the surface of the clouds. And now you can even see the antennas on the roofs of high buildings and then tree branches... Do not be afraid, this is just a thought exercise, there is no impact on the ground. The history of the universe is quite similar. First, the universe was opaque to photons. The CMB photons come from the surface of last scattering, which is analogous to the surface of the clouds in our imaginary exercise. After that the universe gets more and more complex, with the formation of the first stars and the end of dark ages. The closer you get to the ground, that is to say to present time, the more you can

see and the more complex things get. But you will never be able to know what was above the surface of the clouds. The CMB radiation is like a photograph of the universe taken at decoupling (380,000 years after the Big Bang). An old, torn and unique photo with yellowed colours, from which a better picture can be obtained with some serious work

[1] is a good introduction to primordial cosmology and the first chapters cover in details the notions introduced in this chapter.

1.1 Metric and Friedmann equation

Modern cosmology was born with the measurement of the expansion of the universe through galaxy redshifts by Hubble and with the so-called Big Bang theory of Lemaître in the late 20s. Cosmology is of course indissociable with Einstein's General Relativity. A founding principle in cosmology is the assumption that the universe is isotropic and homogeneous. This is named this the cosmological principle. It has an important consequence on the geometry of the universe : the universe must be of constant curvature (it is either a sphere, an Euclidian space that is to say a flat space, or an hyperboloid such as a saddle.) Space-time is described by a Friedmann-Lemaître-Robertson-Walker metric :

$$ds^2 = -dt^2 + a^2(t)g_{ij}dx^i dx^j \quad (1.1)$$

where t is the cosmic time, $a(t)$ the scale factor and g_{ij} the metric of hypersurfaces of constant time such that

$$g_{ij}dx^i dx^j = dr^2 + f_K^2(r)d\Omega^2 \quad (1.2)$$

with r the radial coordinate, $d\Omega^2$ the elementary solid angle and the function f_K which depends on the curvature :

$$\begin{aligned} f_K(r) &= K^{-1/2} \sin(\sqrt{K}r) && \text{for } K > 0 \\ &= r && \text{for } K = 0 \\ &= (-K)^{-1/2} \sinh(\sqrt{-K}r) && \text{for } K < 0 \end{aligned} \quad (1.3)$$

Note for the rest of this thesis that we choose the signature to be $(-,+,+,+)$ and we set $c = 1$.

The scale factor denotes the expansion of the universe, the fact that scales are being stretched out in time. Hence there is a fundamental difference between a physical distance and a comoving distance.

Since the universe is expanding, wavelengths are redshifted. The redshift is defined as

$$1 + z = \frac{a(t_{\text{observation}})}{a(t_{\text{emission}})} \quad (1.4)$$

The redshift is often used as a time measurement. For instance, decoupling occurred at $z_{\text{dec}} \sim \frac{T_{\text{dec}}}{T_0} \sim 1100$. A radial distance cannot be measured directly but is obtained from the redshift and the expansion law of the universe (see the following equation 1.26).

The Hubble rate

$$H = \frac{\dot{a}}{a} \quad (1.5)$$

is the velocity of the expansion of the universe. Present measurements (for a review on the subject see [2]) give

$$H_0 = 100h \text{ km s}^{-1} \text{ Mpc}^{-1} \text{ with } h = 0.72 \pm 0.08 \quad (1.6)$$

The farther two galaxies or clusters are, the faster they seem to part.

For a time-space to be compatible with (1.1-1.3), the energy-momentum tensor has to be of the form :

$$T_{\mu\nu} = -\frac{2}{\sqrt{-g}} \frac{\delta S}{\delta g^{\mu\nu}} = \rho u_\mu u_\nu + p g_{\mu\nu} \quad (1.7)$$

which describes a perfect fluid with an energy density ρ and a pressure p .

Einstein equations are the fundamental equations for cosmology, they link the geometry to the energy distribution.

$$G_{\mu\nu} = R_{\mu\nu} - \frac{1}{2} R g_{\mu\nu} = 8\pi G T_{\mu\nu} \quad (1.8)$$

$R_{\mu\nu}$ is the Ricci tensor, it is the contraction of the Riemann tensor :

$$R_{\mu\nu} = R_{\alpha\mu\nu}{}^\alpha \quad (1.9)$$

$$R_{\lambda\mu\nu}^\rho = \partial_\lambda \Gamma_{\mu\nu}^\rho - \partial_\mu \Gamma_{\lambda\nu}^\rho + \Gamma_{\mu\nu}^\sigma \Gamma_{\sigma\lambda}^\rho - \Gamma_{\lambda\nu}^\sigma \Gamma_{\sigma\mu}^\rho \quad (1.10)$$

with Christoffel symbols

$$\Gamma_{\mu\nu}^\lambda = \frac{1}{2} g^{\lambda\sigma} (\partial_\mu g_{\nu\sigma} + \partial_\nu g_{\sigma\mu} - \partial_\sigma g_{\mu\nu}) \quad (1.11)$$

We will often use the Planck mass $M_p^2 = (8\pi G)^{-1}$ or the kappa factor $\kappa = 8\pi G$ rather than the Newtonian gravitational constant.

From the form of the Einstein tensor, we deduce the Bianchi identity

$$\nabla_\mu T_\nu^\mu = 0 \quad (1.12)$$

Substituting the components of the Ricci tensor for a FLRW metric and the components of the diagonal energy-momentum tensor $T_\nu^\mu = (-\rho, p, p, p)$ in the Einstein equations we obtain the Friedmann equation

$$H^2 = \frac{\dot{a}^2}{a^2} = \frac{\kappa}{3} \rho - \frac{K}{a^2} + \frac{\Lambda}{3} \quad (1.13)$$

and the Raychaudhuri equation

$$\frac{\ddot{a}}{a} = -\frac{\kappa}{6}(\rho + 3p) + \frac{\Lambda}{3} \quad (1.14)$$

The conservation equation is derived from the Bianchi identity

$$\dot{\rho} + 3H(\rho + p) = 0 \quad (1.15)$$

These three equations (1.13, 1.14, 1.15) are the key equations of basic cosmology. No a priori knowledge on the contents of the universe is required to write those equations, the only hypothesis is that of a perfect fluid or fluid mixture with a pressure

$$p = \frac{1}{3}T_i^i \quad (1.16)$$

and energy density

$$\rho = -T_0^0 \quad (1.17)$$

The Λ cosmological constant has a physical interpretation, it is either a vacuum energy or a new form of energy called dark energy. If we use conformal time $dt = ad\eta$ instead of cosmic time, equations (1.13, 1.14) become :

$$\frac{a''}{a} - \mathcal{H}^2 = -\frac{\kappa}{6}a^2(\rho + 3p) + \frac{\Lambda a^2}{3} \quad (1.18)$$

$$\mathcal{H}^2 = \frac{\kappa}{3}\rho a^2 - K + \frac{\Lambda a^2}{3} \quad (1.19)$$

We often define dimensionless variables which represent the ratio of each fluid in the total energy density of the universe

$$\Omega_\Lambda = \frac{\Lambda}{3H^2} \quad (1.20)$$

$$\Omega_K = \frac{-K}{a^2 H^2} \quad (1.21)$$

For the matter part, we can distinguish the fluids with different equations of state

$$\Omega_m = \frac{\kappa\rho}{3H^2} = \sum_i \Omega_i = \sum_i \frac{\kappa\rho_i}{3H^2} = \sum_i \frac{\rho_i}{\rho_c} \quad (1.22)$$

with the critical density being $\rho_c = 3H^2/\kappa$. Then the dimensionless Friedmann equation is :

$$\Omega_m + \Omega_K + \Omega_\Lambda = 1 \quad (1.23)$$

From different observations one gets that the curvature K is zero at one percent of precision (see section 1.3 and figure 1.3) and that

$$\Omega_{\Lambda 0} = 0.73 \quad \text{and} \quad \Omega_{m 0} = 0.27 \quad (1.24)$$

Precise data on Ω_{m0} can be found in table 1 of [3]. Today the universe contains roughly 73% of dark energy which is responsible for the recent cosmic acceleration. Dark energy is an anti-gravitating fluid. The universe also contains 27% of matter : 23% of cold dark matter, that is to say non-relativistic matter with unknown intrinsic properties which only interacts gravitationally and 4% of usual baryonic matter. This is what is called the Λ CDM model describing the universe. There are some refined alternatives as we will see in section 1.4.3.

With these equations (1.13, 1.14) we see that the evolution of the universe depends on the curvature and the equation of state of the fluid

$$w = \frac{p}{\rho} \quad (1.25)$$

The equation of state for radiation is $w_{\text{rad}} = 1/3$, for non-relativistic matter in particular for cold dark matter $w_m = 0$ and for a pure cosmological constant $w_\lambda = -1$. The scale factor evolves as

$$a(t) \propto t^{\frac{2}{3(1+w)}} \quad (1.26)$$

when $w \neq -1$. For a purely cosmological constant, the scale factor is exponential. The energy density evolves as

$$\rho_i \propto a^{-3(1+w_i)} \quad (1.27)$$

so that

$$\rho_{\text{rad}} \propto a^{-4} \quad \text{and} \quad \rho_m \propto a^{-3} \quad (1.28)$$

In section 1.2, we will see that first radiation was dominant, then matter became dominant and now dark energy starts to dominate. The time of matter radiation equality is given by

$$1 + z_{\text{eq}} = 2.4 \cdot 10^4 \Omega_m h^2 \quad (1.29)$$

namely $z_{\text{eq}} \sim 3700$. More details on how to derive this formula are given in appendix A.

As we will discuss in section 1.4.3, it is quite intriguing that we live precisely at the time when matter and the cosmological constant are of the same order. One is a constant whereas the other bears a dilution factor of a^{-3} . This is the coincidence problem. It may be eluded using static or dynamical alternatives to the cosmological constant.

The total energy-momentum tensor is the sum of the energy-momentum tensors of radiation (negligible today), baryons, dark matter and dark energy.

1.2 Brief history of the universe

As we have just seen, the universe is not static. It has expanded and evolved greatly after the Big Bang. In the very early stage, when the temperature was

greater than a few GeV's, the universe was a plasma of quarks and leptons. For $T > 10 \text{ MeV}$ ¹, relativistic particles : electrons, positrons, neutrinos and photons were in equilibrium with non-relativistic particles : baryons and anti-baryons. There was an initial asymmetry in the number of baryons and antibaryons. Its origin is still subject of many different interpretations. Here what we mean by equilibrium is that the reaction rate is much greater than the expansion rate. At $T = 800 \text{ keV}$, the weak interactions freeze-out and the ratio neutrons over protons drops to about 1/5. This is the time when the neutrinos decouple. For $100 \text{ keV} < T < 800 \text{ keV}$, electrons and positrons annihilate and atomic nuclei are formed. When $60 \text{ keV} < T < 100 \text{ keV}$, light elements are synthesized. The synthesis of light elements can only start when the deuterium is no longer at equilibrium. At about $T = 1 \text{ eV}$, recombination takes place $p + e^- \rightarrow H + \gamma$. Right after recombination, photons decouple. Before that decoupling, photons and electrons were coupled via Compton scattering and light could not propagate. Decoupling and recombination occur when the universe is already well into the matter-dominated era. This phase is then marked by the formation of the first stars and the first galaxies (at about $T = 10^{-4} \text{ eV}$). Heavy elements are synthesized inside the stars. And very recently ($z \sim 2$) dark energy became dominant over matter and the expansion of the universe accelerated. In the Λ CDM standard model of the Big Bang it is expected that it will continue to accelerate indefinitely.

1.3 Observations and consequences

Today, we have a few quasi-certainties about cosmology thanks to observations. First the existence of dark matter was suggested by Zwicky who measured the velocity dispersions of the galaxies in the Coma cluster and found that some of the gravitational mass was missing [4]. Another solid evidence of “unseen” mass is the flatness of the rotation curves of observed galaxies that can't be explained by the visible mass of the galaxies alone [5]. The general idea is that the rotation velocity is a function of the inner mass (virial theorem). The missing matter is to be found in the dark matter halo of the galaxy. Another additional proof of the existence of dark matter is strong lensing, the light coming from distant galaxies is deviated by the presence of dark matter. Numerical simulations [6] highlight the necessity to include dark matter, otherwise the formation of large-scale structures does not start at the right time. Nevertheless, dark matter has not been detected yet and some alternatives to DM theories have been developed. The famous MOND (MODified Newtonian Gravity) theory tends to explain the rotation curves by a modification of Newtonian gravity for very small accelerations. This was first proposed by Milgrom [7]. But the observations of the bullet cluster [8] (see figure 1.1) are in contradiction with such theories and are strong evidence in favor of dark matter.

1. the conversion is $\frac{1\text{eV}}{k_B} \equiv 1.1 \cdot 10^4 \text{ K}$

Second, the study of the CMB has suggested the flatness of the universe. Here the general idea is that for an adiabatic model, the position of the first peak is relevant to the curvature of space-time.

Third, as we have explained, Hubble measured the expansion of the universe (see figure 1.2) but much more recently it has been understood that this expansion is actually accelerating thanks to the analysis of the standard candle SNIa data [9, 10].

Fourth, information about nucleosynthesis can be obtained from measurements of the relative abundances of light elements (H, He, Li, Be) in stars, galaxies and in the interstellar medium.

Fifth, the last observational pillar is the Cosmic Microwave Background radiation (CMBR), which we will discuss in much greater details in chapter 5. Let's just say that it is an incomparable source of information for the cosmologist. Precise constraints on cosmological parameters have been obtained from CMB data.

Other great sources of information are the large sky survey (LSS), the Lyman- α forest of absorption rays in quasar spectra, 21cm physics and the detection of gravitational waves.

We can list the cosmological parameters of Big Bang models : H_0 , Ω_{K0} , $\Omega_{\text{CDM}0}$, Ω_{b0} , $\Omega_{\gamma0}$, $\Omega_{\nu0}$, $\Omega_{\Lambda0}$ and we can add w the equation of state parameter for dark energy. There are all tightly constrained by the mentioned observations. Other interesting quantities from the Big Bang Nucleosynthesis are worth listing : η the baryon to photon ratio, T_0 today's temperature of the universe (the temperature of the CMB photons), z_{eq} (refer to 1.29), T_{eq} the temperature of the universe at equality, z_{dec} the decoupling redshift, Δz_{dec} the width, T_{dec} the decoupling temperature, z_{BBN} and T_{BBN} the redshift and temperature at primordial nucleosynthesis.

1.4 The Hot Big Bang limitations

1.4.1 The horizon problem

Since the Big Bang, the photons can only have travelled a finite distance. The universe has an horizon. The comoving Hubble radius $(aH)^{-1}$ can be seen as the maximal distance separating two particles above which it is non longer possible for a photon emitted from particle 1 to eventually reach particle 2. On such a distance, the expansion of the universe prevails. On the other hand, if two particles are separated by a distance larger than the horizon, it means that they have never been in causal contact. From 1.26, we see that

$$(aH)^{-1} \propto t^{\frac{1+3w}{3(1+w)}} \propto t^{1/2} \quad (\text{Radiation era}) \quad (1.30)$$

$$\propto t^{1/3} \quad (\text{Matter era}) \quad (1.31)$$

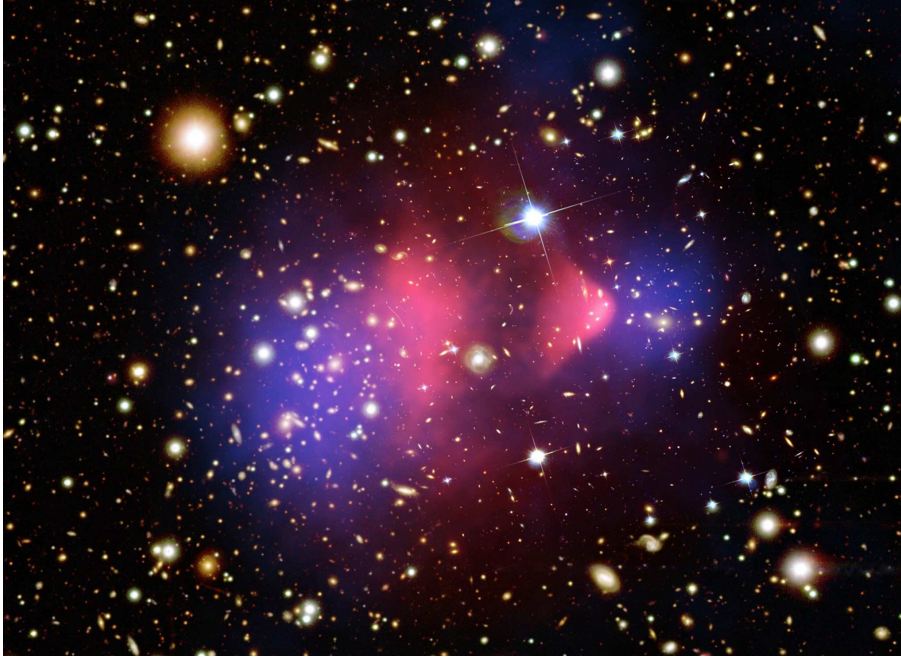


Figure 1.1: The matter in galaxy cluster 1E 0657-56, known as the bullet cluster, is shown in this composite image. A mere 3.4 billion light-years away, the bullet cluster's individual galaxies are seen in the optical image data, but their total mass adds up to far less than the mass of the cluster's two clouds of hot x-ray emitting gas shown in red. Representing even more mass than the optical galaxies and x-ray gas combined, the blue hues show the distribution of dark matter in the cluster. Otherwise invisible to telescopic views, the dark matter was mapped by observations of gravitational lensing of background galaxies. In a text book example of a shock front, the bullet-shaped cloud of gas at the right was distorted during the titanic collision between two galaxy clusters that created the larger bullet cluster itself. But the dark matter present has not interacted with the cluster gas except by gravity. The clear separation of dark matter and gas clouds is considered direct evidence that dark matter exists. *From NASA APOD*

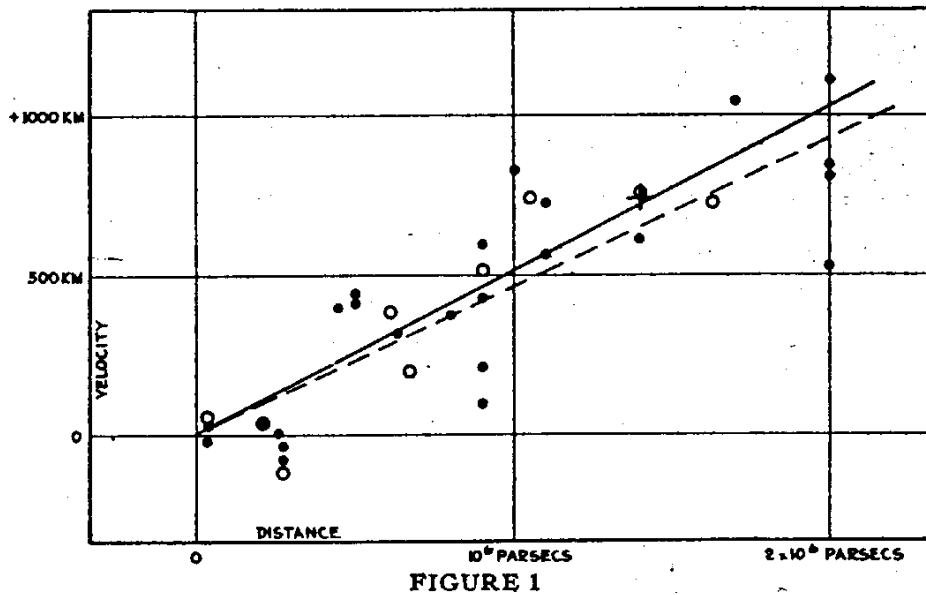


Figure 1.2: Original plot of E. Hubble from [11]. Radial velocities, corrected for solar motion, are plotted against distances estimated from involved stars and mean luminosities of nebulae in a cluster. The black discs and full line represent the solution for solar motion using the nebulae individually; the circles and broken line represent the solution combining the nebulae into groups; the cross represents the mean velocity corresponding to the mean distance of 22 nebulae whose distances could not be estimated individually.

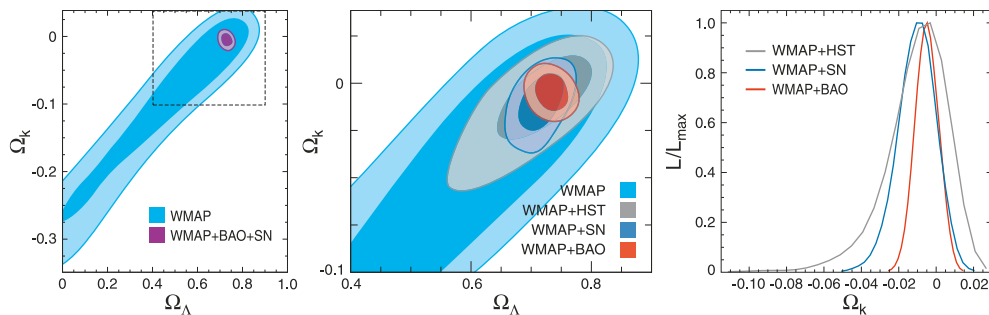


Figure 1.3: Constraints from WMAP and other observations (HST=Hubble space telescope, SN=supernovae, BAO=Baryonic Acoustic Oscillations) on the ratio Ω_K/Ω_Λ , from [3].

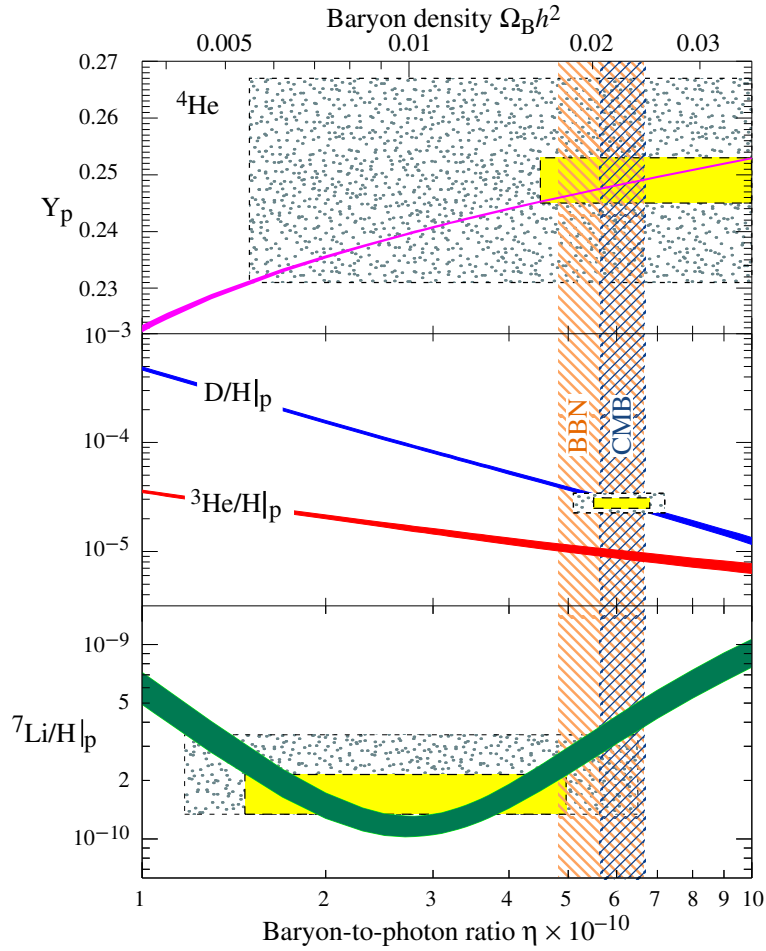


Figure 1.4: The abundances of ${}^4\text{He}$, D, ${}^3\text{He}$ and ${}^7\text{Li}$ as predicted by the standard model of big-bang nucleosynthesis. Boxes indicate the observed light element abundances (smaller boxes: 2σ statistical errors; larger boxes: $\pm 2\sigma$ statistical and systematic errors). The narrow vertical band indicates the CMB measure of the cosmic baryon density. Figure from [12]

so it seems that the comoving Hubble radius has always been increasing in the history of the universe.

The comoving horizon is

$$d_H(t) = \int_0^t \frac{dt'}{a(t')} \quad (1.32)$$

If we consider a universe which is exclusively matter-dominated,

$$a(t) = \left(\frac{t}{t_0}\right)^{2/3} \quad (1.33)$$

the ratio between the comoving particle horizon at decoupling and today is roughly

$$\frac{d_H(t_{\text{dec}})}{d_H(t_0)} = \left(\frac{t_{\text{dec}}}{t_0}\right)^{1/3} \sim 10^{-2} \quad (1.34)$$

The causally connected regions at last scattering are smaller than the observable universe. Their angular size is typically 1 degree. However, the sky is very homogeneous on large-scale. The CMB temperature is the same in all directions with a precision of 10^{-5} . It is surprising that far-away patches of the sky happen to be at the same temperature even though they are causally disconnected and thermalization of the whole universe was not possible.

1.4.2 The flatness problem

From (1.23), we know that

$$|\Omega_m + \Omega_\Lambda - 1| = \frac{|K|}{a^2 H^2} \quad (1.35)$$

Current observations suggest that the universe is flat with a precision of at least

$$|\Omega_{m0} + \Omega_{\Lambda0} - 1| = |\Omega_K| < 10^{-1} \quad (1.36)$$

which implies that at the Planck time

$$|\Omega_{mP} + \Omega_{\Lambda P} - 1| \sim |\Omega_{m0} + \Omega_{\Lambda0} - 1| \left(\frac{a_0 H_0}{a_P H_P}\right)^2 < 10^{-57} \quad (1.37)$$

which is an unreasonably small precision. A theory with fine-tuning issues seems rather limited in its predictions.

1.4.3 The dark energy problem

As we discussed briefly in section 1.1, the cosmological constant in Einstein equations can be seen as a vacuum energy or dark energy. But it can also be seen as a gauge choice : a cosmological constant proportional to the metric can be added in the equations since the energy-momentum tensor is in the kernel

of the metric. One cannot put numbers on the dark energy density but one can very roughly estimate it in natural units

$$\rho_\Lambda \sim M_p^4 \sim 10^{123} \text{ GeV m}^{-3} \sim 10^{122} \rho_c \quad (1.38)$$

this qualitative estimation is in disagreement with the observation by a factor of 10^{122} . The dark energy density cannot be associated with any energy scale in particle physics.

The other problem which arises when thinking about dark energy is the coincidence problem. It can be eluded using more sophisticated models than the pure cosmological constant. For instance, the dark energy could be of the form of quintessence [13] where its equation of state evolves in time and depends on the background [14]. There are claims that acceleration is only a misinterpretation of the data. Modified gravity (at large scales) could explain the observations without requiring dark energy. A good example would be $f(R)$ -chameleons theories, which will be reviewed in chapter 7.

1.4.4 Other puzzles

We have no explanation for the formation of large-scale structures from the global picture of section 1.1. Nothing can *a priori* source the initial inhomogeneities. Another bothering point is the monopole problem, also called the relic problem or the defect problem. This problem arises only if the high-energy theory predicts that symmetries are broken when the universe cools down after the Big Bang. This is predicted for instance in Grand Unified Theories. During phase transitions, topological defects appear, such as domain walls or cosmic strings, with a typical density of one per Hubble volume. The creation of those monopoles, that is to say, very massive (magnetic or non-magnetic) relics, might spoil nucleosynthesis or later-times physics of the Big Bang standard model. Monopoles should a priori dominate over radiation.

The Big Bang theory seems to be a very good model to describe the history of our universe and accounts for most observations but it has some serious limitations, some of which will be suppressed by the introduction of the paradigm of inflation in chapter 3.

String Theory

"IIB or not IIB: that is the question", free adaptation from W. Shakespeare

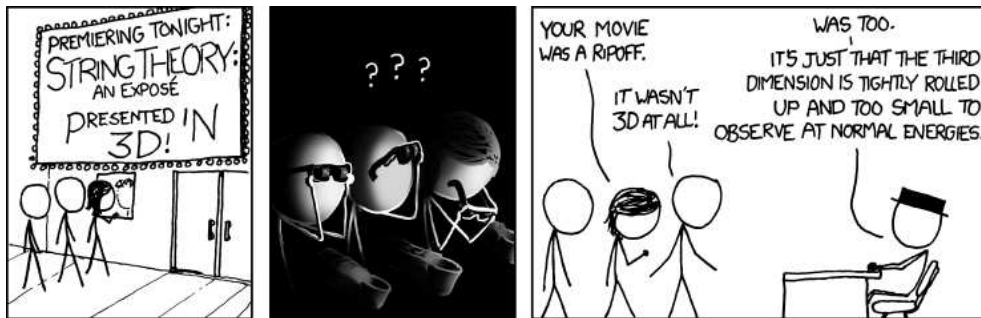


Figure 2.1: enlightning comic strip from XKCD

It is useful to recall some notions of string theory so as to understand brane inflation scenarios discussed later. For a real introduction to string theory, the courses of Polchinski or Kiritsis are a great help [15, 16].

2.1 Introduction

String theory is a complex theory which aims at combining both quantum physics and gravity in a unified theory. In this theory, new fundamental objects appear: strings (1d objects, either open or closed). Their low-energy modes give the massless and massive particles of the Standard Model. This theory has many consequences but very few potentially observational consequences. When including supersymmetry, the string theory becomes the superstring theory. The theory of superstrings is coherent (Lorentz-invariant and ghost-free) in 10 dimensions.

This means that the 6 extra spatial dimensions must be compactified (cf. section 2.4).

There are 5 distinct superstring theories : type I, type IIA, type IIB, heterotic $E_8 \times E_8$ and heterotic $SO(32)$. Their differences lie in the choice of orienting strings or not, on considering open strings or only closed ones and on choosing the same or opposite chirality for fermions. Heterotic theories mix bosonic and superstring theories. M theory [17] is believed to be a unified theory of those 5 realizations. It lives in 11d and its fundamental objects are membranes instead of strings. In this work, we will always be in the type IIB framework.

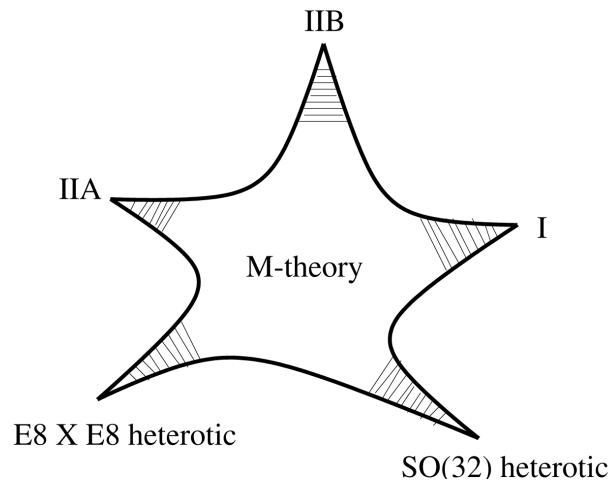


Figure 2.2: Different string theories, supposedly unified in M-theory

Type IIB describes closed oriented superstrings. It has $\mathcal{N} = 2$ supersymmetry. Fermions have the same chirality. Type IIB has no gauge symmetry and can only describe gravity and it thus cannot be the whole story. Superstring theory still needs lots of improvements to reach a viable unified theory.

2.2 From the bosonic string to the superstring

The coordinates on the worldsheet (σ, τ) are mapped onto space-time by the string coordinates $X^\mu(\sigma, \tau)$. The bosonic string is described either by the Nambu-Goto action or the Polyakov action.

$$S_{\text{NG}} = -T \int d\sigma d\tau \sqrt{(X_{,\tau} \cdot X_{,\sigma})^2 - (X_{,\tau})^2 (X_{,\sigma})^2} \quad (2.1)$$

$$S_{\text{P}} = -\frac{T}{2} \int d\sigma d\tau \sqrt{-g} g^{\alpha\beta} \partial_\alpha X^\mu \partial_\beta X^\nu \eta_{\mu\nu} \quad (2.2)$$

in a flat Euclidean metric and where the rank 2 worldsheet metric is used as an auxiliary field and $T = 1/2\pi\alpha'$ is the string tension and α' is the Regge slope.

The solutions can be decomposed into left and right movers.

$$X_L^\mu = \frac{x^\mu}{2} + \frac{l_s^2}{2} p^\mu (\tau + \sigma) + i \frac{l_s}{\sqrt{2}} \sum_{m \neq 0} \frac{\alpha_m^\mu}{m} e^{-im(\tau + \sigma)} \quad (2.3)$$

$$X_R^\mu = \frac{x^\mu}{2} + \frac{l_s^2}{2} p^\mu (\tau - \sigma) + i \frac{l_s}{\sqrt{2}} \sum_{m \neq 0} \frac{\bar{\alpha}_m^\mu}{m} e^{-im(\tau - \sigma)} \quad (2.4)$$

with l_s the string length. The strings are quantized.

$$[\alpha_m^\mu, \alpha_n^\nu] = m \eta^{\mu\nu} \delta_{m+n,0} \quad (2.5)$$

Free fermions are included using the Ramond-Neveu-Schwarz formalism. It involves adding a Dirac action for the fermionic fields (Majorana spinors). There is a freedom in the choice of the boundary conditions both for the left and right-movers. For the closed strings :

$$\psi(\sigma, \tau) = +\psi(\sigma + \pi, \tau) \text{ Ramond sector} \quad (2.6)$$

$$= -\psi(\sigma + \pi, \tau) \text{ Neveu-Schwarz sector} \quad (2.7)$$

There are four different possibilities : the NS-NS and R-R sectors give rise to space-time bosons while the NS-R and R-NS sectors give rise to space-time fermions. Each sector has its own spectrum of states. For example, in type IIB, the R-R sector massless spectrum contains a scalar, a 2-form gauge field and a 4-form gauge field. The IIB theory also includes the dilaton, the metric and its bosonic partner and a rank 2 antisymmetric potential: the Kalb Ramond field B_{MN} , plus (as we will see later) the coordinates of each brane.

2.3 D-branes

Other key objects arise in string theory. A Dp-brane [18] is an extended object or hypersurface of p spatial dimension. For instance it is a point if $p = 0$, it is a string if $p = 1$ and it is space-filling if $p = 9$. Our universe could be a D3 brane or a stack of coincident D3 branes, on which the Standard Model interactions are confined. Only gravity is propagating in the bulk. This gives a phenomenological explanation of the weakness of the gravitational interaction.

Even though it breaks Lorentz invariance, open strings can have Dirichlet boundary conditions on certain directions. They have to end on specified hypersurfaces : Dp-branes, such that

$$\partial_\sigma X^\mu(0/\pi, \tau) = 0 \quad \mu = 0 \dots p \quad (\text{Neumann condition}) \quad (2.8)$$

$$\partial_\tau X^i(0/\pi, \tau) = 0 \quad i = p + 1 \dots 9 \quad (\text{Dirichlet condition}) \quad (2.9)$$

Open strings are constrained to end on branes with Dirichlet boundary conditions while closed strings can live in the bulk and interact with the branes. Another

way to see D-branes is as the natural objects which are minimally coupled to the RR potentials. A p-brane is charged under a massless (p+1)-form.

In type IIA, the RR sector contains a 1-form and a 3-form gauge field so that D0 and D2 branes are electrically coupled to them and D4 and D6 branes are magnetically coupled to their (Hodge) duals. D8 branes are also present in IIA string theory. As previously stated, in type IIB, the RR sector contains a 0-form, a 2-form and a 4-form gauge field. D(-1) and D1 branes are coupled electrically. A D(-1) brane is equivalent to a soliton in an Euclidean theory. D3 branes are coupled both electrically and magnetically. D5 and D7 branes couple magnetically. D9 branes may also be considered in IIB as stable branes.

To put things in a nutshell, we can say that in type IIB string theory Dp branes are stable if p is an odd number and in type IIA p should be even. Under those conditions the spectrum of open strings that start and end on the D-brane is tachyon-free. D-branes are BPS states. They are sometimes called half-BPS because they conserve half of the supersymmetry. Their charge equals their tension that is to say that the RR Coulomb interaction is cancelled by the gravitational interaction. Therefore a stack of parallel D-branes is stable.

We will often refer to anti-D-branes or $\overline{\text{D}}$ -branes. A $\overline{\text{D}}p$ -brane is the charge-conjugate of the Dp-brane.

Born and Infeld have proposed a non-linear generalization of Maxwell action

$$S_{\text{BI}} \sim \int \sqrt{-\det(\eta_{\alpha\beta} + kF_{\alpha\beta})} d^4\sigma \quad (2.10)$$

This structure appears in low-energy effective D-brane actions. When generalizing to higher dimensions, this Born-Infeld action combines with the usual Nambu-Goto action for a Dp-brane and we obtain the (p+1)-dimensional Dirac-Born-Infeld action.

$$S_{\text{DBI}} = -T_{D_p} \int \sqrt{-\det(G_{\alpha\beta} + k\mathcal{F}_{\alpha\beta})} d^{p+1}\sigma \quad (2.11)$$

where $k = 2\pi\alpha'$, the brane tension $T_{D_p} = (g_s(2\pi)^p\alpha'^{(p+1)/2})^{-1}$, $G_{\alpha\beta}$ is the induced metric and $\mathcal{F}_{\alpha\beta} = F_{\alpha\beta} + B_{\alpha\beta}$ is the sum of the antisymmetric Kalb Ramond field $B_{\alpha\beta}$ and the form $F_{\alpha\beta}$ arising from a U(1) gauge potential associated with strings with both ends on the brane. This action for the dynamical brane is fully computed for instance in [18]. A Chern-Simons action must be added in order to implement the kappa-symmetry so as to have the right number of fermionic degrees of freedom. It is the integral of a (p + 1)-form, coming from the R-R sector.

$$S_{\text{CS}} = \mu_p \int (C e^{B+kF})_{p+1} \quad (2.12)$$

μ_p is the electric charge, the generalized Dirac quantization gives $\mu_p\mu_{6-p} \in 2\pi\mathbb{Z}$. Since an anti-Dp brane has the same tension as a Dp-brane but opposite five-form charge, it is described by a similar action where the sign of the Chern-Simons

term is reversed. In the abelian case the DBI action can be written as

$$S_{\text{DBI}} = -T_{D_p} \int e^{-\varphi_0} \sqrt{-\det(g_{\alpha\beta} + B_{\alpha\beta} + k^2 \partial_\alpha \phi^i \partial_\beta \phi^i + k F_{\alpha\beta})} d^{p+1} \sigma \quad (2.13)$$

where the dilaton, the graviton and the 2-form B come from the NS-NS sector.

2.4 Compactification

The 6 extra spatial dimensions need to be compactified in order to obtain our observed 4d world. The simplest example of compactification is the Kaluza-Klein theory where there is one additional dimension which is curled up in a circle of sufficiently small radius. When compactifying, it is important to preserve the Poincaré invariance in the remaining 4 dimensions. Kaluza-Klein theory is essential to the understanding of compactification issues and of how compactification affects the mass spectrum.

Here we will focus on compactifications of 10d type IIB string theory on 6d Calabi-Yau spaces. A compact Calabi-Yau manifold is Ricci flat ($R_{MN} = 0$). We can characterize distinct compactifications by their topology, geometry and discrete data such as quantized fluxes and wrapped D-branes. It is important to understand how to derive the corresponding 4d effective theories. The choice made in the compactifying process influence the resulting 4d physics at low energy.

When compactifying, the 10d metric is split in a direct product of an external and an internal manifold. The internal metric does not depend on the external coordinates. It must allow the presence of branes and non vanishing background fluxes.

$$ds_{10}^2 = h^{-1/2}(y) \eta_{\mu\nu} dx^\mu dx^\nu + h^{1/2}(y) g_{MN}(y) dy^\mu dy^\nu \quad (2.14)$$

The metric is a warped product of a Minkowski space and an internal manifold. The function $h(y)$ is the warp factor. The Calabi-Yau metric g_{MN} can be approximated in some region by a cone over a five-dimensional Einstein manifold. The internal space may be deformed in several regions into conifolds with different warp factors. Inflation can be produced in one of the conifolds.

Conifold geometries typically arise when the Minkowski space is replaced by an anti-de Sitter (AdS) space (a space with negative curvature, which also satisfies Lorentz invariance). The simplest example is when the manifold is the product of an anti-de Sitter space and a sphere $\text{AdS}_5 \times S_5$

$$ds_{10}^2 = h^{-1/2}(r) \eta_{\mu\nu} dx^\mu dx^\nu + h^{1/2}(r) dr^2 + h^{1/2}(r) r^2 d\Omega_5^2 \quad (2.15)$$

If we generalize from the sphere to any Einstein space, we obtain

$$ds_{10}^2 = h^{-1/2}(r) \eta_{\mu\nu} dx^\mu dx^\nu + h^{1/2}(r) dr^2 + h^{1/2}(r) r^2 ds_{X_5}^2 \quad (2.16)$$

The 6 compact dimensions form a cone of radial direction r . (2.16) is valid far away enough from the throat tip and top. Space-time with an $\text{AdS}_5 \times X_5$ structure is of particular interest because of the AdS/CFT correspondence which will be described in section 2.6.

The Klebanov-Strassler (KS) geometry [19] is an example of such a warped throat caused by a stack of D3 branes where $X_5 = (SU(2) \times SU(2))/U(1)$. The singularity at the tip of the throat $r = 0$ is smoothed by appropriate fluxes. The UV top of the throat is somehow glued into an unwarped bulk geometry. The warp factor is proportional to R^4/r^4 with R the radius of compactification.

2.5 Moduli stabilization

Moduli are parameters used in the geometry description. Moduli are classically massless and are naturally good candidate scalar fields for the 4D effective theory and might play the role of the inflaton.

A very simple example to understand what moduli are is the example of the torus compactification. Consider a 2d torus with a zero Riemann tensor with the boundary conditions : $y^1 = y^1 + 1$ and $y^2 = y^2 + 1$. The metric is

$$ds^2 = a(dy^1)^2 + bdy^1dy^2 + c(dy^2)^2 \quad (2.17)$$

The a , b and c constants are the three moduli of the 2d torus. In a CY geometry, there can be hundreds of moduli.

Moduli are either related to the complex structure of compactification or the Kahler structure. A deformation of the Einstein equations in the direction of a moduli field comes without energy cost. So the moduli do not contribute to the effective potential in 4d at lowest order and are generically unfixed. But it is expected that loop corrections, SUSY breaking and non-perturbative effects generate a potential for moduli.

Branes and fluxes can remove moduli. For instance, wrapped D7 branes can remove some of the moduli describing the volume of the 4-cycle about which the branes wrap.

We may distinguish between light and heavy moduli : heavy moduli are frozen during inflation and must be integrated out, this moduli stabilization induces contribution to the potential. Light moduli ($m < H$) are all relevant for the dynamics during inflation. They must all be taken in account. Even if the multi-field description is suitable for inflation, light moduli might spoil successful light elements abundances predictions from nucleosynthesis. A relevant example of moduli is given by the positions of branes.

2.6 Gauge/gravity duality

The AdS/CFT correspondence is a quantum correspondence between a conformal field theory on the boundary and string theory on certain types of curved background such as an anti de Sitter space. In conifold geometries, such as those described in section 2.4, a stack of N D3-branes is often localized at the tip ($r \rightarrow 0$) of the throat. The AdS/CFT correspondence states that the low-energy world-volume gauge theory on these coincident branes is dual to the string theory in the near-horizon limit (ie close to the branes). This means that those two theories describe the same physics but in different regimes of coupling. When the gauge theory is weakly coupled, the supergravity theory is strongly curved since the correspondence gives

$$g_{\text{YM}}^2 \Leftrightarrow 4\pi g_s \quad \text{and} \quad g_{\text{YM}} \sqrt{N/v} \Leftrightarrow \frac{R^2}{\alpha'} \quad (2.18)$$

where $v = \text{Vol}(X_5)/\text{Vol}(S_5)$ depends on the Einstein manifold. A more precise formulation of the correspondence is the Maldacena conjecture which states that type IIB string theory on $\text{AdS}_5 \times S^5$ is equivalent to $\mathcal{N} = 4$ super Yang-Mills gauge theory in 4d.

2.7 String theory and cosmology

Primordial cosmology and in particular inflation are sensitive to UV-physics, so it is natural to try to associate string theory to inflationary cosmology. The main motivation is to build a coherent inflationary theory. But inflationary cosmology can also be seen as a test for string theory [20]. Cosmology is one of the only field where stringy predictions may be tested, along with super-collider physics. It might be too ambitious to intend to experimentally test string theory since most stringy cosmological models are often only inspired by string theory and their stringy features are not manifest. It is one thing to succeed in constraining parameters but it is a whole different story to validate a theory.

There are three relevant scales in string inflation : the string scale, the compactification scale and the inflationary scale. The 4d Planck mass is calculable in terms of those scales. If $H_I \approx M_I^2/M_p \ll M_c \ll M_s$ then inflation is well-described by a 4d effective theory. This energy condition will always be satisfied in our framework. So we would only be probing the 4d consequences of a theory living in 10d. There is a great number of parameters in string theory and we cannot expect to have as many inflationary observables. Currently, meaningful constraints exist only for the set of parameters (n_s, r, f_{NL}) . In the rest of this thesis we will link those constraints to a certain type of brane inflation predictions.

The important and distinguishing ingredient of inflationary models is the inflaton potential. Most often, the computation of this potential in brane inflation is

difficult to carry out. In section 6.1 of this manuscript, the different contributions to this potential are listed in the context of DBI inflation and CMB observables are expressed in terms of slow-roll parameters which themselves depend on the potential and its derivatives.

Evidence for string inflation could come from elsewhere than the CMB. For instance, strong, weak and micro-lensing could contain information about cosmic strings [21, 22, 23, 24], as well as the observation of inflationary gravitational waves [25].

Inflation

“The world is a stage, but the play is badly cast”, O. Wilde

Two good reviews on the subject are for instance [26, 27].

3.1 The paradigm of inflation

The paradigm of inflation was first introduced by Guth in 1981 to solve problems of the Hot Big Bang Theory. Other precursors of inflation are Linde, Starobinsky, Steinhardt and Albrecht. Getting rid of the horizon problem requires that the universe went through a phase before the radiation era during which the comoving Hubble radius decreased.

$$\frac{d}{dt} \left(\frac{1}{aH} \right) < 0 \Leftrightarrow \ddot{a} > 0 \quad (3.1)$$

Inflation is a phase of exponential expansion of the universe, which occurred just after the Big Bang and before nucleosynthesis. The existence of this phase solves the horizon problem. In fact, as illustrated in figure 3.1, the horizon is much larger than today’s Hubble radius. It is actually much greater than the size of the observable horizon. Figure 3.2 shows that two distant points at last scattering on an observer’s light cone which seem to belong to two distinct causal patches were actually in causal contact if we assume a primordial phase of inflation.

Inflation also solves the flatness and relic problems. From chapter 1 it is clear that Ω_K evolves as the square of the comoving Hubble radius. Since during inflation the comoving Hubble radius decreases exponentially, no matter what the initial conditions are, Ω_K will always tend to a tiny value at the end of inflation. Besides, during inflation, hypothetical monopoles simply get diluted by the expansion. It is natural that no monopole is observed today because the size of the observable universe is limited.

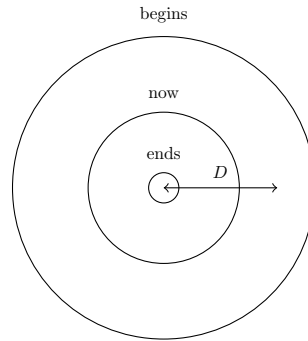


Figure 3.1: Evolution of the comoving Hubble radius since the beginning of inflation. The comoving Hubble radius decreased during inflation and has been increasing ever since. If two points are separated by a distance D they cannot communicate now but they were in causal contact in the early universe.

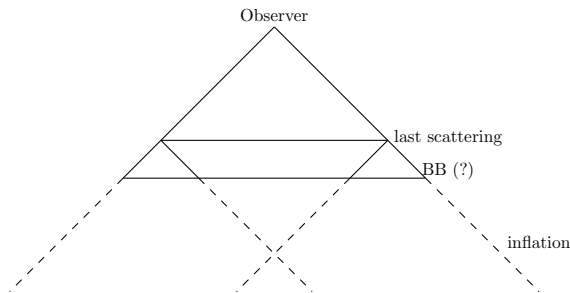


Figure 3.2: Past light cone of an observer. Two regions which seemed totally causally disconnected at last scattering were actually connected if we assume a preliminary phase of inflation (dashed lines). In this scheme, the Big Bang does not correspond to $\eta \rightarrow 0$. Negative conformal time have to be considered when introducing the phase of inflation.

We define N the number of e-folds, which is a convenient time variable for the phase of inflation

$$N_f - N_i = \ln \left(\frac{a_f}{a_i} \right) \quad (3.2)$$

Inflation must last at least about 60 e-folds so as to solve the horizon problem today. The size of a causal region must be at least as large as the size of the observable universe.

Some alternatives to the inflation paradigm are being investigated, such as the ekpyrotic or cyclic universe [28, 29, 30, 31] or string gas cosmology [32, 33]. But there is a strong consensus in favor of the more plausible theory of inflation. The success of inflation lies also in the elegant explanation it offers for

the origin of CMB anisotropies. The quantum fluctuations of the inflaton are the seeds of large-scale structures. We will see in chapter 5 the evolution of those perturbations on super-Hubble scales.

3.2 Old and new inflation

In old inflation [34], a scalar field in a metastable equilibrium subject to a constant potential creates an exponential expansion. When the field tunnels out to its true vacuum state, a bubble is created with very specific properties. The universe is then composed of several bubbles with distinct properties and is necessarily very inhomogeneous. This model was ruled out because of this disturbingly high inhomogeneity. The original proposal of Guth, old inflation, is no longer of interest and now the simplest viable scenario for a phase of cosmic inflation, referred to as “new inflation” [35], requires a scalar field, the so-called inflaton, that slowly rolls down a very flat potential.

$$S_\phi = - \int d^4x \sqrt{-g} \left(\frac{1}{2} g^{\mu\nu} \partial_\mu \phi \partial_\nu \phi + V(\phi) \right) \quad (3.3)$$

In a FLRW universe, the field is spatially homogeneous at linear order. It is described by :

$$\rho_\phi = \frac{1}{2} \dot{\phi}^2 + V(\phi) \quad (3.4)$$

$$p_\phi = \frac{1}{2} \dot{\phi}^2 - V(\phi) \quad (3.5)$$

The Klein-Gordon equation yields

$$\ddot{\phi} + 3H\dot{\phi} + \frac{dV}{d\phi} = 0 \quad (3.6)$$

The expansion of the universe contributes as a friction term in the equation of motion for the inflaton. It can be easier to integrate this equation in terms of the number of e-folds :

$$\frac{d^2\phi}{dN^2} + \left(3H^2 + \frac{1}{H} \frac{dH}{dN} \right) \frac{d\phi}{dN} + \frac{dV}{d\phi} = 0 \quad (3.7)$$

To realize inflation we must have :

$$\ddot{a} > 0 \Leftrightarrow \rho + 3p < 0 \Leftrightarrow 2 \left(\dot{\phi}^2 - V \right) < 0 \Leftrightarrow \dot{\phi}^2 < V \quad (3.8)$$

The equation of state for the inflaton is constrained

$$w_\phi < -\frac{1}{3} \quad (3.9)$$

The contributions of all other components are completely negligible at this stage. The simplest example of inflation is the de Sitter universe where the Hubble rate

H is constant and the scale factor is exponential, though in such a case inflation is eternal.

We define the slow-roll parameters.

$$\epsilon = \frac{-\dot{H}}{H^2} \quad (3.10)$$

and

$$\eta = \eta_V = 2\epsilon - \frac{\dot{\epsilon}}{2\epsilon H} \quad (3.11)$$

In a universe dominated by the inflaton,

$$H^2 = \frac{\kappa}{3 - \epsilon} V \quad (3.12)$$

and

$$\frac{\ddot{a}}{a} = H^2(1 - \epsilon) \quad (3.13)$$

In an inflationary universe, the slow-roll parameter ϵ must be smaller than one. In the slow-roll regime ($|\epsilon|, |\eta| \ll 1$), the right-hand side of the Friedmann equation reduces to the contribution of the potential. The Klein-Gordon equation reduces to

$$3H\dot{\phi} \approx -V' \quad (3.14)$$

where the $'$ denotes a derivative with respect to the inflaton. The slow-roll parameters may be written in terms of the potential and its derivatives. For a smooth potential

$$\epsilon = \frac{1}{2\kappa} \left(\frac{V'}{V} \right)^2 \quad (3.15)$$

and

$$\eta = \eta_V = \frac{1}{\kappa} \frac{V''}{V} \quad (3.16)$$

To realize slow-roll, not only the inflaton speed must be small but its acceleration must also be negligible compared to the Hubble friction term. The criterion on the inflaton potential is its flatness in the domain of interest. Note that there are different commonly used definitions of the slow-roll parameters which are not equivalent. We might define higher-order slow-roll parameters with the generic definition

$$\epsilon_{i+1} = \frac{d \ln|\epsilon_i|}{dN} \text{ with } \epsilon_0 = \frac{1}{H} \quad (3.17)$$

then $\epsilon_1 = \epsilon$ but $\epsilon_2 \neq \eta$. The slow-roll parameters are used for a perturbative expansion around a pure de Sitter universe.

3.2.1 Example of inflation with a quadratic potential

$$V(\phi) = \frac{1}{2}m^2\phi^2 \quad (3.18)$$

The Friedmann equation is roughly

$$H^2 = \frac{\kappa}{6}m^2\phi^2 \quad (3.19)$$

Substituting this Hubble rate H in the simplified Klein-Gordon equation (3.14) we find that the inflaton decreases linearly in time

$$\phi(t) = \phi_i - m\sqrt{\frac{2}{3\kappa}}t \quad (3.20)$$

and the scale factor is exponential

$$a(t) = a_i \exp\left(\frac{\kappa}{4}(\phi_i^2 - \phi^2(t))\right) \quad (3.21)$$

The slow-roll parameters are

$$\epsilon = \eta = \frac{2}{\kappa\phi^2} \quad (3.22)$$

so inflation lasts as long as the inflaton is trans-Planckian.

3.2.2 Preheating and reheating

Successful inflation must last for at least sixty e-folds and possess a graceful exit into a decelerating universe. Inflation ends when the slow-roll parameter ϵ becomes of order one. At the end of inflation, the inflaton oscillates around its (zero) minimum and decays to hot radiation to recover the usual Big Bang model. This process is called reheating [36, 37, 38, 39]. Reheating can be either perturbative or non-perturbative. In this latter case of preheating, particles are usually created via parametric resonance. The physics of reheating depends on the inflationary model and the underlying particle physics theory considered. The comprehension of the mechanisms at stake (including rescattering, fragmentation, turbulence and thermalization) is highly important because it is the source of all elementary particles. Signatures of (p)reheating are typically non-Gaussianities [40, 41] and gravitational waves (probably a stochastic GWs background) [42, 43, 44].

3.2.3 Shortcomings of this model

This model is not very natural because it does not provide any explanation for the origin of the inflaton scalar field. Besides it is difficult to embed all this in a higher-energy theory. If we take into account corrections from supergravity, it adds a mass term in the potential, which spoils slow-roll inflation. This is the

so-called η problem. In any case one needs to know the whole high-energy picture to check the validity of the approximations. In addition, even though inflation was precisely introduced to solve fine-tuning problems, some subtle fine-tuning issues remain. We cannot choose any set of initial conditions or we risk missing inflation. For instance, in the overshoot problem, if the initial kinetic term is too large inflation stops before reaching its attractor solution on which the inflaton should slow-roll.

3.3 The inflationary zoology

The very simple phenomenological model of inflation previously developed satisfies all current observational constraints. But we want to go farther in model-building because new inflation is limited in its predictions. Inflation is only a framework and there are basically an infinity of possible scenarios. We have to check the consistency with particle physics and the consistency with observational data. We can go beyond this simple model exploring different leads. We may modify the kinetic term or the inflaton potential or gravity. Let's first distinguish between two classes of models : small and large field inflation. Either the inflaton is sub-Planckian and $\eta < 0 < \epsilon$ so as to comply with slow-roll, either it is trans-Planckian and quite often $0 < \eta \leq \epsilon$. After giving some examples of both large and small field inflation, we will present different scenarios of inflating universe.

3.3.1 Small-field inflation

In small-field inflation, the field does not evolve much, it moves over a sub-Planckian distance $\Delta\phi < M_p$. Small-field inflation is often associated with spontaneous symmetry breaking where the inflaton field rolls off an unstable equilibrium towards a displaced vacuum, along a Higgs-like potential

$$V(\phi) = V_0 \left(1 - \left(\frac{\phi}{\mu} \right)^2 \right)^2 \quad \text{with } \mu > M_p > \phi \quad (3.23)$$

Generically the dominant term is

$$V(\phi) = V_0 \left(1 - \left(\frac{\phi}{\mu} \right)^p \right) \quad \text{with } p > 1 \quad (3.24)$$

A famously related potential is the Coleman-Weinberg potential

$$V(\phi) = V_0 \left(\frac{1}{4} + \left(\frac{\phi}{\mu} \right)^4 \left(\ln \left(\frac{\phi}{\mu} \right) - \frac{1}{4} \right) \right) \quad (3.25)$$

originally introduced for radiatively induced symmetry breaking in electroweak and grand unified theories.

An interesting feature of small-field inflation models is that one does not expect to detect gravitational waves from inflation. Their amplitude is most probably too small since the tensor-to-scalar ratio

$$r = 16\epsilon = 8 \left(\frac{M_p}{\phi} \right)^2 \left(\frac{\phi}{\mu} \right)^{2p} < 8 \left(\frac{\phi}{\mu} \right)^{2p-2} < 10^{-2} \quad (3.26)$$

for the potential (3.24).

3.3.2 Large-field inflation

In large-field inflation, the inflaton often moves over a large distance down to its minimum at zero. Chaotic inflation is the prototype of large-field inflation, the potential is dominated by a monomial term $\lambda_p \phi^p$ with $\lambda_p \ll M_p^{4-p}$ or an exponential potential. The best example is that of a free massive scalar field (see in the previous subsection 3.2.1). Another example is natural inflation where the inflaton is an axion and the potential is periodic

$$V(\phi) = V_0 \left(\cos \left(\frac{\phi}{\mu} \right) + 1 \right) \quad (3.27)$$

with $\mu > M_p$.

According to Lyth [45], primordial gravitational waves contribution would be detected if

$$r > 0.07 \quad (3.28)$$

which corresponds to the Lyth bound

$$\Delta\phi > 0.46 M_p \quad (3.29)$$

because

$$\frac{\Delta\phi}{M_p} \approx 0.46 \left(\frac{r}{0.07} \right)^{1/2} \quad (3.30)$$

so that large-field models predict that the primordial GWs contribution is detectable. It could be detected by on-earth large interferometers (LIRGO, VIRGO) or future spatial interferometers (LISA or equivalent).

3.4 Multi-field inflation

Up to now, we have exclusively considered single-field inflation models. This was a question of simplicity and minimization of the assumptions. But we can extend inflation to multi-field realizations. As we will see in the next chapter there are sometimes strong motivations for considering multiple scalar fields. As we will see now, an additional field can be a way out of many issues. Though it just adds the question of the origin of this scalar field.

3.4.1 Hybrid inflation

In this model, one scalar field ϕ drives inflation and another scalar field ψ is necessary to end inflation. The inflaton potential is of the form

$$V(\phi, \psi) = \frac{1}{2}m^2\phi^2 + \frac{1}{2}\lambda'\psi^2\phi^2 + \frac{1}{4}\lambda(M^2 - \psi^2)^2 \quad (3.31)$$

For $\phi > \phi_c = \lambda M^2/\lambda'$, ψ is trapped at the minimum $\psi_0 = 0$. Inflation is realized in this false vacuum. When ϕ becomes smaller than the critical value ϕ_c , the ψ field rolls down to one of the new minima $\psi_0 = \pm M$ and inflation ends. Above the critical value ϕ_c , the effective inflaton potential consists of a constant part and a power-law part

$$V(\phi) = V_0 + \frac{1}{2}m^2\phi^2 \quad (3.32)$$

and it is just similar to single-field inflation with $0 < \epsilon < \eta$. The inflaton field does not need to be super-Planckian. A great advantage of this model is that it can be embedded in SUSY or SUGRA theories. And fine-tuning problems can be eliminated. For more details, refer to [46, 47, 48].

3.4.2 Curvaton scenario

In the curvaton scenario, the first scalar field the inflaton is responsible for the phase of cosmic acceleration and the second scalar field the curvaton plays a role at the end of inflation and is responsible for curvature perturbations. The curvaton must be light during inflation and must decay to matter and radiation at the end. There are now attempts to build a supersymmetric model of inflation with a curvaton [49].

3.5 K-inflation

The name k-inflation refers to a theory of inflation where the kinetic term is non-canonical [50, 51]. There are several consistent models of k-inflation among which DBI inflation, which is of special interest for us and which will be discussed extensively in the next chapter. The effective action of those kinds of models can be written generically as

$$S_\phi = \int d^4x \sqrt{-g} \mathcal{P}(\phi, X) \quad (3.33)$$

with $X = \frac{1}{2}g^{\mu\nu}\partial_\mu\phi\partial_\nu\phi$. The inflaton dynamics are governed by the energy density

$$\rho_\phi = -\mathcal{P} + 2X \frac{\partial\mathcal{P}}{\partial X} \quad (3.34)$$

and the pressure

$$p_\phi = \mathcal{P} \quad (3.35)$$

In particular we find that

$$\frac{\partial \mathcal{P}}{\partial X} = \frac{\rho_\phi + p_\phi}{2X} \quad (3.36)$$

In k-inflation the sound speed is non trivial

$$c_s^2 = \frac{\partial p / \partial X}{\partial \rho / \partial X} = \frac{\frac{\partial \mathcal{P}}{\partial X}}{\frac{\partial \mathcal{P}}{\partial X} + 2X \frac{\partial^2 \mathcal{P}}{\partial X^2}} \quad (3.37)$$

The Klein-Gordon equation is given by

$$\frac{\partial \mathcal{P}}{\partial \phi} + \frac{\partial \mathcal{P}}{\partial X} (\ddot{\phi} + 3H\dot{\phi}) + \dot{\phi} \frac{d}{dt} \left(\frac{\partial \mathcal{P}}{\partial X} \right) = 0 \quad (3.38)$$

which can be recast in

$$\ddot{\phi} \left(\frac{\partial \mathcal{P}}{\partial X} + 2X \frac{\partial^2 \mathcal{P}}{\partial X^2} \right) = - \left(\frac{\partial \mathcal{P}}{\partial \phi} - 2X \frac{\partial^2 \mathcal{P}}{\partial \phi \partial X} + 3H\dot{\phi} \frac{\partial \mathcal{P}}{\partial X} \right) \quad (3.39)$$

when expanding the time derivative in the third term. We recover usual canonical inflation for $\mathcal{P} = -X - V(\phi)$. It is generally possible to obtain an equivalent of the slow-roll regime in k-inflation. We can then extend this formalism and build models with multiple kinetically modified fields with the formalism

$$S_\phi = \int d^4x \sqrt{-g} \mathcal{P}(\phi^K, X^{IJ}) \quad \text{with } X^{IJ} = \frac{1}{2} g^{\mu\nu} \partial_\mu \phi^I \partial_\nu \phi^J \quad (3.40)$$

we can generalize previous equations

$$\rho_\phi = -\mathcal{P} + 2X^{IJ} \mathcal{P}_{<IJ>} \quad (3.41)$$

and

$$p_\phi = \mathcal{P} \quad (3.42)$$

and Klein-Gordon equation becomes

$$\ddot{\phi}^J \left(\mathcal{P}_{<IJ>} + \dot{\phi}^L \dot{\phi}^K \mathcal{P}_{<IL>, <JK>} \right) = \mathcal{P}_{,I} - 3H\dot{\phi}^J \mathcal{P}_{<IJ>} - \dot{\phi}^J \dot{\phi}^K \mathcal{P}_{<IJ>, K} \quad (3.43)$$

where $_{,I}$ denotes a derivative with respect to ϕ^I and

$$\mathcal{P}_{<IJ>} = \frac{1}{2} \left(\frac{\partial \mathcal{P}}{\partial X^{IJ}} + \frac{\partial \mathcal{P}}{\partial X^{JI}} \right) \quad (3.44)$$

3.6 Brane inflation

It is only natural to try to build inflationary scenarios derived from superstring theory [52]. But we must face many difficulties to obtain a consistent construction. The obvious advantage of string theory is the plethora of scalar fields

(moduli) which might serve as candidates for the inflaton. An interesting class of stringy inflation is brane inflation. Historically, it was introduced by Dvali and Tye [53] more than a decade ago. In D/anti-D scenarios [54, 55, 56, 57], it is the relative motion of the pair of branes that triggers inflation. The reference paper on the subject is the famous KKLMMT paper [58] (which relies on the previous [59]) where the compactification manifold contains a warped throat described by the Klebanov-Strassler solution (KS) [19]. The KS geometry is a non-compact 10d solution to type IIB supergravity in the presence of background fluxes. The 6d internal space has a tip which is smoothed into a S^3 of finite size. As seen in chapter 2, far from the tip, the geometry is approximatively a cone over the Einstein manifold $T^{1,1}$.

$$ds^2 = h^{-1/2} \eta_{\mu\nu} dx^\mu dx^\nu + h^{1/2} (dr^2 + r^2 ds_{T^{1,1}}^2) \quad (3.45)$$

The background fluxes are such that

$$M = \frac{1}{(2\pi)^2 \alpha'} \int_{S^3} F \gg 1 \quad (3.46)$$

and

$$-K = \frac{1}{(2\pi)^2 \alpha'} \int_B H \gg 1 \quad (3.47)$$

where M and K are two integers and B is the Poincaré-dual to the three-cycle of the S^3 at the tip. The warp factor h is given by

$$h(r) = \frac{27\pi}{4r^2} \alpha'^2 g_s M \left(K + g_s M \left(\frac{3}{8\pi} + \frac{3}{2\pi} \ln \left(\frac{r}{r_{\max}} \right) \right) \right) \quad (3.48)$$

At the location $r = r_{\max}$ the warped throat is smoothly glued to the Calabi-Yau orientifold. One finds that approximately

$$R^4 = \frac{27}{4} \pi g_s N \alpha'^2 \quad (\text{because } v_{T^{1,1}} = 16/27 \text{ [60]}) \quad \text{and } N = MK \quad (3.49)$$

The exact derivation and understanding of all those terms is well beyond the scope of this thesis. But the important thing to know is that inflation can be achieved from the motion of a D3 brane in the KS region with an additional anti-D3 brane at the tip of the conifold (thus its energy is minimal). The attraction between the brane and anti-brane in the throat is described by the Coulomb potential and is roughly in r^{-4} (since it is in 6d). The potential is *a priori* very flat. The work of KKLMMT was precisely to rule on how flat this potential could remain when including volume stabilization effects. They investigated two scenarios of volume stabilization: superpotential stabilization and Kahler stabilization. The challenge is still to reproduce slow-roll. Volume stabilization tends to steepen dramatically the inflaton potential. Moreover the interaction of the inflaton with other moduli might stop inflation. The many possible choices of

fluxes and compactifications enable discrete fine-tuning. For very specific choices of the background and of the stabilization mechanism, one can find a sufficiently flat inflaton potential.

From this initially valid and thoroughly examined scenario of brane inflation, many others were derived. The one of interest to us, DBI inflation, will be detailed in chapter 6. It is remarkable because DBI inflation occurs even when the potential is very steep. An analogous case is [61] where warm D/\bar{D} inflation is investigated and strong dissipative effects are expected to counterbalance the inflaton fast motion.

There are many examples of inflation theories inspired by open or closed string theory. As we have just said the inflaton can be the radial distance between a D brane and an anti D-brane, it can also be the dilaton, or an axion or a Kahler modulus [62, 63, 64, 65, 66] or pretty much any other modulus.

The physics of early inflation is quite similar to the physics of late acceleration so it is tempting to try to find a unique theory (maybe with a unique scalar field) which could explain both. In the context of string theory, galileons were first introduced to explain cosmic acceleration through modified gravity theories where the graviton becomes massive in the infra-red. Then it was noticed that galileon-like scalar fields could drive inflation. The main challenge in galileon inflation (or G-inflation) [67, 68, 69, 70, 71] is to get rid of ghosts.

3.7 Tests for inflation

We have seen a few examples of inflationary classes and models. But there is literally a huge number of plausible models. Observations may help discriminate among different models of inflation and thus different high-energy theories or at least it may help constraining the theory parameters. This is one of the main motivation for studying inflation. The best thing we can do is to investigate as many consistent models as possible and identify their specific observational predictions as a preliminary work before the production of future data. All those models are pretty much identical at linear order so one must go to higher-order predictions. The quantities of interest are : the amplitude of scalar perturbation and the spectral index (the scale dependence of scalar modes), the amplitude of tensor modes (the detection of primordial CMB B-modes would be virtually impossible to explain by anything other than inflationary gravitational waves [72]. Moreover the tensor amplitude is directly linked with the energy scale of inflation) and then the measurement of f_{NL} for different shapes of non-Gaussianities.

We have to keep in mind that inflation is only a theory and it has not been proven that the universe underwent this hypothetical phase. Though it is reasonable to say that it is the best (let say minimal) theory to explain temperature fluctuations of the CMB. Anyway it is difficult to select a good scenario among the plethora of models, and this is without saying anything about the embedding

of the model in a more generic high-energy theory.

Perturbation theory

“Toute matière commence par un grand dérangement spirituel”, A. Artaud

For a review on the subject, [73] is a judicious reading. [1] is very pedagogical.

4.1 Basics on usual perturbation theory

The motivation is to understand the formation of large scale structures from small initial density fluctuations.

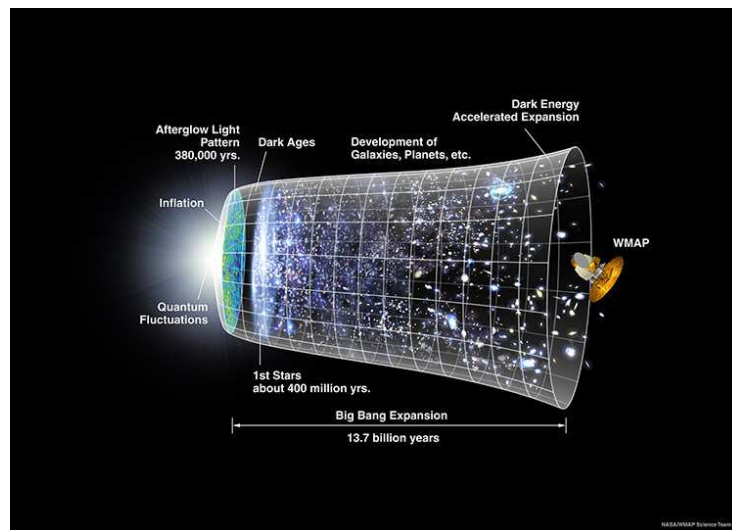


Figure 4.1: Timeline of the Universe (credit: NASA/WMAP Science Team). Small initial density perturbations as seen in the CMB are amplified through gravitational instability. Baryons follow the collapse of the dark matter halos to form the first stars and the first galaxies in their midst.

We trust that all cosmological quantities can be expanded in a Taylor way as a sum of a background value plus smaller and smaller perturbations. This approach is very general in physics but it is here a bit trickier than usual since we must take into account the gravitational dynamics. Those fluctuations are necessarily present due to the quantum nature of the fields. Depending on what we are investigating the linear perturbation theory can be sufficient or not. Most of the time it is. Though, for a strictly meticulous study, one should always check that higher order contributions are negligible. In this chapter we will restrain to the linear (first order perturbation) theory.

Generically, the perturbed metric is expressed as :

$$ds^2 = a(\eta)^2(-1 + 2A)d\eta^2 + 2B_i dx^i d\eta + (\gamma_{ij} + h_{ij})dx^i dx^j \quad (4.1)$$

where $\gamma_{ij} = \delta_{ij}$. In the scalar-vector-tensor (SVT) decomposition, a vector is written as

$$B^i = D^i B + \bar{B}^i \quad \text{with } D^i \bar{B}_i = 0 \quad (4.2)$$

The vector is decomposed into a scalar and a divergenceless vector. It is exactly the same thing we do when we write a velocity in terms of the potential and the vorticity field. Similarly, the decomposition of a tensor gives

$$h_{ij} = 2C\delta_{ij} + 2D_i D_j E + 2D_{(i} \bar{E}_{j)} + 2\bar{E}_{ij} \quad \text{with } D_i \bar{E}^{ij} = 0 \quad \text{and } \bar{E}_i^i = 0 \quad (4.3)$$

This SVT decomposition is very useful because scalar perturbations, vector perturbations and tensor perturbations get all decoupled and can be studied separately.

Now we compute the perturbation of the perfect fluid.

$$\delta T_{\mu\nu} = (\delta\rho + \delta p)\bar{u}_\mu \bar{u}_\nu + \delta p \bar{g}_{\mu\nu} + 2(\rho + p)\bar{u}_{(\mu} \delta u_{\nu)} + p\delta g_{\mu\nu} + a^2 p \pi_{\mu\nu} \quad (4.4)$$

where $\pi_{\mu\nu}$ is the anisotropic stress tensor. Without losing in generality we can choose $\pi_{00} = \pi_{0i} = 0$

$$\pi_{ij} = \left(D_i D_j - \frac{1}{3} \delta_{ij} \Delta \right) \bar{\pi} + D_{(i} \bar{\pi}_{j)} + \bar{\pi}_{ij} \quad (4.5)$$

In most cases, the perturbed fluid is also a perfect fluid and this anisotropic stress tensor is zero. The 4-velocity is

$$u^\mu = \bar{u}^\mu + \delta u^\mu \quad (4.6)$$

with the normalization

$$u^\mu u_\mu = -1 \quad (4.7)$$

$$\bar{u}^\mu = (-a^{-1}, 0, 0, 0) \quad (4.8)$$

and we find that

$$\delta u^\mu = a^{-1}(-A, v^i) \quad \text{with } v_i = D_i v + \bar{v}_i \quad (4.9)$$

So finally, the components of the energy-momentum tensor are :

$$\delta T_{00} = \rho a^2 \left(\frac{\delta \rho}{\rho} + 2A \right) \quad (4.10)$$

$$\delta T_{0i} = -\rho a^2 \left((1+w)(D_i v + \bar{v}_i) + D_i B + \bar{B}_i \right) \quad (4.11)$$

$$\delta T_{ij} = p a^2 \left(h_{ij} + \frac{\delta p}{p} \delta_{ij} + \pi_{ij} \right) \quad (4.12)$$

For later use we also write the components

$$\delta T_0^0 = -\delta \rho \quad (4.13)$$

$$\delta T_i^0 = -\rho \left((1+w)(D_i v + \bar{v}_i) + D_i B + \bar{B}_i \right) \quad (4.14)$$

We define the entropy perturbation Γ such that

$$\delta p = c_s^2 \delta \rho + p \Gamma \quad (4.15)$$

Most often it can be neglected in a universe dominated by a single-field. Entropy perturbations are relevant when taking into account several fluids (see [74]).

It is necessary to fix the gauge. The non-physical degrees of freedom come from the choice of system of coordinates, for the unperturbed and perturbed space-times. We need to build gauge-invariant quantities. Under the transformation

$$x^\mu \rightarrow x^\mu - \xi^\mu \quad \text{with } \xi^\mu = (T, L^i = D^i L + \bar{L}^i) \quad (4.16)$$

a scalar is transformed as

$$\delta Q \rightarrow \delta Q + \mathcal{L}_\xi \bar{Q} \quad (4.17)$$

and only the quantities with zero Lie derivative

$$\mathcal{L}_\xi \bar{Q} = 0 \quad \forall \xi$$

are gauge-invariant (Stewart-Walker lemma). The metric perturbation transforms as

$$\delta g_{\mu\nu} \rightarrow \delta g_{\mu\nu} + \mathcal{L}_\xi \bar{g}_{\mu\nu} \quad (4.18)$$

which gives :

$$A \rightarrow A + T' + \mathcal{H}T \quad (4.19)$$

$$B \rightarrow B - T + L' \quad (4.20)$$

$$C \rightarrow C + \mathcal{H}T \quad (4.21)$$

$$E \rightarrow E + L \quad (4.22)$$

$$\bar{B}^i \rightarrow \bar{B}^i + \bar{L}^{i'} \quad (4.23)$$

$$\bar{E}^i \rightarrow \bar{E}^i + \bar{L}^i \quad (4.24)$$

$$\bar{E}^{ij} \rightarrow \bar{E}^{ij} \quad (4.25)$$

There seems to be 10 degrees of freedom, but only 6 are physically relevant. We may define the following gauge-invariant quantities

$$\psi = -C - \mathcal{H}(B - E') \quad (4.26)$$

$$\varphi = A + \mathcal{H}(B - E') + (B - E')' \quad (4.27)$$

$$\varphi^i = \bar{E}^{i'} - \bar{B}^i \quad (4.28)$$

$$\bar{E}^{ij} \quad (4.29)$$

which do not depend on L^i or T .

In our work, we will often choose the Newtonian gauge: $B = 0$, $E = 0$ and $\bar{B}_i = 0$. In this case, the Bardeen potentials $A = \varphi$ and $-C = \psi$ can be equal when the scalar component of the anisotropic stress tensor is zero. There are lots of other common gauges: flat-slicing, synchronous, comoving... The choice of gauge is guided by a concern for the simplicity of the calculations.

The next step is to derive the perturbed Einstein equations. We compute independently the S, V and T parts. The tensor part is of interest for the study of gravitational waves during inflation. In a flat universe, the equation for the tensor mode is

$$u_T'' + \left(-\Delta - \frac{a''}{a}\right) u_T = \kappa a^2 p \bar{\pi}_{ij} \quad (4.30)$$

where $u_T = a \bar{E}_{ij} = a \sum_{\lambda} \bar{E}_{\lambda} \epsilon_{ij}^{\lambda}$. The GWs have been expanded into their polarization tensors. Note that in most cases, the source term is null and there is no coupling with any of the fields (inflaton or matter).

The vector modes are not very interesting. They play no role in the formation of large-scale structures because the perturbations are diluted by the expansion of the universe.

For the scalar modes we get six relevant equations : two constraint equations (the analogue of Poisson equation and the equation relating A and C), two fluid equations (a conservation equation and an Euler equation) and two equations of evolution, one of which is

$$A'' + 3\mathcal{H}(1 + c_s^2)A' + (2\mathcal{H}' + \mathcal{H}^2(1 + 3c_s^2))A - c_s^2 \Delta A = \frac{\kappa}{2} a^2 p \Gamma \quad (4.31)$$

in a flat universe when neglecting the scalar component of the anisotropic stress tensor. This equation can be recast in

$$u_s'' - \left(\frac{\theta''}{\theta} + c_s^2 \Delta\right) u_s = \frac{\kappa}{3} \frac{\theta}{\mathcal{H}} a^4 p \Gamma \quad (4.32)$$

where

$$\theta = \frac{\mathcal{H}}{a} \left(\frac{2}{3}(\mathcal{H}^2 - \mathcal{H}')\right)^{-1/2} \quad \text{and} \quad u_s = \frac{2}{3} \frac{a^2 \theta}{\mathcal{H}} A \quad (4.33)$$

4.2 Perturbations in k-inflation

Usually, matter is absent during inflation and only the inflaton field

$$\phi \rightarrow \phi(t) + \delta\phi(t, \mathbf{x}) \quad (4.34)$$

and the metric have to be perturbed. If several dynamical fields are present during inflation, it leads to entropy (or isocurvature) perturbations. A specific example of inflation coupled to matter will be studied in chapter 9. Following the Mukhanov & Garriga approach [75], we derive the perturbation equations and recast them in a simple and convenient form for any model of single-field k-inflation with a lagrangian $\mathcal{P}(\phi, X)$.

We choose the Newtonian (or longitudinal) gauge, in which the metric takes the form

$$ds^2 = -(1 + 2\varphi_N)dt^2 + a^2(t)(1 - 2\varphi_N)\delta_{ij}dx^i dx^j \quad (4.35)$$

We write two perturbed Einstein equations for the 0_0 component and the 0_i component. First the perturbed Einstein tensor components are

$$\delta G^0_0 = -2 \left(\frac{\Delta\varphi_N}{a^2} - 3H(\dot{\varphi}_N + H\varphi_N) \right) \quad (4.36)$$

and

$$\delta G^0_i = -2 \partial_i (\dot{\varphi}_N + H\varphi_N) \quad (4.37)$$

The fluid 4-velocity is defined as

$$u_\mu = \frac{\partial_\mu \phi}{\sqrt{g^{\alpha\beta} \partial_\alpha \phi \partial_\beta \phi}} \quad (4.38)$$

With (4.9, 4.13, 4.14) in the Newtonian gauge, we find that the perturbed energy-momentum tensor components are respectively

$$\delta T^0_0 = -\delta\rho \quad (4.39)$$

and

$$\delta T^0_i = \partial_i q \quad \text{with } q = -(\rho + p) \frac{\delta\phi}{\dot{\phi}} \quad (4.40)$$

The energy density perturbation is

$$\delta\rho = \frac{\partial\rho}{\partial\phi} \delta\phi + \frac{\partial\rho}{\partial X} \delta X \quad (4.41)$$

The conservation equation for the total energy density gives

$$\dot{\rho} = -3H(\rho + p) = \frac{\partial\rho}{\partial\phi} \dot{\phi} + \frac{\partial\rho}{\partial X} \dot{X} \quad (4.42)$$

together with (3.36, 3.37) comes

$$\delta\rho = -3H(\rho + p)\frac{\delta\phi}{\dot{\phi}} + \frac{\rho + p}{2c_s^2 X} \left(\delta X - \dot{X} \frac{\delta\phi}{\dot{\phi}} \right) \quad (4.43)$$

and since $\delta X = -2\varphi_N X - \dot{\phi} \delta\phi$ we find that

$$\delta\rho = -3H(\rho + p)\frac{\delta\phi}{\dot{\phi}} + \frac{\rho + p}{c_s^2} \left(\frac{d}{dt} \left(\frac{\delta\phi}{\dot{\phi}} \right) - \varphi_N \right) \quad (4.44)$$

So finally our two coupled perturbed Einstein equations are :

$$\dot{\varphi}_N + H\varphi_N = 4\pi G(\rho + p)\frac{\delta\phi}{\dot{\phi}} \quad (4.45)$$

$$\frac{d}{dt} \left(\frac{\delta\phi}{\dot{\phi}} \right) = \varphi_N + \frac{c_s^2}{4\pi G a^2 (\rho + p)} \Delta\varphi_N \quad (4.46)$$

where the first equation has been used to simplify the second one. We define the gauge-invariant comoving curvature perturbation

$$\mathcal{R} = \varphi_N - \frac{H}{\rho + p} q = \varphi_N + H \frac{\delta\phi}{\dot{\phi}} \quad (4.47)$$

From the previous paragraph, we know that $\delta\phi$ transforms as $\delta\phi \rightarrow \delta\phi + \phi'T$ and also that $\varphi_N = -C \rightarrow \varphi_N - \mathcal{H}T$ so we can check that the combination in \mathcal{R} gives a gauge-invariant variable. The name ‘‘comoving’’ is given to this quantity because it reduces to $-C$ in the comoving gauge where $\delta\phi = 0$. The time derivative of the comoving curvature perturbation is

$$\dot{\mathcal{R}} = \dot{\varphi}_N + \dot{H} \frac{\delta\phi}{\dot{\phi}} + H \frac{d}{dt} \left(\frac{\delta\phi}{\dot{\phi}} \right) \quad (4.48)$$

One useful background equation is

$$\dot{H} = -4\pi G(\rho + p) \quad (4.49)$$

which is obtained from the derivative of the Friedmann equation combined with the conservation equation. Reporting this in (4.48) leads to a nice cancellation thanks to (4.45) and we find that

$$\dot{\mathcal{R}} = \frac{c_s^2 H}{4\pi G a^2 (\rho + p)} \Delta\varphi_N \quad (4.50)$$

We realize that the comoving curvature perturbation is constant for large-scales. So outside the horizon $k \ll aH$, the curvature perturbation is nearly constant. We derive a second-order differential equation for the quantity \mathcal{R}

$$\ddot{\mathcal{R}} + \left(H - \frac{\dot{C}}{C} - \frac{\dot{H}}{H} \right) \dot{\mathcal{R}} - \frac{c_s^2 \Delta}{a^2} \mathcal{R} = 0 \quad (4.51)$$

where C is the operator

$$C = \frac{c_s^2 H \Delta}{4\pi G a^2 (\rho + p)} \quad (4.52)$$

Going to conformal time

$$\mathcal{R}'' - \frac{(4\pi G H C)'}{4\pi G H C} \mathcal{R}' + c_s^2 \Delta \mathcal{R} = 0 \quad (4.53)$$

So as to eliminate the first-order time derivative, we change variable to the Mukhanov-Sasaki variable

$$v = -z\mathcal{R} \quad (4.54)$$

The variable v becomes an operator in second quantization and its expansion in Fourier modes is

$$v(x, \eta) = \int \frac{d^3k}{(2\pi)^{3/2}} (\hat{a}_k v_k(\eta) e^{i c_s k \cdot x} + \hat{a}_k^\dagger v_k^*(\eta) e^{-i c_s k \cdot x}) \quad (4.55)$$

The wronskian normalization is

$$v_k v_k'^* - v_k^* v_k' = i \quad (4.56)$$

where v' is the conjugate momentum of v . The variable z is

$$z = \exp \left(-\frac{1}{2} \int \frac{\left(\frac{c_s^2 H^2}{a^2 (\rho + p)} \right)'}{\frac{c_s^2 H^2}{a^2 (\rho + p)}} d\eta \right) = \left| \frac{c_s^2 H^2}{a^2 (\rho + p)} \right|^{-1/2} = \frac{a(\rho + p)^{1/2}}{c_s H} \quad (4.57)$$

We obtain the perturbation equation for the Fourier mode of momentum k

$$v_k'' + \left(c_s^2 k^2 - \frac{z''}{z} \right) v_k = 0 \quad (4.58)$$

The perturbation equation is similar to a Schrödinger equation.

We will now focus on canonical standard inflation $c_s = 1$,

$$z = \frac{a\dot{\phi}}{H} \quad (4.59)$$

and the perturbation equation is of the form

$$v_k'' + \left(k^2 - \frac{\nu^2 - 1/4}{\eta^2} \right) v_k = 0 \quad (4.60)$$

The general solution is a combination of the Hankel functions of index ν of first and second kind.

$$v_k = \sqrt{-\eta} \left(A(k) H_\nu^{(1)}(-k\eta) + B(k) H_\nu^{(2)}(-k\eta) \right) \quad (4.61)$$

We need to evaluate the value of ν^2 . It is useful to express the potential part in terms of the slow-roll coefficients. Using the definition (3.17), we find

$$\frac{z''}{z} = \mathcal{H}^2 \left(2 - \epsilon_1 + \frac{3}{2}\epsilon_2 + \mathcal{O}(\epsilon^2) \right) \quad (4.62)$$

so that

$$\nu^2 = \frac{9}{4} - \epsilon_1 + \frac{3}{2}\epsilon_2 + \mathcal{O}(\epsilon^2) \quad (4.63)$$

In a de Sitter universe the index is $\nu^2 = 9/4$ and the Mukhanov-Sasaki variable is

$$v_k(\eta) = A(k)e^{-ik\eta} \left(1 + \frac{1}{ik\eta} \right) + B(k)e^{ik\eta} \left(1 - \frac{1}{ik\eta} \right) \quad (4.64)$$

We often assume that the initial state is a Bunch-Davies vacuum $v_k \rightarrow e^{-ik\eta}/\sqrt{2k}$. It corresponds to a vacuum state which minimizes the energy for each mode in its infinite de Sitter past $\eta \rightarrow -\infty$. We are interested in the evolution of both sub-Hubble $k \gg aH$ and super-Hubble $k \ll aH$ modes. The perturbation equation (4.60) can be studied in both limits. Super-Hubble modes are frozen and an initially sub-Hubble mode oscillates as its wavelength grows and then freezes when it becomes super-Hubble. If c_s is non trivial (see equations 4.58 and 4.30), the sound horizon is different from the Hubble horizon and the scalar modes freeze out at sound horizon crossing whereas the tensor modes freeze out at Hubble horizon crossing.

In a universe which first underwent a phase of cosmic acceleration before being radiation and matter-dominated, small scales are the last to exit the horizon but the first to re-enter (see figure 4.2). It is the exact opposite for large scales. Perturbations which are about the same size as our horizon today exited the horizon during inflation about 60 e-folds before the end of inflation. Therefore only the last 60 e-folds of inflation are accessible to us. Perturbations which exited the horizon earlier than that are still larger than our horizon today.

The quantity of interest to us is the comoving curvature perturbation \mathcal{R} or the curvature perturbation on uniform-density hypersurfaces ζ .

$$\zeta = -\varphi_N - H \frac{\delta\rho}{\dot{\rho}} \quad (4.65)$$

The variable ζ reduces to C when $\delta\rho = 0$.

$$-\zeta - \mathcal{R} = H \left(\frac{\delta\rho}{\dot{\rho}} - \frac{\delta\phi}{\dot{\phi}} \right) = H \frac{\rho + p}{c_s^2 \dot{\rho}} \left(\frac{d}{dt} \left(\frac{\delta\phi}{\dot{\phi}} \right) - \varphi_N \right) \quad (4.66)$$

and from (4.46)

$$-\zeta - \mathcal{R} = \frac{\Delta\varphi_N}{3a^2\dot{H}} \quad (4.67)$$

In the large scale limit (modes with $k \rightarrow 0$), one finds the equality of the two quantities.

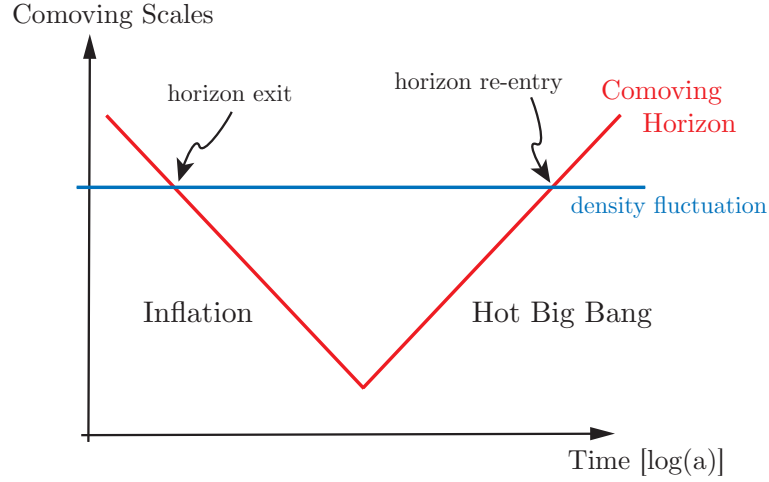


Figure 4.2: Evolution of perturbations in our universe. While comoving scales remain constant the comoving Hubble radius evolves, it first shrinks during inflation and then grows. Figure from [26].

We will see in chapter 5 how inflation imprints on the CMB and how to relate CMB observations to the spectrum of curvature perturbation. We need to define some relevant quantities

4.2.1 Interesting quantities

The Fourier transform of the two-point function gives the spectrum of curvature perturbation

$$\langle \mathcal{R}_{\mathbf{k}} \mathcal{R}_{\mathbf{k}'} \rangle = (2\pi)^3 \delta(\mathbf{k} + \mathbf{k}') \mathcal{P}_R \quad (4.68)$$

$$\Delta_{\mathcal{R}}^2 = \frac{k^3}{2\pi^2} \mathcal{P}_R(k) = \frac{k^3}{2\pi^2} \frac{|v_k|^2}{|z|^2} \quad (4.69)$$

where each mode is evaluated at horizon crossing. The spectral index gives the scale dependence of the scalar power spectrum

$$n_s - 1 = \frac{d \ln \Delta_{\mathcal{R}}^2}{d \ln k} \quad (4.70)$$

We may also define the running of the spectral index :

$$\alpha_s = \frac{dn_s}{d \ln k} \quad (4.71)$$

We define as well the power spectrum of the tensor perturbation

$$\Delta_T^2 = \frac{k^3}{2\pi^2} \frac{64\pi}{M_p^2} \left| \frac{u_T}{a} \right|^2 \quad (4.72)$$

where each polarization contributes equally. Similarly for tensor modes,

$$n_T = \frac{d \ln \Delta_T^2}{d \ln k} \quad (4.73)$$

and

$$\alpha_T = \frac{dn_T}{d \ln k} \quad (4.74)$$

The tensor to scalar ratio is another key quantity

$$r = \frac{\mathcal{P}_T}{\mathcal{P}_R} \quad (4.75)$$

With some knowledge on the Hankel functions we find that the solution of the perturbation equation which tends to a Bunch-Davies vacuum initially is

$$v_k(\eta) = \frac{\sqrt{-\pi\eta}}{2} i^{\nu+1/2} H_\nu^{(1)}(-k\eta) \quad (4.76)$$

Its limit is

$$v_k(\eta \rightarrow 0) = \frac{1}{\sqrt{2k}} (-k\eta)^{-\nu+1/2} 2^{\nu-3/2} i^{\nu+1/2} \frac{\Gamma(\nu)}{\Gamma(3/2)} \quad (4.77)$$

so that

$$\Delta_{\mathcal{R}}^2 \sim \frac{1}{2\pi^2} \left(\frac{k}{aH} \right)^{3-2\nu} \left| \frac{H^4}{\dot{\phi}^2} \right|_{k=aH} \quad (4.78)$$

in a nearly de Sitter situation. We use that $aH \sim -1/\eta$. To find the dependence of the spectral index and the other quantities on the slow-roll parameters in canonical inflation from (4.63), the calculation is non-trivial and must be carried out very cautiously.

$$n_s - 1 = -2\epsilon_1 - \epsilon_2 \quad (4.79)$$

$$\alpha_s = -2\epsilon_1\epsilon_2 - \epsilon_2\epsilon_3 \quad (4.80)$$

$$n_T = -2\epsilon_1 \quad (4.81)$$

$$\alpha_T = -2\epsilon_1\epsilon_2 \quad (4.82)$$

$$r = 16\epsilon_1 \quad (4.83)$$

It expresses the deviation from the perfect Harrison Zel'dovich spectrum. Of course, those quantities are expected to be rather small but we will discuss with more precision in chapter 5 the constraints derived from the CMB on those quantities.

4.2.2 Non-Gaussianities

With the refined precision of the CMB data, information on the bispectrum are obtained. As a first approximation the CMB is gaussian, but only at the first

level of approximation. The Fourier transform of the three-point function, the bispectrum, is non-zero

$$\langle \mathcal{R}_{k_1} \mathcal{R}_{k_2} \mathcal{R}_{k_3} \rangle = (2\pi)^3 \delta(\mathbf{k}_1 + \mathbf{k}_2 + \mathbf{k}_3) \mathcal{B}_R \quad (4.84)$$

They are different ways of characterizing the degree of non-Gaussianity. We use $f_{\text{NL}}^{\text{local}}$ to parametrize non-gaussianities as a non-linear correction to a purely gaussian perturbation.

$$\mathcal{R}(x) = \mathcal{R}_g(x) + \frac{3}{5} f_{\text{NL}}^{\text{local}} (\mathcal{R}_g(x)^2 - \langle \mathcal{R}_g(x)^2 \rangle) \quad (4.85)$$

For arbitrary shape functions, we define the generalized f_{NL} parameter

$$f_{\text{NL}} = \frac{5}{18} \frac{\mathcal{B}_R(k, k, k)}{\mathcal{P}_R(k)^2} \quad (4.86)$$

There are different typical shapes : squeezed limit, equilateral, folded. The shape function is defined as

$$S(k_1, k_2, k_3) = N(k_1 k_2 k_3)^2 \mathcal{B}_R(k_1, k_2, k_3) \quad (4.87)$$

where $N(k_1 k_2 k_3)$ is a normalization factor. The two most common shapes are :

$$S^{\text{local}}(k_1, k_2, k_3) \propto \frac{K_3}{K_{111}} \quad (4.88)$$

$$S^{\text{equil}}(k_1, k_2, k_3) \propto \frac{\tilde{k}_1 \tilde{k}_2 \tilde{k}_3}{K_{111}} \quad (4.89)$$

with the notations defined in [76]

$$K_p = \sum_i (k_i)^p \quad (4.90)$$

$$K_{pq} = \frac{1}{\Delta_{pq}} \sum_{i \neq j} (k_i)^p (k_j)^q \quad (4.91)$$

$$K_{pqr} = \frac{1}{\Delta_{pqr}} \sum_{i \neq j \neq l} (k_i)^p (k_j)^q (k_l)^r \quad (4.92)$$

$$\tilde{k}_i = K_1 - 2k_i \quad (4.93)$$

with $\Delta_{pq} = 1 + \delta_{pq}$ and $\Delta_{pqr} = \Delta_{pq}(\Delta_{qr} + \delta_{pr})$ (no summation).

There is an important property of the non-gaussianities worth mentioning : Maldacena's theorem, which states that in single-field inflation, non-Gaussianities in the squeezed limit are suppressed by a factor of $(1 - n_s)$

$$\lim_{k_3 \rightarrow 0} \langle \mathcal{R}_{k_1} \mathcal{R}_{k_2} \mathcal{R}_{k_3} \rangle = (2\pi)^3 \delta(\mathbf{k}_1 + \mathbf{k}_2 + \mathbf{k}_3) (1 - n_s) \mathcal{P}_R(k_1) \mathcal{P}_R(k_3) \quad (4.94)$$

Should we discover non-Gaussianities in the squeezed limit, all single-field inflation models would be ruled out.

Current constraints both from the CMB and the Sloan Digital Sky Survey (SDSS) ([77, 78], see also [79]) are

$$-4 < f_{\text{NL}}^{\text{local}} < +70 \text{ at 95\% CL} \quad (4.95)$$

$$-125 < f_{\text{NL}}^{\text{equil}} < +435 \text{ at 95\% CL} \quad (4.96)$$

Non-Gaussianities are extremely important because they are model-dependent distinguishable features.

The Cosmic Microwave Background Radiation

“Il faut se résigner à n’avoir qu’une pensée d’homme, à mesurer l’univers avec ce millimètre”, H. Bazin

A good text book on the subject is [80].

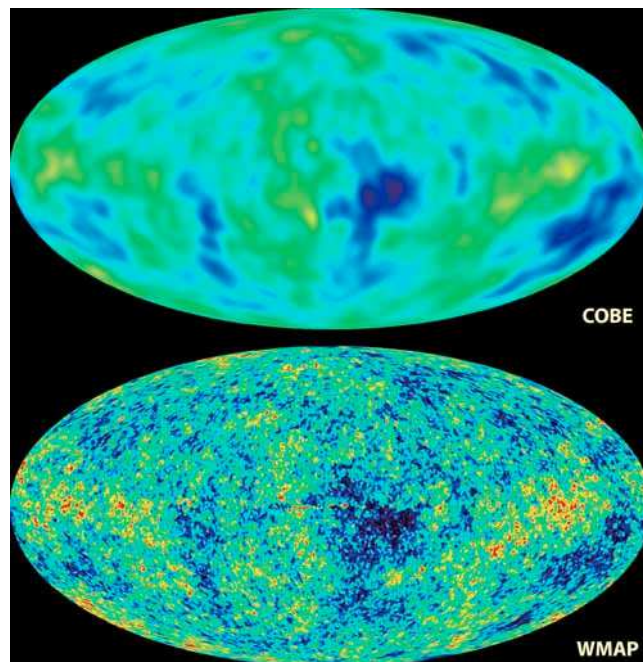


Figure 5.1: Anisotropies in the CMB temperature viewed by COBE and WMAP. Colors indicate “warmer” (yellow, red) and “cooler” (dark blue) spots. The signal from our galaxy has been subtracted using the multi-frequency data.

5.1 History

The Cosmic Microwave Background Radiation, CMBR in short, was discovered fortuitously by Penzias and Wilson in 1965 with their radio-telescope. They received the Nobel prize for their contribution in 1978. But the CMBR was predicted years before, in 1948, by Alpher, Gamow and Hermann who had estimated the background temperature at 5 K. The measured temperature today is

$$T_0 = 2.725 \text{ K} \quad (5.1)$$

Three satellites have been launched to measure the CMBR temperature, first COBE (the COsmic Background Explorer, NASA) in 1989, whose results were rewarded by a Nobel prize to Smoot and Mather, then WMAP (Wilkinson Microwave Anisotropy Probe, NASA) in 2001 and Planck (ESA) in 2009 [81]. The community is looking forward to the data release of Planck. Last January, the Planck collaboration published their first results [82]. They have compiled a catalog of compact sources, it also includes a sample of galaxy clusters detected through the Sunyaev-Zel'dovich effect and a list of cold molecular cloud cores distributed throughout the Milky Way. Results on CMB temperature anisotropies have not yet been obtained. Planck's improvements compared to its predecessors are a higher angular resolution and a better sensitivity. Planck satellite exceeds the expectations from its specifications and should run longer than initially planned.

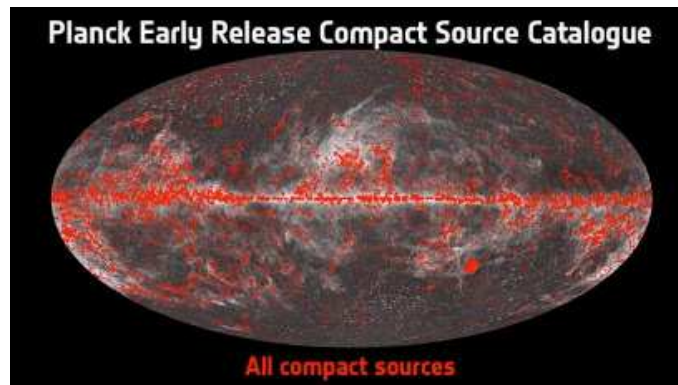


Figure 5.2: This image illustrates the position on the sky of all compact sources detected by Planck during its first all-sky survey and listed in the Early Release Compact Source Catalog (ERCSC). The ERCSC contains more than 15,000 unique compact sources. These sources have been extracted from the individual lists of sources detected at each of the frequencies probed by Planck. The size of the spots displayed in the image reflects the brightness of the sources.

5.2 Physics

The CMBR is the bath of photons from the surface of last-scattering we detect today. Those photons were the first free-moving photons after recombination. The CMBR is equivalent to the radiation from an almost perfect black body with a peak temperature redshifted by the expansion of the universe. This temperature is roughly the same in any direction. Thanks to the COBE mission, it has been realized that there are some colder and some hotter than average spots in the sky.

A sky map of the CMB temperature fluctuations can be fully characterized by an infinite series of correlation functions. Our first and main source of information is the 2-point correlation function (temperature autocorrelation function, we will refer to it as the CMB spectrum). A purely Gaussian spectrum is expected to give only even number-point non-zero correlation functions, all of which can be expressed in terms of the 2-point correlation function. So the CMB bispectrum is a test of non-Gaussian contributions. Since the CMBR is polarized, we could in theory extract more information from the autocorrelation of E and B modes or from cross-correlations. Planck CMBPol mission should provide a precise polarization map of the sky. If the B-mode is detected it would give observational proof of primordial gravitational waves. As a first approximation, the anisotropies are nearly Gaussian, nearly scale-invariant and nearly adiabatic. And they are correlated over large scales. Measurements of the deviation of the CMB from the ideal homogeneity, gaussianity, adiabaticity and scale-invariance give precious information on the primordial universe, not only on recombination but also on the inflationary phase.

Inflationary perturbations (curvature perturbations) are linked to the density perturbations at recombination thus to the CMB temperature inhomogeneities. As explained in chapter 4, the scales we observe today were inside the Hubble radius at the beginning of inflation and exited the Hubble radius between 40 and 60 e-folds before the end of inflation. Small scales exit the Hubble radius last and re-enter first (hence during the radiation-dominated era). On the contrary the largest scales re-enter during matter-dominated era. On large scales, the comoving curvature perturbation coincides with the curvature perturbation on uniform density hypersurfaces and we know the evolution of this ζ in a universe dominated by any fluid with any equation of state w .

The transfer function between the primordial scalar and tensor power spectra and the CMB angular power spectrum is easier to calculate for large scales. Large scales were still outside the Hubble radius at recombination and thus were not affected by the sub-horizon evolution (we say they were frozen, see 4.2). Their evolution is roughly only determined by the Sachs-Wolfe effect. It is determined by the gravitational potential at the time of recombination

$$\frac{\delta T}{T} \sim \frac{1}{3} A \tag{5.2}$$

This relation is central, it gives the correspondence between the temperature fluctuation and the Newtonian potential. The physics of photons propagating in an inhomogeneous media include several effects. The Doppler effect is corrected when mapping the CMB temperature fluctuations map. There are some subtler but sub-dominant effects such as the Sunyaev-Zeldovich effect (Compton diffusion on ionized gas in galaxy clusters).

On the contrary small scales have a much more complex evolution. They provide information on the cosmological parameters. Angular scales smaller than 1 degree, which is the angular scale corresponding to the Hubble radius at recombination, correspond to very large l . Small-scales perturbations are partly suppressed by the thickness of the surface of last-scattering.

The transfer function which relates \mathcal{R} to δT is usually computed numerically. The evolution through reheating can be modeled by the evolution in a universe dominated by a fluid with a well-fitting effective equation of state w . There is no need of a better microphysical understanding of reheating. Assuming a model of inflation and specifying the inflaton potential, we can derive the CMB spectra and observables using numerical codes. We always assume that perturbations are coherent as predicted by inflationary scenarios. The reverse procedure is also carried out numerically. From the CMB temperature map we extract the CMB spectrum and bispectrum and derive constraints on cosmological and inflationary parameters. For example, first-year results from WMAP and implications for inflation are found in [83].

The relative temperature measured from a photon from the direction \mathbf{n} is decomposed in spherical harmonics $Y_{lm}(\mathbf{n}) = Y_{lm}(\theta, \varphi)$ on the celestial sphere

$$\frac{\delta T}{T}(\mathbf{n}) = \sum_{l=1}^{\infty} \sum_{m=-l}^l a_{lm} Y_{lm}(\theta, \varphi) \quad (5.3)$$

The 2-point correlation function is

$$\left\langle \frac{\delta T}{T}(\mathbf{n}) \frac{\delta T}{T}(\mathbf{n}') \right\rangle = \sum_{l,l',m,m'} \langle a_{lm} a_{l'm'}^* \rangle Y_{lm}(\mathbf{n}) Y_{l'm'}(\mathbf{n}') \quad (5.4)$$

$$= \sum_l C_l \sum_m Y_{lm}(\mathbf{n}) Y_{l'm'}(\mathbf{n}') \quad (5.5)$$

$$= \frac{1}{4\pi} \sum_{l=0}^{\infty} (2l+1) C_l P_l(\mathbf{n} \cdot \mathbf{n}') \quad (5.6)$$

where the P_l are the Legendre polynomials. Anisotropies in the angular power spectrum are typically of order

$$\frac{\delta T}{T} = 10^{-5} \quad (5.7)$$

so that

$$\mathcal{R} \sim 10^{-5} \text{ and } \zeta \sim 10^{-5} \quad (5.8)$$

The averaging in (5.4) is done on a small number of realizations, especially for small l (large-scales), because we are observing from only one position in only one universe. So our results are plagued by the so-called cosmic variance.

We could as well write the 3-point correlation function which corresponds to the bispectrum. For more information on non-Gaussianities refer to the end of chapter 4.

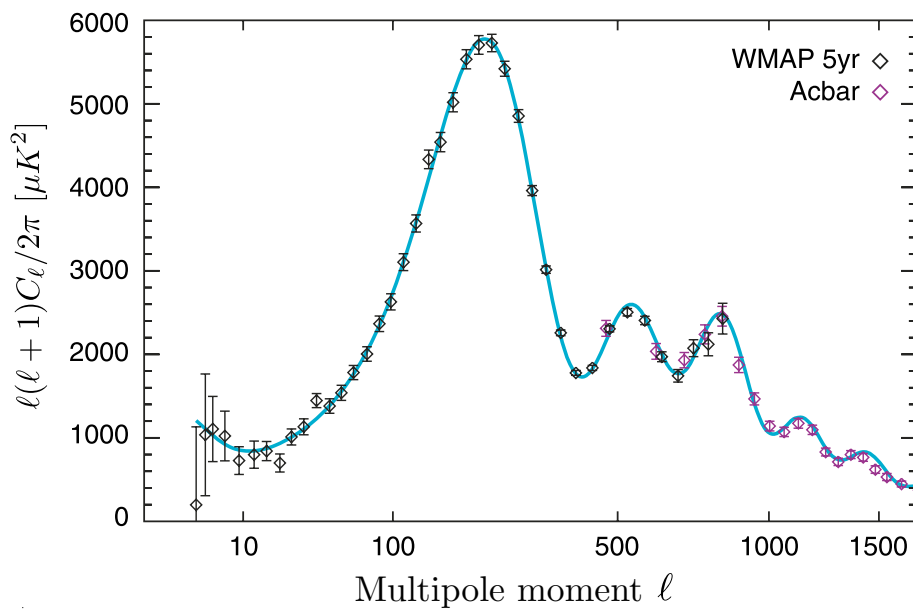


Figure 5.3: CMB spectrum of anisotropies from WMAP5 and ACBAR : Legendre coefficients for the CMBR temperature correlations, as measured by WMAP5 and ACBAR

The two most important characteristics of the angular power spectrum is the Sachs-Wolfe plateau for small l and the acoustic peaks for larger l values. The multipole moments C_l are almost independent of l for $l < 20$ so that the plot contains a plateau. The height and slope of this plateau depend on the amplitude of scalar and tensor perturbations and on the spectral index. For larger l values, there are acoustic peaks related to baryonic acoustic oscillations (BAO) in the plasma at the time of recombination. Basically what happens is that density fluctuations create temperature fluctuations since the gas heats as it compresses and cools as it expands. This part of the angular power spectrum is partially shaped

by the values of the cosmological parameters. It also gives information on inflation of course. For instance, the peak structure depends on possible isocurvature fluctuations. So it delivers constraints on multi-field inflation models. Besides, the peak structure requires the coherence of the primordial fluctuations and is thus interpreted as strong evidence for inflation.

In chapter 4, we give the link between CMB observables and inflationary quantities and current constraints on non-Gaussianities from the latest data. An example of constraining is also given just below for the relation between the tensor-to-scalar ratio and the scalar tilt.

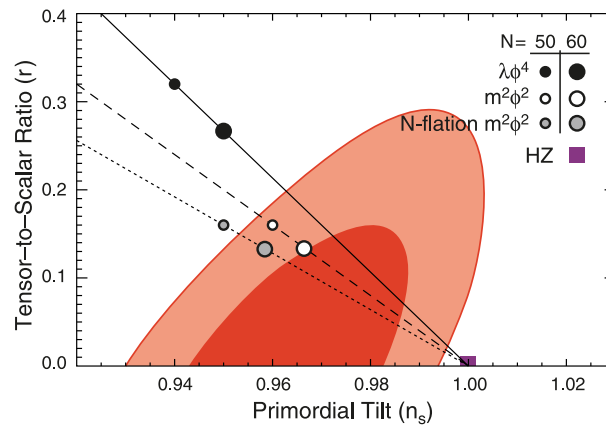


Figure 5.4: Two-dimensional joint marginalized constraint (68% and 95% CL) on the primordial tilt n_s and the tensor-to-scalar ratio r derived from the data combination of WMAP+BAO+H0. The symbols show the predictions from chaotic inflation models whose potential is given by $V(\phi) \propto \phi^\alpha$ (Linde 1983), with $\alpha = 4$ (solid) and $\alpha = 2$ (dashed) for single-field models, and $\alpha = 2$ for multi-axion field models with $\beta = 1/2$ (dotted; Easther & McAllister 2006). Plot from [79].

It appears from the plot 5.4 that the spectrum has a slightly red tilt, the spectral index n_s is smaller than 1 by a few percent. For a vanishing tensor amplitude, $n_s = 0.96$. CMB temperature fluctuations are dominated by the scalar modes and we can calculate that the tensor-to-scalar ratio is small $r < 0.3$.

Dirac-Born-Infeld Inflation

“Quand admettra-t-on qu'on ne saurait arriver à maîtriser l'inflation sans avoir recours aux solutions casse-cou ?”, J. Delacour

In DBI inflation [84, 85], the situation is very similar to KKLMMT (see 3.6). It is the motion of a test D3 brane inside a strongly warped throat which generates inflation. In this scheme, the inflaton represents the radial distance between the test D3 brane and the $\overline{D3}$ inside the throat : $\phi = \sqrt{T_3}r$ where $T_3 = \frac{1}{(2\pi)^3 g_s \alpha'^2}$ is the brane tension.

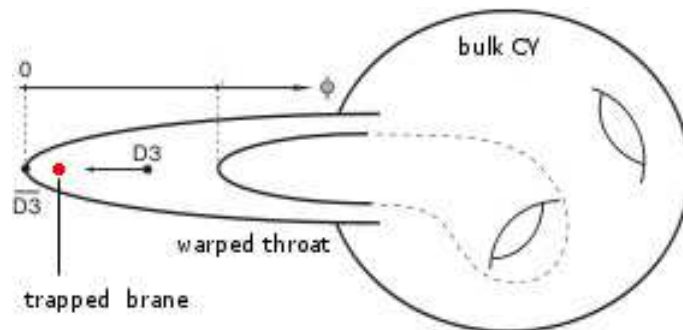


Figure 6.1: DBI inflation scenario

6.1 Action

The name DBI inflation comes from the effective 4-dimensional action which describes the motion of the probe D3 brane inside the warped throat. It is the Dirac-Born-Infeld action. It contains an uncommon non-canonical kinetic term. The DBI action and the Chern-Simons part are given in equations (2.11) and

(2.12). The $B_{\alpha\beta}$ form is null on the brane and $F_{\alpha\beta}$ is set to zero. Hence we are left with the computation of the induced metric $G_{\alpha\beta}$ and its determinant. It depends on the warp function $h(r)$. In the derivation of the Chern-Simons action, we use that the charge equals the tension. We obtain the following action

$$S = -\frac{1}{g_s} \int d^4x \sqrt{-g} \left(\frac{1}{f(\phi)} \sqrt{1 + f(\phi) g_{\mu\nu} \partial^\mu \phi \partial^\nu \phi} - \frac{1}{f(\phi)} + V(\phi) + g_{\mu\nu} \partial^\mu \chi \partial^\nu \chi + \frac{g^2}{2} \chi^2 |\phi - \phi_1|^2 \right) \quad (6.1)$$

where we have assumed that there is also a trapped brane stuck at ϕ_1 along the throat. Trapped branes may be present due to fixed points in the compactification manifold. Particles χ on the trapped brane are coupled to the inflationary brane with a quartic coupling at leading order. We will see later on that this coupling is responsible for the slowing down of the inflationary brane when crossing the trapped brane. The coupling is equivalent to the one between the inflaton and brane degrees of freedom on a trapped brane fixed along the inflationary valley [86]. We should of course add the Einstein-Hilbert action to get the complete action.

The warp factor $h(r)$ is re-expressed as an inflaton-dependent function $f(\phi)$ rather than a function depending on the radial direction. We will exclusively focus on a warped case with an AdS throat where $f(\phi) = \frac{\lambda}{\phi^4}$. The 't Hooft coupling is $\lambda = R^4/\alpha'^2 = R^4/l_s^4$ where R is the radius of compactification. The form of the warp factor $f(\phi)$ is crucial for the DBI dynamics. The coupling constants g_s and g are respectively the string coupling and the Yukawa coupling where $g_s \approx g^2$.

The inflaton potential $V(\phi)$ is highly-non trivial. It consists of several contributions. Its whole computation is still a work in progress. For a good review on the subject, refer to [87] or see the more recent papers [88, 89, 90]. The easy part to calculate is the Coulomb potential which describes the attraction between the D3 and $\overline{\text{D3}}$

$$V_{\text{D3}-\overline{\text{D3}}} = D \left(1 - \frac{3D}{16\pi^2 \phi^4} \right) \quad (6.2)$$

with $D = \frac{2}{f(\phi_{\text{IR}})}$, where f is evaluated at the tip of the throat. There is also a mass term $V_2 \phi^2$ coming from radiative and supergravity corrections to the potential. In general the mass term V_2 is positive apart from the case of a probe brane starting at the tip of the throat and moving towards the bulk [91, 92]. Corrections to the potential coming from bulk effects have to be added too. Those corrections have integer and half-integer powers of ϕ and depend on the bulk of the compactification. The leading correction is proportional to $\phi^{3/2}$ or ϕ^2 (if some discrete symmetry forbids the lowest eigenvalue). In the first case, the mass term $V_2 \phi^2$ and a negative $\phi^{3/2}$ term imply the existence of an inflection point [93] around which the potential becomes $V_0 + V_1(\phi - \phi_{\text{inflection}})$. Slow roll

inflation is tunable in this context and requires a choice of initial conditions to overcome the overshooting problem [94, 95]. In the second case, the DBI model is inflationary when the branes are sufficiently apart under the influence of the quadratic potential.

DBI inflation is very specific because it does not reproduce slow-roll conditions, in particular the potential does not need to be flat. The square-root action is consistent in the relativistic regime where higher time derivatives are negligible.

6.2 Dynamics

In this section and the following, we do not consider the coupling with matter. We define the equivalent of the Lorentz factor γ

$$\gamma = \frac{1}{\sqrt{1 + f(\phi)g_{\mu\nu}\partial^\mu\phi\partial^\nu\phi}} = \frac{1}{\sqrt{1 - f\dot{\phi}^2}}. \quad (6.3)$$

The maximal brane velocity is determined by the warp factor $f\dot{\phi}^2 \leq 1$. When approaching the maximal brane velocity the γ factor tends to infinity. On the contrary we recover $\gamma = 1$ in the standard case $f(\phi) \rightarrow 0$. The energy density and the pressure of the inflaton field are given by :

$$\rho_\phi = \frac{\gamma - 1}{f} + V \quad (6.4)$$

$$p_\phi = \frac{\gamma - 1}{\gamma f} - V \quad (6.5)$$

In this model, the sound speed is non trivial

$$c_s = \frac{1}{\gamma} \quad (6.6)$$

The inflationary dynamics are governed by the Klein Gordon equation for the spatially homogeneous inflaton field ϕ

$$\ddot{\phi} + 3H\dot{\phi} + \frac{\dot{\gamma}}{\gamma}\dot{\phi} + \frac{1}{\gamma}\frac{dV}{d\phi} + \frac{1}{\gamma f^2}\frac{df}{d\phi} - \frac{1}{\gamma^2 f^2}\frac{df}{d\phi} - \frac{\dot{\phi}^2}{2f}\frac{df}{d\phi} = 0 \quad (6.7)$$

or equivalently

$$\ddot{\phi} + \frac{3H}{\gamma^2}\dot{\phi} + \frac{1}{\gamma^3}\left(\frac{dV}{d\phi} + \frac{1}{f^2}\frac{df}{d\phi}\right) - \frac{1}{f^2}\frac{df}{d\phi} + \frac{3}{2}\dot{\phi}^2\frac{1}{f}\frac{df}{d\phi} = 0 \quad (6.8)$$

In the ultrarelativistic limit, both the potential term and the friction term coming from the expansion of the universe are subdominant.

With the warp factor $f(\phi) = \frac{\lambda}{\phi^4}$, equation (6.7) becomes :

$$\ddot{\phi} + 3H\dot{\phi} + \frac{\dot{\gamma}}{\gamma}\dot{\phi} + \frac{1}{\gamma}\frac{dV}{d\phi} - \frac{4\phi^3}{\lambda\gamma} + \frac{4\phi^3}{\lambda\gamma^2} + \frac{2\dot{\phi}^2}{\phi} = 0 \quad (6.9)$$

It may be easier to analyze the DBI dynamics using the Hamilton-Jacobi formalism.

As in canonical inflation, we can compute everything in terms of the slow-roll parameters defined in (3.17). Here the first slow-roll parameter ϵ_1 is proportional to $1/\gamma$, inflation is possible in the ultra-relativistic regime even with a large mass term. This solves the η problem [96]. In k-inflation, a new class of slow-roll parameters must be defined

$$\delta_{i+1} = \frac{d \ln |\delta_i|}{dN} \quad \text{with} \quad \delta_0 = \frac{1}{c_s} = \gamma \quad (6.10)$$

They measure the deviation from canonical inflation. Let's for example reexpress the Friedmann equation with slow-roll parameters :

$$H^2 = \frac{\kappa V}{3 - \frac{2\gamma}{\gamma+1}\epsilon_1} \quad (6.11)$$

6.2.1 Hamilton-Jacobi formalism

In the Hamilton-Jacobi formalism, every function is re-expressed as a function of ϕ . Using the Friedmann equation, the potential can be written as

$$V(\phi) = 3M_P^2 g_s H^2 - \frac{\gamma}{f} + \frac{1}{f} \quad (6.12)$$

If we differentiate (6.11) and upon using the Klein-Gordon equation we can express $\frac{dV}{d\phi}$ and obtain

$$\dot{\phi} = -2M_P^2 g_s \frac{1}{\gamma} \frac{dH}{d\phi} \quad (6.13)$$

Similarly, the γ factor can be written in terms of functions of ϕ

$$\gamma(\phi) = \sqrt{1 + 4M_P^4 g_s^2 f(\phi) \left(\frac{dH}{d\phi} \right)^2} \quad (6.14)$$

The DBI analogue to the standard slow-roll trajectory is readily obtained [97] from the Hamilton-Jacobi approach assuming $\epsilon_1, |\epsilon_2| \ll 1$

$$N(\phi) = -\kappa \int_{\phi_i}^{\phi} \sqrt{\left(\frac{V(\psi)}{V'(\psi)} \right)^2 + \frac{f(\psi)V(\psi)}{3\kappa}} d\psi \quad (6.15)$$

For a given potential, the Hubble function of ϕ is solution of a differential equation. It is possible to solve it for some simple potentials. It is also possible to use a Taylor expansion ansatz for H and assume a vanishing ϕ field at late times.

6.2.2 Example of a quadratic potential

This is precisely what we do in the case of a quadratic potential. There are co-dominant terms in (6.12) and one finds

$$H = \frac{1}{3\sqrt{\lambda}} \left(1 + \sqrt{1 + \frac{3m^2\lambda}{M_P^2 g_s}} \right) \phi \quad (6.16)$$

the relativistic factor is dominated by

$$\gamma(\phi) \approx 2M_P^2 g_s \sqrt{f(\phi)} \left| \frac{dH}{d\phi} \right| \quad (6.17)$$

As a result, the inflaton follows a universal trajectory dictated by the warp factor $f(\phi)$

$$\dot{\phi} \approx -\frac{1}{\sqrt{f(\phi)}} \quad \text{and} \quad \phi(t) = \frac{\sqrt{\lambda}}{t} \quad (6.18)$$

The potential term has an influence on the scale factor only.

$$\frac{a}{a_0} = \left(\frac{t}{t_0} \right)^{1/\epsilon} \quad (6.19)$$

where

$$\frac{1}{\epsilon} = \frac{1}{3} \left(1 + \sqrt{1 + \frac{3m^2\lambda}{M_P^2 g_s}} \right) \approx \sqrt{\frac{\lambda}{3g_s}} \frac{m}{M_P}. \quad (6.20)$$

Inflation occurs when $\epsilon < 1$. The coupling $\frac{\lambda}{g_s}$ and $\frac{m}{M_P}$ must be adjusted. The γ factor may be written as

$$\gamma = \frac{2M_P^2 g_s}{\lambda} \frac{1}{\epsilon} t^2 \quad (6.21)$$

These expressions are valid only at late times. In conformal time we find that

$$a(\eta) \propto \left(\frac{1-\epsilon}{\epsilon} \right)^{\frac{1}{\epsilon-1}} \left(\frac{\eta}{\eta_0} \right)^{\frac{1}{\epsilon-1}} \quad (6.22)$$

in such a way that

$$\mathcal{H} \approx -\eta^{-1}, \quad \frac{a''}{a} \approx 2\eta^{-2} \quad (6.23)$$

We deduce $\phi \propto \left(\frac{\eta}{\eta_0} \right)^{-\frac{\epsilon}{\epsilon-1}} \approx \left(\frac{\eta}{\eta_0} \right)^\epsilon$ to leading order.

In the case of this purely quadratic potential, the integration (6.15) can be performed explicitly in the slow-roll regime.

6.3 Perturbations

We use the results from the chapter 4 about k-inflation with

$$\mathcal{P}(\phi, X) = -\frac{1}{f(\phi)} \left(\sqrt{1 + 2f(\phi)X} - 1 \right) - V(\phi) \quad (6.24)$$

and we find that the perturbation equation is

$$v_k'' + \left(c_s^2 k^2 - \frac{z''}{z} \right) v_k = 0 \quad (6.25)$$

with

$$z = \frac{a\gamma^{3/2}\dot{\phi}}{H} = a\gamma\sqrt{\frac{2}{\kappa}\epsilon_1} \quad (6.26)$$

There are some γ corrections compared to standard slow-roll inflation. The term

$$\frac{z''}{z} = a^2 H^2 \left(2 - \epsilon_1 + \frac{3}{2}\epsilon_2 + \frac{1}{4}\epsilon_2^2 - \frac{1}{2}\epsilon_1\epsilon_2 + \frac{1}{2}\epsilon_2\epsilon_3 + (3 - \epsilon_1 + \epsilon_2)\delta_1 + \delta_1^2 + \delta_1\delta_2 \right) \quad (6.27)$$

in the perturbation equation can be rewritten in term of the smallest-order slow-roll parameters and of V'' and f'' as we will see in chapter 8.

In a quasi de Sitter universe, the approximation $\frac{z''}{z} \sim \frac{2}{\eta^2}$ is still valid in DBI slow-roll. However the solutions of the perturbation equation are not simply Hankel functions. Most often the solution is derived claiming that c_s is a slowly varying function but this might be wrong in some cases. One has to check afterward one's initial assumptions. With the uniform approximation, we obtain a solution for the Mukhanov-Sasaki variable in terms of Airy function [97]

$$v_k(\eta) = A(k) \left(\frac{f}{g} \right)^{1/4} \text{Ai}(f) + B(k) \left(\frac{f}{g} \right)^{1/4} \text{Bi}(f) \quad (6.28)$$

where the function

$$g(\eta) = \frac{\nu^2}{\eta^2} - c_s^2 k^2 \quad (6.29)$$

has a turning point η_* . The function $f(k, \eta)$ is defined by

$$f(k, \eta) = \frac{|\eta - \eta_*|}{\eta - \eta_*} \left| \frac{3}{2} \int_{\eta_*}^{\eta} \sqrt{|g(\tau)|} d\tau \right|^{2/3} \quad (6.30)$$

We assume that $1/c_s$ admits a polynomial expansion around η_* and we find

$$\frac{1}{c_s(\eta)} = \frac{1}{c_{s*}} \left(1 - \delta_{1*} \ln \frac{\eta}{\eta_*} \right) + \mathcal{O}(\epsilon\delta) \quad (6.31)$$

We expand as well $\nu(\eta)$. This all leads to the scalar power spectrum. At first order in the slow-roll parameters

$$\Delta_{\mathcal{R}}^2 = \frac{H^2}{\pi M_p^2 \epsilon_1 c_s} (18e^{-3}) \left(1 - 2(D+1)\epsilon_1 - D\epsilon_2 + (D+2)\delta_1 - (2\epsilon_1 + \epsilon_2 - \delta_1) \ln \frac{k}{\tilde{k}} \right) \quad (6.32)$$

where $D = 1/3 - \ln(3)$ and everything is evaluated at sound horizon crossing $-\tilde{k}\eta = 1/c_s(\eta)$.

6.4 Characteristics, observational signatures

When going to higher-orders, we derive precise values for all relevant inflationary quantities. At second order, the spectral index is given by

$$n_s - 1 = -2\epsilon_1 - \epsilon_2 + \delta_1 - 2\epsilon_1^2 - (2D+3)\epsilon_1\epsilon_2 + 3\epsilon_1\delta_1 + \epsilon_2\delta_1 - D\epsilon_2\epsilon_3 - \delta_1^2 + (D+2)\delta_1\delta_2 \quad (6.33)$$

For a quadratic potential, the scalar spectrum is extremely flat : $n_s - 1 = \mathcal{O}(\epsilon^3, \delta^3, \epsilon_i\delta_j)$ with $i + j = 3$.

The tensor to scalar ratio is at first order

$$r = 16c_s\epsilon_1 \propto 1/\gamma^2 \quad (6.34)$$

so it gets quite close to zero.

In DBI inflation, the non-Gaussianities are expected to be larger [136], typically proportional to γ^2 . For example for the quadratic potential

$$f_{\text{NL}}^{\text{equil}} = \frac{35}{108}(1 - \gamma^2) \quad \text{and} \quad f_{\text{NL}}^{\text{local}} = \mathcal{O}(\epsilon_i, \delta_i) \quad (6.35)$$

So current data (see inequality 4.96 and figure 5.4) imply that the γ factor cannot be very high ($\gamma \lesssim 19$). Typically during the observable e-folds of inflation γ should be of order 10, so not in a specially ultra-fast moving brane scenario.

In [98], a good but now outdated comparison between observations and DBI predictions can be found. In [99, 51], parameters of the theory are bounded from observational data analysis.

6.5 Brane annihilation and reheating

When the inflationary D3 brane approaches within a string length the $\overline{\text{D3}}$, they annihilate via tachyonic instability. Cosmic strings are expected to be produced at the end of this process. This production is characteristic of string inflation models. The precise mechanism which ends DBI inflation is not yet well understood and is being investigated by string theorists and cosmologists. One tricky point is how the energy is transferred to the brane where the Standard Model particles live. Reheating and preheating in DBI inflation are treated in [100, 101].

6.6 A word on multi-field DBI inflation

Taking into account the angular coordinates of the moving inflationary brane leads to a multi-field scenario since each brane coordinate in the extra dimensions gives rise to a scalar field from the effective four-dimensional point of view.

$$\mathcal{P} = -\frac{1}{f(\phi^I)} \left(\sqrt{\det(\delta_\nu^\mu + f G_{IJ} \partial^\mu \phi^I \partial_\nu \phi^J)} - 1 \right) - V(\phi^I) \quad (6.36)$$

where G_{IJ} is the metric of the internal compact space. We have included a potential term, which contains the brane interactions with the bulk and possibly with other branes. For a detailed analysis of perturbations in multi-field DBI inflation, refer to [102, 103].

Scalar-tensor theories

“L’univers entier se conduirait par une seule loi, si cette loi était bonne”,
Marquis de Sade

7.1 Brans-Dicke theories, $f(R)$ theories and chameleons

Scalar-tensor theories are modifications of the general relativity where a scalar field couples both to gravity and matter. In the Jordan frame, the generic form of the action in this theory is

$$S = \int d^4x \sqrt{-g} \left(\frac{F(\phi)R}{16\pi G_N} - g^{\mu\nu} \frac{Z(\phi)}{2} \partial_\mu \phi \partial_\nu \phi - U(\phi) \right) + S_m[g_{\mu\nu}, \text{matter}] \quad (7.1)$$

where G_N is the bare gravitational constant, F and Z are two dimensionless arbitrary functions, U is the potential. Only two of those three functions are parameters, the other one can be reabsorbed in a redefinition of the scalar field. It is simple to choose $Z(\phi) = 1$ and leave $F(\phi)$ unspecified. It can sometimes be more convenient to choose the Brans-Dicke parameterization with $Z(\phi) = \omega(\phi)/\phi$ and $F(\phi) = \phi$. In this frame, the matter fields are minimally coupled to gravity. On the contrary, in the Einstein frame, the metric is related to the Jordan-frame metric through a conformal transformation

$$g_{\mu\nu}^* = F(\phi)g_{\mu\nu} \quad (7.2)$$

and the Einstein-Hilbert action is unmodified

$$S = \int d^4x \sqrt{-g_*} \left(\frac{R_*}{16\pi G_N} - g_*^{\mu\nu} \partial_\mu \phi_* \partial_\nu \phi_* - V(\phi_*) \right) + S_m[g_{\mu\nu}, \text{matter}] \quad (7.3)$$

The relations between the Jordan and Einstein frames are the following :

$$\frac{d\phi_*}{d\phi} = \sqrt{\frac{3}{4} \left(\frac{d \ln F(\phi)}{d\phi} \right)^2 + \frac{Z(\phi)}{2F(\phi)}} \quad (7.4)$$

$$A(\phi_*) = F^{-1/2}(\phi) \quad (7.5)$$

$$V(\phi_*) = U(\phi)F^{-2}(\phi) \quad (7.6)$$

In the Brans-Dicke parameterization, we find that $\omega = -3/2$ and the two fields are equal $\phi = \phi_*$. The energy-momentum tensor in the Einstein frame is different from the one in the Jordan frame and we do not have the usual conservation of matter

$$T_{*;\mu}^{\mu\nu} = 0 \text{ but } T_{*;\mu}^{\mu\nu} = \beta T^* \partial^\nu \phi_* \neq 0 \text{ with } \beta = \frac{d \ln A}{d\phi_*} \quad (7.7)$$

where T^* is the trace of the Einstein-frame energy-momentum tensor

$$T_*^{\mu\nu} = \frac{2}{\sqrt{-g_*}} \frac{\delta S_m}{\delta g_{\mu\nu}^*} \quad (7.8)$$

In the cosmological context this leads to

$$\dot{\rho} + 3H(\rho + p) = \beta \dot{\phi}_*(\rho - 3p) \quad (7.9)$$

We may write the Einstein equations in either the Jordan frame

$$\begin{aligned} F(\phi)G_{\mu\nu} = 8\pi G_N T_{\mu\nu} + Z(\phi) \left(\partial_\mu \phi \partial_\nu \phi - \frac{1}{2} g_{\mu\nu} \partial_\alpha \phi \partial^\alpha \phi \right) \\ + \nabla_\mu \partial_\nu F(\phi) - g_{\mu\nu} \square F(\phi) - g_{\mu\nu} U(\phi) \end{aligned} \quad (7.10)$$

or the Einstein frame

$$G_{\mu\nu}^* = 8\pi G_N T_{\mu\nu}^* + 2\partial_\mu \phi_* \partial_\nu \phi_* - g_{\mu\nu}^* \partial_\alpha \phi_* \partial^\alpha \phi_* - g_{\mu\nu}^* V \quad (7.11)$$

The Klein-Gordon equation in the Jordan frame reads

$$Z(\phi)\square\phi = \frac{dU}{d\phi} - \frac{1}{2} \frac{dF}{d\phi} R - \frac{1}{2} \frac{dZ}{d\phi} (\partial_\alpha \phi)^2 \quad (7.12)$$

and in the Einstein frame

$$\square_* \phi_* = \frac{dV}{d\phi_*} - \beta T^* \quad (7.13)$$

It is equivalent to the usual Klein-Gordon equation with the effective potential

$$V_{\text{eff}} = V - A(\phi_*)T \quad (7.14)$$

The mass of each matter particle is rescaled by a factor $A(\phi_*)$. It is now interesting to notice that the scalar field induces a modification of the effective gravitational constant

$$G_{N \text{ eff}} = (1 + 2\beta^2)G_N \quad (7.15)$$

and the Newtonian constant measured in a Cavendish experiment is

$$G_{N \text{ Cav}} = (1 + 2\beta^2)A^2(\phi_*)G_N \quad (7.16)$$

The coupling constant β is constrained by solar system gravity tests

$$\beta^2 \leq 4.10^{-5} \quad (7.17)$$

Besides, microscopic physics give another bound on the coupling when the mass of the scalar field is small, deduced from the bound on the violation of the equivalence principle

$$\beta \leq 10^{-5} \quad (7.18)$$

This bound is stronger than the previous one. But the violation of the equivalence principle can be averted by certain scalar-tensor theories : chameleon theories. When the function $A(\phi)$ is an increasing function, the effective potential for a pressure-less matter fluid

$$V_{\text{eff}}(\phi) = V(\phi) + A(\phi)\rho_m \quad (7.19)$$

has a mass which depends on the local density and can thus evade lab tests. Some chameleons theories are equivalent to a particular class of theories where the Einstein-Hilbert action depends not directly on the curvature R but on an arbitrary function $f(R)$ of the curvature. $f(R)$ theories are extensions of the general relativity theory, which contain no ghost. They are described by

$$S = \frac{1}{16\pi G_N} \int d^4x \sqrt{-g} f(R) + S_m[g_{\mu\nu}, \text{matter}] \quad (7.20)$$

The related Einstein equation is

$$R_{\mu\nu} f'(R) - \frac{1}{2} f(R) g_{\mu\nu} - \nabla_\mu \nabla_\nu f'(R) + g_{\mu\nu} \square f'(R) = 8\pi G_N T_{\mu\nu} \quad (7.21)$$

These theories of modified gravity can be rewritten as scalar-tensor theories via the following conformal transformation :

$$\bar{g}_{\mu\nu} = e^{-\frac{2\beta\phi^*}{M_{\text{P}}}} g_{\mu\nu} \quad \text{with } \phi^* \text{ such that } f'(R) = e^{-\frac{2\beta\phi^*}{M_{\text{P}}}} \quad (7.22)$$

where the coupling is fixed and large $\beta = 1/\sqrt{6}$ implying that the scalar field must be a chameleon field. In the Einstein frame

$$S = \int d^4x \sqrt{-g} \left(\frac{1}{2} M_{\text{P}}^2 \bar{R} - \frac{1}{2} \bar{g}^{\mu\nu} \nabla_\mu \phi^* \nabla_\nu \phi^* - V(\phi^*) \right) + S_m \left[e^{\frac{2\beta\phi^*}{M_{\text{P}}}} \bar{g}_{\mu\nu}, \text{matter} \right] \quad (7.23)$$

with the potential

$$V(\phi) = \frac{M_{\text{P}}^2 (R f'(R) - f(R))}{2 f'(R)^2} \quad (7.24)$$

If $m_{\phi^*} = \sqrt{V_{,\phi^*\phi^*}}$ is strongly dependent on the ambient density of matter, ϕ^* can be heavy enough in the environment of the laboratory tests so as to evade them, whilst remaining relatively light on cosmological scales.

This brief introduction to scalar-tensor theories will prove useful in chapter 9 and the interested reader can find more details in [105, 106, 107, 108, 109, 110, 111, 112] and in [113], a scalar-tensor theory with a DBI matter component is even investigated.

Part II
PhD researches

Features

“The most important scientific revolutions all include, as their only common feature, the dethronement of human arrogance from one pedestal after another of previous convictions about our centrality in the cosmos”, S. Jay Gould

8.1 Starobinsky’s model : background

I am referring to Starobinsky’s paper [114], which was the first to consider a perturbation equation with a dirac term giving rise to features in the scalar power spectrum. It provides a very good toy model. Consider canonical inflation with a linear potential but with a sudden change of slope

$$V(\phi) = V_0 + A_+(\phi - \phi_1) \text{ for } \phi > \phi_1 \quad (8.1)$$

$$= V_0 + A_-(\phi - \phi_1) \text{ for } \phi < \phi_1 \quad (8.2)$$

This potential is continuous but its derivatives are not. Consequently, the slow-roll regime is disrupted for a few e-folds after crossing the feature $\phi = \phi_1$. In the case $A_+ > A_-$, the inflaton should tend to acquire a smaller velocity after the feature. Slow-roll (SR) can be violated even though the speed of the inflaton decreases. It is important to notice that in this toy-model the first slow-roll parameter ϵ_1 always remains much smaller than one (see figure 8.1). Therefore the Friedmann equation reduces to

$$H^2 \approx \frac{\kappa V}{3} \quad (8.3)$$

and only depends on the potential. The parameters are such that the Hubble rate is, to a good level of approximation, constant.

$$H^2 \approx H_0^2 = \frac{\kappa V_0}{3} \quad (8.4)$$

We can check numerically that the slow-roll solution with a constant Hubble rate is very close to the real solution. We replace the Hubble rate by the constant

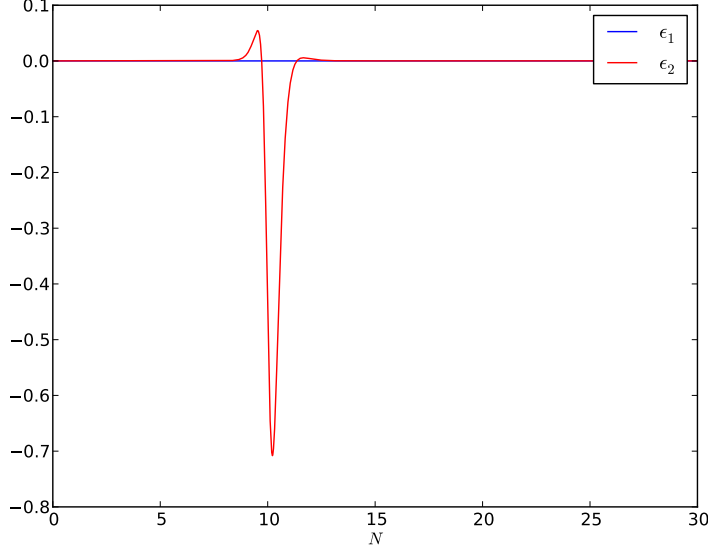


Figure 8.1: Slow-roll parameters in Starobinsky's model in canonical inflation : $\epsilon_1 \ll 1$ while $|\epsilon_2| \sim 1$. We notice that the fast-roll regime lasts typically one, at most two e-folds. Here the parameters obey $N_1 = 10$, $A_-/A_+ = 10^{-2}$ and $\dot{\phi}_{\text{ini}} = -A_+/3H_{\text{ini}}$.

value H_0 in the end in all expressions but it does not mean that we neglect the derivatives of H , on the contrary. As explained in [114] or [115], the slow-roll regime is violated for a very few e-folds after $\phi = \phi_1$ with $\epsilon_1 < 1$ but $|\epsilon_2| \gtrsim 1$ corresponding to

$$\frac{1}{2\kappa} \left(\frac{V'}{V} \right)^2 < 1 \Rightarrow \frac{1}{2\kappa} \left(\frac{A_{\pm}}{V_0} \right)^2 < 1 \quad (8.5)$$

but

$$\frac{1}{\kappa} \left| \frac{V''}{V} \right| \approx \frac{1}{\kappa} \left| \frac{V'_+ - V'_-}{\phi_1 V} \right| \gtrsim 1 \quad (8.6)$$

roughly

$$\frac{1}{\kappa} |A_+ - A_-| \gtrsim \phi_1 V_0 \quad (8.7)$$

From COBE normalization, we get another constraining condition on the parameters

$$\mathcal{P}_{\mathcal{R}} \sim \frac{\kappa H^2}{\epsilon_1} \sim \kappa^3 \frac{V_0^3}{A_{\pm}^2} \sim 10^{-10} \quad (8.8)$$

The inflaton must be sub-Planckian when going through the feature

$$\phi_1 < 1/\sqrt{\kappa} \quad (8.9)$$

The Klein-Gordon equation reads :

$$\ddot{\phi} + 3H\dot{\phi} + \frac{dV}{d\phi} = 0 \quad (8.10)$$

We know that in standard inflation, after about 60 e-folds, the inflaton oscillates around its minimum. The N -dependent Klein Gordon equation is

$$H^2 \frac{d^2\phi}{dN^2} + H \frac{dH}{dN} \frac{d\phi}{dN} + 3H^2 \frac{d\phi}{dN} + \frac{dV}{d\phi} = 0 \quad (8.11)$$

For a constant Hubble ratio, we thus have

$$\frac{d^2\phi}{dN^2} + 3 \frac{d\phi}{dN} + \frac{1}{H_0^2} \frac{dV}{d\phi} = 0 \quad (8.12)$$

We assume that before the feature the universe is inflating in the slow-roll regime. Numerically, we either tune the initial conditions to start with slow-roll or let the system evolve freely for a certain amount of time so that the inflaton reaches its slow-roll solution before it reaches the feature. In slow-roll we can neglect the second derivative so $\phi(N)$ satisfies

$$\frac{d\phi}{dN} = -\frac{A_{\pm}}{3H_0^2} \quad (8.13)$$

So before the feature :

$$\phi_+(N) = \phi_{\text{ini}} - \frac{A_+ N}{3H_0^2} \quad (8.14)$$

When reaching the feature at $\phi = \phi_1$, this SR approximation (8.13) is no longer valid. Solving the whole differential equation (8.12) and using the continuity of ϕ and $d\phi/dN$ gives us the expression of $\phi(N) < \phi_1$

$$\frac{d\phi_-}{dN} = \frac{(A_- - A_+)e^{-3(N-N_1)} - A_-}{3H_0^2} \quad (8.15)$$

and

$$\phi_-(N) = \phi_1 + \frac{A_+ - A_-}{9H_0^2} (e^{-3(N-N_1)} - 1) - (N - N_1) \frac{A_-}{3H_0^2} \quad (8.16)$$

with

$$N_1 = \frac{3H_0^2}{A_+} (\phi_{\text{ini}} - \phi_1) \quad (8.17)$$

Starobinsky also calculated the expression of the derivative of the inflaton both before and after the feature but with respect to the cosmic time and not the number of e-folds. Here we favor the variable N because it is a better choice for the evolution parameter in a numerical resolution since inflation lasts over a too

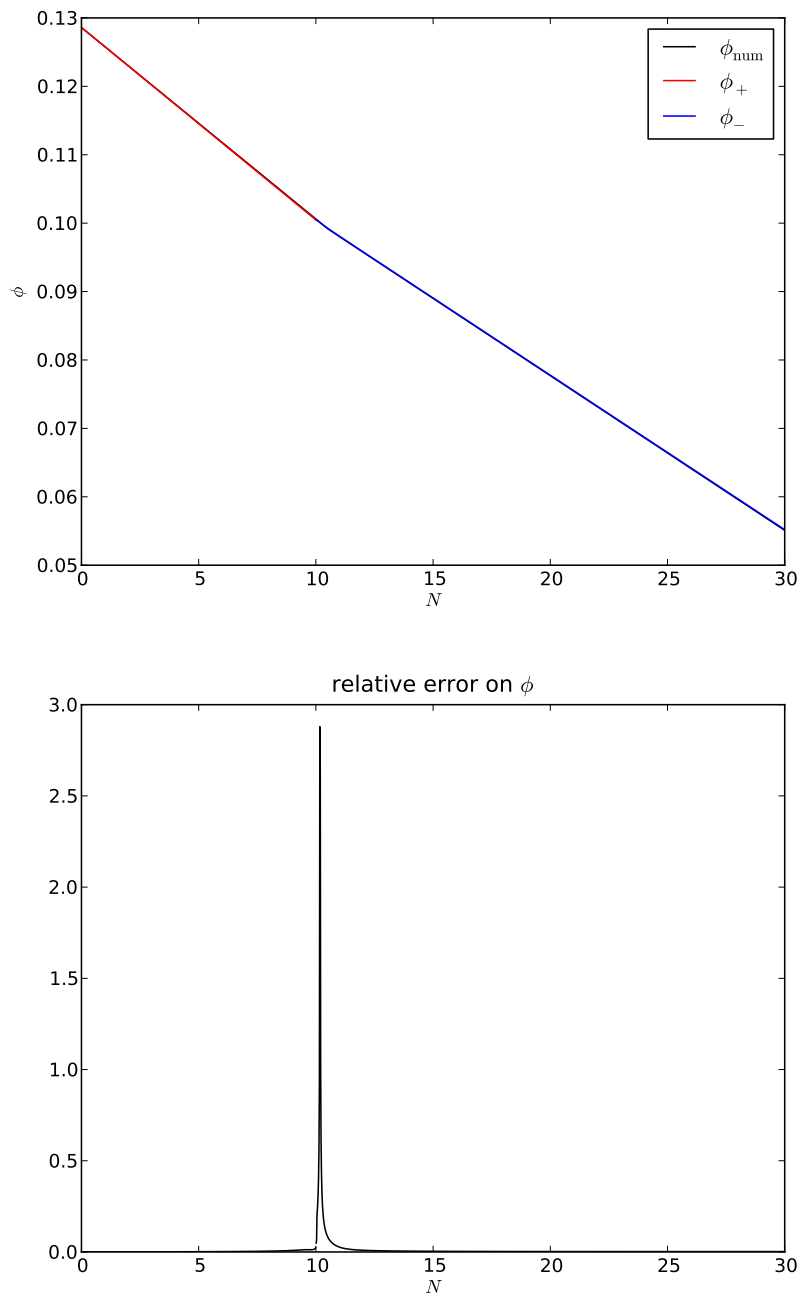


Figure 8.2: Comparison of the analytical solution with the numerical solution in Starobinsky's original model with $N_1 = 10$. The error is completely negligible (the pic is just a numerical artifact due to the non perfect gluing of the analytical solution before to the analytical solution after). Same parameters as in figure 8.1.

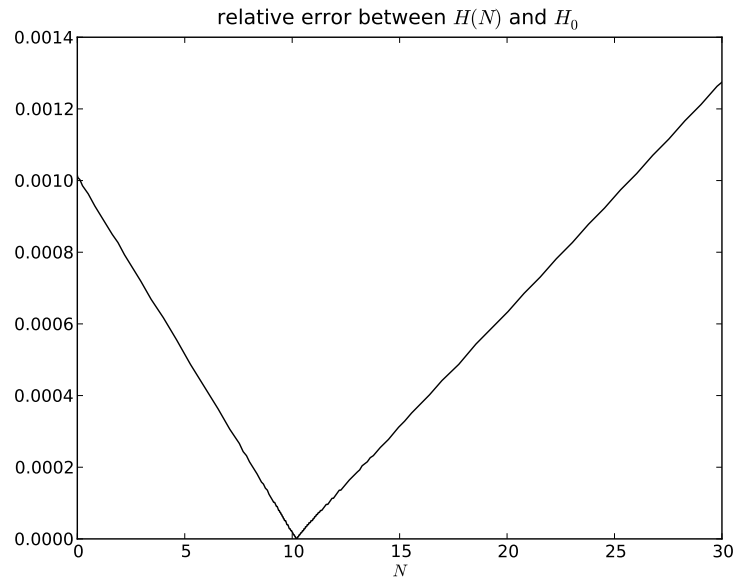


Figure 8.3: Consistency of the approximation of a constant Hubble rate (only 0.1% error). Same parameters as in figure 8.1.

wide range of cosmic times. In fact we can check the solution (8.14) and (8.16) numerically with great accuracy (see figure 8.2). Considering that the Hubble rate is constant is a very good approximation (see figure 8.3). The exponential in (8.16) decreases very fast in terms of e-folds. The fast-roll regime is expected to last typically for $\Delta N = 1/3$. Numerical simulations confirm that fast-roll lasts less than one e-fold.

8.2 Starobinsky's potential in DBI inflation

We want to study this same potential in DBI inflation and see the effect of the feature. In DBI inflation, the dynamics highly depend on the form of the warp factor $f(\phi)$. We wonder whether the “DBI slow-roll” regime breaks down here. What we call “DBI slow-roll” regime here is the regime where all slow-roll parameters (ϵ_i) and (δ_i) are small. It has nothing to do with usual slow-roll in canonical inflation since the inflaton speed is large. In DBI also, ϵ_1 always remains smaller than unity with Starobinsky's potential (see figure 8.4).

The Klein-Gordon equation reads

$$\ddot{\phi} + \frac{3H}{\gamma^2} \dot{\phi} + \frac{3\gamma - \gamma^3 - 2}{2\gamma^3} \frac{d}{d\phi} \left(\frac{1}{f} \right) + \frac{1}{\gamma^3} \frac{dV}{d\phi} = 0 \quad (8.18)$$

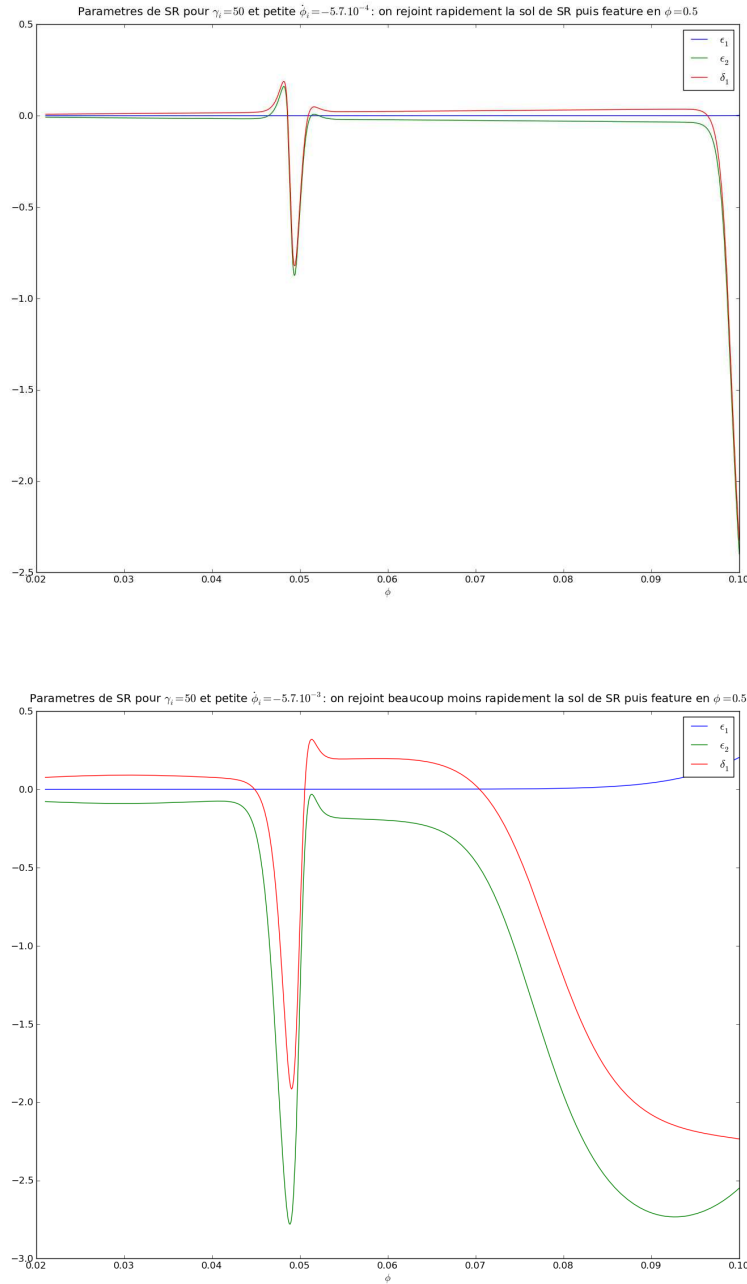


Figure 8.4: First slow-roll parameters in DBI inflation with a Starobinsky potential with a feature at $\phi_1 = 0.05 M_p$ and $A_-/A_+ = 10^{-2}$, for different initial velocities (the velocity above is ten times smaller than the velocity below). The slow-roll is reached earlier for a smaller initial velocity. The parameter ϵ_1 (blue curve) remains very close to zero whereas the absolute values of ϵ_2 (green curve) and δ_1 (red curve) become larger than unity at the feature.

We compute the slow-roll parameters, starting from some partially random initial conditions ($\phi_{\text{ini}} = 0.1 M_p$ and $\gamma_{\text{ini}} = 50$). After some e-folds, we reach the slow-roll regime then, as the inflaton rolls down its potential, the inflaton encounters the feature.

We have noticed that the behavior of the slow roll parameters are independent of the initial value of the γ factor. This is because the inflaton has already reached the SR solution when passing the feature and there is no memory of initial conditions.

and the Friedmann equation is

$$H^2 = \frac{\kappa V}{3 - 2\gamma\epsilon_1/(\gamma + 1)} \approx \frac{\kappa V}{3} \approx \frac{\kappa V_0}{3} \quad (8.19)$$

With the Hamilton-Jacobi approach, we can write every quantity as a function of ϕ . So with the expression (6.14) of the γ factor comes :

$$\left(\frac{d\phi}{dN}\right)^2 = \left(\frac{\dot{\phi}}{H}\right)^2 = \frac{\gamma^2 - 1}{\gamma^2 H^2 f} \quad (8.20)$$

It is easier to compute $N(\phi)$ than $\phi(N)$.

$$\frac{dN}{d\phi} = -\sqrt{H^2 f + \frac{\kappa^2}{4} \frac{H^2}{(dH/d\phi)^2}} \quad (8.21)$$

In our case $|\epsilon_1| \ll 1$ and $|\epsilon_2| \gtrsim 1$ at the feature, it is correct to replace H^2 by $\kappa V/3$ but $dH^2/d\phi$ is not simply proportional to $dV/d\phi$. On the contrary, in pure slow-roll, the expression (8.21) reduces to

$$N(\phi) = -\kappa \int_{\phi_i}^{\phi} \sqrt{\left(\frac{V(\psi)}{V'(\psi)}\right)^2 + \frac{f(\psi)V(\psi)}{3\kappa}} d\psi \quad (8.22)$$

This was derived for example in [97]. With our approximation $V_0 \gg A_{\pm}\phi_0$, the slow-roll solution can be written

$$N(\phi) = -\kappa \int_{\phi_i}^{\phi} \sqrt{\left(\frac{V_0}{A_{\pm}}\right)^2 + \frac{\lambda V_0}{3\kappa\psi^4}} d\psi \quad (8.23)$$

This integral can be expressed in terms of extended elliptic integrals of first and second kind.

$$\begin{aligned} N(\phi) = & -\phi \sqrt{\left(\frac{V_0}{A_{\pm}}\right)^2 + \frac{\lambda V_0}{3\kappa\phi^4}} + \phi_{\text{ini}} \sqrt{\left(\frac{V_0}{A_{\pm}}\right)^2 + \frac{\lambda V_0}{3\kappa\phi_{\text{ini}}^4}} \\ & + 2i \frac{V_0^2}{A_{\pm}^2} \sqrt{\frac{3\kappa}{\lambda V_0}} \left(\frac{i}{A_{\pm}} \sqrt{\frac{3\kappa V_0}{\lambda}}\right)^{-3/2} \left(\mathcal{E} \left[i \operatorname{sh}^{-1} \left(\phi \sqrt{\frac{i}{A_{\pm}}} \sqrt{\frac{3\kappa V_0}{\lambda}} \right) / -1 \right] \right. \\ & - \mathcal{E} \left[i \operatorname{sh}^{-1} \left(\phi_{\text{ini}} \sqrt{\frac{i}{A_{\pm}}} \sqrt{\frac{3\kappa V_0}{\lambda}} \right) / -1 \right] - \mathcal{F} \left[i \operatorname{sh}^{-1} \left(\phi \sqrt{\frac{i}{A_{\pm}}} \sqrt{\frac{3\kappa V_0}{\lambda}} \right) / -1 \right] \\ & \left. + \mathcal{F} \left[i \operatorname{sh}^{-1} \left(\phi_{\text{ini}} \sqrt{\frac{i}{A_{\pm}}} \sqrt{\frac{3\kappa V_0}{\lambda}} \right) / -1 \right] \right) \quad (8.24) \end{aligned}$$

We cannot derive analytically the solution $\phi(N)$ or $N(\phi)$ in the fast-roll regime. We can only compute it numerically. Here in DBI the Hubble rate H can also be replaced by a constant. The potential is continuous and its derivative are not thus the inflaton field ϕ , its derivative $\dot{\phi}$, the γ factor, the Hubble rate H and its first derivative H' are continuous but $\ddot{\phi}$, $\dot{\gamma}$, H'' are not. The jump in $\dot{\gamma}$ can be re-expressed in terms of the jump in $\ddot{\phi}$ or in H''

$$\dot{\gamma} = \gamma^3 \frac{\lambda \dot{\phi}^2}{\phi^4} \left(\frac{\ddot{\phi}}{\dot{\phi}} - \frac{2\dot{\phi}}{\phi} \right) \quad (8.25)$$

$$[\dot{\gamma}]_{-}^{+} = \gamma_0^3 \frac{\lambda \dot{\phi}_0}{\phi_0^4} [\ddot{\phi}]_{-}^{+} \quad (8.26)$$

The γ factor is continuous but evolves quite drastically during the fast-roll regime as we observe in the simulations.

8.3 DBI perturbation equation

We know from (4.58) that the perturbation equation can be formulated as

$$v_k'' + \left(c_s^2 k^2 - \frac{z''}{z} \right) v_k = 0 \quad (8.27)$$

where $c_s = 1/\gamma$ and where the variable

$$z = a\gamma^{3/2} \frac{d\phi}{dN} \quad (8.28)$$

depends on the potential. Here, z is continuous but its derivative are not. The computations of z''/z is carried out in the general framework of DBI in the following lines. We recall from chapter 6 that

$$\frac{z''}{z} = a^2 H^2 \left(2 - \epsilon_1 + \frac{3}{2}\epsilon_2 + \frac{1}{4}\epsilon_2^2 - \frac{1}{2}\epsilon_1\epsilon_2 + \frac{1}{2}\epsilon_2\epsilon_3 + (3 - \epsilon_1 + \epsilon_2)\delta_1 + \delta_1^2 + \delta_1\delta_2 \right) \quad (8.29)$$

The perturbation equation can be rewritten in term of the smallest-order slow-roll parameters and of V'' and f'' . Using

$$\epsilon_1 = -\frac{\dot{H}}{H^2} = \frac{2}{\kappa\gamma} \frac{1}{H^2} \left(\frac{dH}{d\phi} \right)^2 = \frac{2}{\kappa\gamma} \left(\frac{d \ln H}{d\phi} \right)^2 \quad (8.30)$$

$$\epsilon_2 = \frac{2}{\kappa\gamma} \left(\frac{2}{H^2} \left(\frac{dH}{d\phi} \right)^2 - \frac{2}{H} \frac{d^2 H}{d\phi^2} + \frac{1}{\gamma} \frac{d\gamma}{d\phi} \frac{1}{H} \frac{dH}{d\phi} \right) \quad (8.31)$$

$$\delta_1 = \frac{\dot{\gamma}}{\gamma H} = -\frac{2}{\kappa\gamma} \frac{1}{\gamma} \frac{d\gamma}{d\phi} \frac{1}{H} \frac{dH}{d\phi} \quad (8.32)$$

$$\delta_2 = \frac{2}{\kappa\gamma} \left(\frac{2}{\gamma} \frac{d\gamma}{d\phi} \frac{1}{H} \frac{dH}{d\phi} - \frac{d^2\gamma/d\phi^2}{d\gamma/d\phi} \frac{1}{H} \frac{dH}{d\phi} + \frac{1}{H^2} \left(\frac{dH}{d\phi} \right)^2 - \frac{1}{H} \frac{d^2 H}{d\phi^2} \right) \quad (8.33)$$

and (6.14, 8.19), we find

$$\begin{aligned}
\epsilon_2 \epsilon_3 &= -\frac{V''}{H^2} \frac{\gamma+1}{\gamma^2} + \frac{1}{\gamma+1} \delta_1 \delta_2 + 3 \frac{(\gamma+1)^2}{\gamma^2} \epsilon_1 - \frac{3}{2} \frac{\gamma+1}{\gamma^2} \epsilon_2 - 2 \left(1 + \frac{1}{\gamma^2}\right) \epsilon_1^2 \\
&+ \left(\frac{1}{2\gamma} - 1\right) \epsilon_2^2 + 5\epsilon_1 \epsilon_2 - \frac{3}{2} \frac{\gamma+1}{\gamma^2} \delta_1 + \left(\frac{1}{\gamma} - \frac{1}{2(\gamma+1)} + \frac{4}{\gamma+1}\right) \epsilon_1 \delta_1 \\
&+ \left(\frac{\gamma+3}{\gamma+1} + \frac{1}{2\gamma}\right) \delta_1 \epsilon_2 + \frac{1}{\gamma+1} \left(\frac{\gamma}{\gamma+1} + \frac{3}{2}\right) \delta_1^2 \tag{8.34}
\end{aligned}$$

and

$$\delta_1 \delta_2 = \frac{1}{2} \left(\epsilon_2 \delta_1 - \frac{\gamma^2+1}{\gamma^2-1} \delta_1^2 - \frac{4}{\sqrt{\gamma^2-1}} \delta_1^2 + \frac{2}{\kappa} \frac{\sqrt{\gamma^2-1}}{\gamma} \epsilon_1 \frac{f''}{f} \right) \tag{8.35}$$

so that

$$\begin{aligned}
\frac{z''}{z} \frac{1}{a^2 H^2} &= 2 - \frac{V''}{2H^2} \frac{\gamma+1}{\gamma^2} + \frac{1}{\kappa} \left(1 + \frac{1}{2(\gamma+1)}\right) \frac{\sqrt{\gamma^2-1}}{\gamma} \epsilon_1 \frac{f''}{f} + \left(\frac{3(\gamma+1)^2}{2\gamma^2} - 1\right) \epsilon_1 \\
&- \left(1 + \frac{1}{\gamma^2}\right) \epsilon_1^2 + 4\epsilon_1 \epsilon_2 + \frac{1}{2} \left(-2 + \frac{1}{\gamma} - \frac{1}{2(\gamma+1)} + \frac{4}{\gamma+1}\right) \epsilon_1 \delta_1 \\
&+ \frac{3}{2} \left(1 - \frac{\gamma+1}{2\gamma^2}\right) \epsilon_2 + \frac{1}{4} \left(\frac{1}{\gamma} - 1\right) \epsilon_2^2 + 3 \left(1 - \frac{\gamma+1}{4\gamma^2}\right) \delta_1 + \left(1 - \frac{2}{\sqrt{\gamma^2-1}}\right) \delta_1^2 \\
&+ \frac{1}{2(\gamma+1)} \left(\frac{3}{2} + \frac{\gamma}{\gamma+1} - \frac{1}{2} \frac{\gamma^2+1}{\gamma^2-1} - \frac{2}{\sqrt{\gamma^2-1}} - \frac{\gamma^2+1}{\gamma-1}\right) \delta_1^2 \\
&+ \frac{1}{2} \left(3 + \frac{\gamma+3}{\gamma+1} + \frac{1}{2\gamma} + \frac{1}{2(\gamma+1)}\right) \epsilon_2 \delta_1 \tag{8.36}
\end{aligned}$$

Details on these computations are given in appendix B. It is interesting to note that z''/z contains both a second derivative of the inflaton potential and a second derivative of the warp factor. So if the warp factor is continuous but its derivatives are not, it can also lead to features in the power spectrum. In [117], they consider a warped throat whose tip can be approximated by a stair-like function¹ and they obtain a perturbation equation with delta functions. This is very specific to brane inflation. However, such features look quite like features from other sources, as will be seen later on. This formula (8.36) is never written this way in the literature, but this form is of great use for the study of features, in particular in canonical inflation.

1. The physics at the tip of the throat is complex, the effect of the inflationary brane on the geometry cannot be neglected thus it is difficult to estimate the warp factor, but the function with steps used in [117] is a fair approximation.

8.4 Starobinsky's perturbation equation in canonical inflation : resolution

In canonical inflation $\gamma = 1$ we see from (8.36) that

$$\frac{z''}{z} = a^2 H^2 \left(2 + \epsilon_1 \mathcal{O}(1) + \mathcal{O}(V''/H^2) \right) \quad (8.37)$$

so that we can neglect all the terms other than the de Sitter term and the second derivative of the potential in Starobinsky's case where $\epsilon_1 \ll 1$ because there is a life-saver cancellation in the first and second order in the SR parameter ϵ_2 . Hence the perturbation equation reduces to

$$v_k'' + \left(k^2 - \frac{2}{\eta^2} + a^2 V'' \right) v_k = 0 \quad (8.38)$$

Starobinsky's potential is such that its second derivative can be seen as a dirac centered at η_1 . Features might seem as mathematical artifacts. It is actually mathematically justified to introduce such a delta function in our equation as shown in appendix C.

$$a^2 V'' = a^2 m_{\text{eff}}^2 = u \delta(\eta - \eta_1) = au \delta(t - t_1) \quad (8.39)$$

The perturbation equation is the de Sitter equation with a dirac term

$$v_k'' + \left(k^2 - \frac{2}{\eta^2} + u \delta(\eta - \eta_1) \right) v_k = 0 \quad (8.40)$$

The coefficient u of the dirac will be calculated in the next section for Starobinsky's potential. But the computation of the solutions of this equation is generic. The solution before the feature is in a Bunch-Davies vacuum at $\eta \rightarrow -\infty$ [116]

$$v_k^+ = \frac{H_0}{\sqrt{2k}} \left(-\eta + \frac{i}{k} \right) e^{-ik\eta} \quad (8.41)$$

and after the feature

$$v_k^- = \frac{H_0}{\sqrt{2k}} \alpha \left(-\eta + \frac{i}{k} \right) e^{-ik\eta} + \frac{H_0}{\sqrt{2k}} \beta \left(-\eta - \frac{i}{k} \right) e^{ik\eta} \quad (8.42)$$

with the junction conditions

$$[v_k]_{\eta_1} = 0 \quad (8.43)$$

$$[v_k']_{\eta_1} = -u v_k(\eta_1) \quad (8.44)$$

the Bogoliubov coefficients are

$$\alpha = 1 + \frac{u}{2ik} \left(1 + \frac{1}{k^2 \eta_1^2} \right) \quad (8.45)$$

$$\beta = \frac{-\eta_1 + \frac{i}{k}}{-\eta_1 - \frac{i}{k}} (1 - \alpha) e^{2ik\eta_1} = -\frac{u}{2ik} e^{-2ik\eta_1} \left(-1 + \frac{i}{k\eta_1} \right)^2 \quad (8.46)$$

8.5 Evaluation of the dirac factor

The dirac function in the perturbation equation comes from the form of the inflaton potential. In this section, we want to derive the coefficient u from the potential in the general framework of DBI inflation. The result in canonical inflation will be obtained with no more effort by taking the $\gamma \rightarrow 1$ limit at the end. Using the Hamilton-Jacobi approach, I can derive the Hubble factor $H(\phi)$ from the expression of the potential $V(\phi)$.

$$V = 3M_p^2 H^2 + \frac{1}{f} \left(1 - \sqrt{1 + 4M_p^4 f \left(\frac{dH}{d\phi} \right)^2} \right) \quad (8.47)$$

Choosing an ansatz

$$H(\phi) = h_0 + h_1(\phi - \phi_1) + h_2(\phi - \phi_1)^2 + h_3(\phi - \phi_1)^3 + \dots \quad (8.48)$$

we find :

$$V_0 = 3M_p^2 h_0^2 + \frac{1}{f(\phi_1)} \left(1 - \sqrt{1 + 4M_p^4 f(\phi_1) h_1^2} \right) \quad (8.49)$$

So we can deduce h_1 from any (V_0, h_0) . The coefficient h_0 remains undetermined. Still with (8.47), equalizing the right and left hand side at next order we find :

$$V_1 = A_{\pm} = 6M_p^2 h_0 h_1 + 4 \frac{\phi_1^3}{\lambda} (1 - \sqrt{R}) - 8M_p^4 \frac{h_1 h_2 - h_1^2 / \phi_1}{\sqrt{R}} \quad (8.50)$$

where we have defined $R = 1 + 4M_p^4 f(\phi_1) h_1^2 = \gamma_1^2$ for simplification. We see that we can deduce h_2 from this equation and express it in terms of V_0 , A_{\pm} and h_0 and that it also depends on the position of the feature ϕ_1 . We also note that h_1 is continuous but h_2 is not. We must define a h_2^+ and a h_2^- . This means that the slow roll parameter ϵ_1 will remain small at the passage of the feature, contrary to ϵ_2 or δ_1 and higher parameters. The parameter δ_1 contains a $d\gamma/d\phi$ that is to say a $d^2 H/d\phi^2$.

At next order, for Starobinsky's potential (8.1)

$$\begin{aligned} V_2 = 0 &= 3M_p^2 (2h_0 h_2 + h_1^2) + \frac{6}{\phi_1^2 f(\phi_1)} (1 - \sqrt{R}) \\ &- \frac{4M_p^4}{\sqrt{R}} \left(\frac{4h_1^2}{\phi_1^2} + 2h_2^2 + 3h_1 h_3 \right) - \frac{32M_p^8}{R^{3/2}} f(\phi_1) h_1^2 \left(h_2 - \frac{h_1}{\phi_1} \right)^2 \end{aligned} \quad (8.51)$$

This equation gives us h_3 . We could go on like this and recursively find h_n up to any n and express it in terms of V_0 , A_{\pm} , h_0 and ϕ_1 . However, we are not particularly interested in higher order coefficients $h_{i>3}$ because z''/z only contains derivatives of H up to the third order. So we will neglect higher order terms in the vicinity of the feature.

We have

$$h_1 = -\frac{1}{2M_p^2} \sqrt{(3M_p^2 h_0^2 - V_0)(2 + f(\phi_1)(3M_p^2 h_0^2 - V_0))} \quad (8.52)$$

and

$$h_2^\pm = -\frac{\sqrt{R}}{8M_p^4 h_1} A_\pm + \frac{h_1}{\phi_1} + \frac{3\sqrt{R}h_0}{4M_p^2} + \frac{\phi_1^3 \sqrt{R}(1-\sqrt{R})}{\lambda 2M_p^4 h_1} \quad (8.53)$$

From these, we can deduce the coefficient u . It is the first term in h_2 which induces the discontinuity. We notice from this computation that h_1 will always be continuous. This means that we cannot obtain a derivative of a dirac δ' in the expression of the z''/z term in the perturbation equation. At best, we obtain a dirac. Features coming from the potential are always of Starobinsky's type (dirac). To obtain representations with derivatives of a dirac, it must come from another source than the potential.

For a generic H with a feature at $\phi = \phi_1$

$$H(\phi) = H_+ Y(\phi - \phi_1) + H_- Y(\phi_1 - \phi) \quad (8.54)$$

where H is the Heaviside function. We choose this writing of $+/-$ to be in accordance with the writing of Starobinsky's potential, $+$ means $\phi > \phi_1$ (before the feature) and $-$ means $\phi < \phi_1$ (after the feature). The correspondence with (8.48) is :

$$H_+ = h_0 + h_1(\phi - \phi_1) + h_2^+(\phi - \phi_1)^2 + h_3^+(\phi - \phi_1)^3 + \dots \quad (8.55)$$

$$H_- = h_0 + h_1(\phi - \phi_1) + h_2^-(\phi - \phi_1)^2 + h_3^-(\phi - \phi_1)^3 + \dots \quad (8.56)$$

From (8.54), we also express the derivatives of the Hubble factor with respect to the inflaton field ϕ

$$\frac{dH}{d\phi}(\phi) = \frac{dH_+}{d\phi} Y(\phi - \phi_1) + \frac{dH_-}{d\phi} Y(\phi_1 - \phi) \quad (8.57)$$

$$\frac{d^2 H}{d\phi^2}(\phi) = \frac{d^2 H_+}{d\phi^2} Y(\phi - \phi_1) + \frac{d^2 H_-}{d\phi^2} Y(\phi_1 - \phi) \quad (8.58)$$

$$\frac{d^3 H}{d\phi^3}(\phi) = \frac{d^3 H_+}{d\phi^3} Y(\phi - \phi_1) + \frac{d^3 H_-}{d\phi^3} Y(\phi_1 - \phi) + \left(\frac{d^2 H_+}{d\phi^2} - \frac{d^2 H_-}{d\phi^2} \right) \delta(\phi - \phi_1) \quad (8.59)$$

We are interested in the last term which is a dirac function. For later use, we rewrite it as

$$\left(\frac{d^2 H_+}{d\phi^2} - \frac{d^2 H_-}{d\phi^2} \right) \delta(\phi - \phi_1) = -2(h_2^+ - h_2^-) \frac{\delta(\eta - \eta_1)}{a_1 \dot{\phi}_1} \quad (8.60)$$

We want to look in more detail at the z''/z term in the perturbation equation. We have written it in terms of the SR coefficients, that is to say in terms of $H(\phi)$ and its derivatives. The ϵ_1 SR parameter can be neglected, but the higher-order SR parameters ϵ_2 , ϵ_3 , δ_1 and δ_2 can't during the fast-roll regime around the feature. ϵ_3 and δ_2 contain third derivatives of H and can thus be represented using δ functions. We can derive the u factor of the $\delta(\eta - \eta_1)$ in the perturbation

equation from a simple analysis of z''/z with $z = a\dot{\phi}\gamma^{3/2}/H$, we see that third derivatives of H can only come from $\dot{\phi}''/\dot{\phi}$ or $\frac{3}{2}\gamma''/\gamma$. We find that

$$u = \frac{2M_p^2 a^2 \dot{\phi}}{\gamma} \frac{d^3 H}{d\phi^3} \left(1 + \frac{2M_p^4}{\gamma^2} f \left(\frac{dH}{d\phi} \right)^2 \right) \quad (8.61)$$

For Starobinsky's potential :

$$u = -\frac{4M_p^2 a_1}{\gamma_1} (h_2^+ - h_2^-) \left(1 + \frac{2M_p^4}{\gamma_1^2} f \left(\frac{dH}{d\phi} \right)^2 \right) \quad (8.62)$$

With (8.53) comes :

$$\begin{aligned} u &= -\frac{4M_p^2 a_1}{\gamma_1} (A_- - A_+) \frac{\gamma_1}{8M_p^4 h_1} \left(1 + \frac{2M_p^4}{\gamma_1^2} f \left(\frac{dH}{d\phi} \right)^2 \right) \\ &= -a_1 \frac{A_+ - A_-}{\gamma_1 \dot{\phi}_1} \left(1 - \frac{1}{2} \left(\frac{1}{\gamma_1^2} - 1 \right) \right) \end{aligned} \quad (8.63)$$

For the canonical case $\gamma = 1$, it simplifies to

$$u = -a_1 \frac{A_+ - A_-}{\dot{\phi}_1} \quad (8.64)$$

with $\dot{\phi}_1 = -A_+/3H_0^2$ comes

$$u = 3H_0 a_1 \left(1 - \frac{A_-}{A_+} \right) \quad (8.65)$$

8.6 Power spectrum and features in canonical inflation

We have solved the perturbation equation (8.40) and we are interested in the long time behavior of the modes evaluated at $\eta_* \rightarrow 0$ implying that

$$v_k(\eta_* \rightarrow 0) = \frac{iH_0}{\sqrt{2}k^{3/2}} (\alpha - \beta) \quad (8.66)$$

From (8.42, 8.45, 8.46) we find that

$$v_k \propto \alpha - \beta = 1 + \frac{u}{k} e^{-ik\eta_1} \frac{1 + \frac{1}{k^2 \eta_1^2}}{i - \frac{1}{k\eta_1}} \left(\cos(k\eta_1) - \frac{\sin(k\eta_1)}{k\eta_1} \right) \quad (8.67)$$

We can study the limits $-k\eta_1 \gg 1$ and $-k\eta_1 \ll 1$. When k is large,

$$(\alpha - \beta)(k \rightarrow \infty) = 1 \quad (8.68)$$

in an oscillatory manner. On the contrary we find that

$$(\alpha - \beta)(k \rightarrow 0) = 1 + \frac{u\eta_1}{3} \quad (8.69)$$

This implies that the power spectrum jumps from small to large k . It is also possible to compute analytically the whole power spectrum so as to predict with more accuracy the form of the spectrum. To do so, we need to compute $|\alpha - \beta|^2$. For $\dot{\phi}_- = -A_-/3H_0$

$$\Delta_{\mathcal{R}}^2 = \frac{9H_0^6}{4\pi^2 a^2 A_-^2} |\alpha - \beta|^2 \quad (8.70)$$

Defining $k_1 = -1/\eta_1$ and $y = k/k_1$ we find

$$\begin{aligned} |\alpha - \beta|^2 = & 1 - \frac{u}{k} \left(\frac{2}{y} \cos(2y) + \left(1 - \frac{1}{y^2}\right) \sin(2y) \right) \\ & + \frac{u^2}{2k^2} \left(1 + \frac{1}{y^2}\right) \left(\left(1 + \frac{1}{y^2}\right) + \left(1 - \frac{1}{y^2}\right) \cos(2y) - \frac{2}{y} \sin(2y) \right) \end{aligned} \quad (8.71)$$

For the factor u in Starobinsky's model given in (8.65)

$$\alpha = 1 + \frac{3i}{2} \frac{k_1}{k} \left(\frac{A_-}{A_+} - 1 \right) \left(1 + \frac{k_1^2}{k^2} \right) \quad (8.72)$$

$$\beta = -\frac{3i}{2} \left(\frac{A_-}{A_+} - 1 \right) e^{2ik/k_1} \frac{k_1}{k} \left(1 + i \frac{k_1}{k} \right)^2 \quad (8.73)$$

and

$$\begin{aligned} |\alpha - \beta|^2 = & 1 + \frac{3}{y} \left(1 - \frac{A_-}{A_+}\right) \left(\frac{2}{y} \cos(2y) + \left(1 - \frac{1}{y^2}\right) \sin(2y) \right) \\ & + \frac{9}{2y^2} \left(1 - \frac{A_-}{A_+}\right)^2 \left(1 + \frac{1}{y^2}\right) \left(1 + \frac{1}{y^2} + \left(1 - \frac{1}{y^2}\right) \cos(2y) - \frac{2}{y} \sin(2y)\right) \end{aligned} \quad (8.74)$$

With this expression, we can plot the power spectrum or study its IR and UV limits

$$|\alpha - \beta|^2(k \rightarrow \infty) \rightarrow 1 \quad (8.75)$$

$$|\alpha - \beta|^2(k = 0) \rightarrow \left(\frac{A_-}{A_+} \right)^2 \quad (8.76)$$

So the jump in the spectrum exclusively depends on the ratio between the slopes of the potential. For details on the computation of these limits, refer to appendix B.

8.7 Perturbation equation in DBI : challenges

The sound speed $c_s = 1/\gamma \neq 1$ is time dependent and evolves consequently during the e-fold of fast-rolling. Hence we do not know how to solve the perturbation equation. We are not even sure that we can match the slow-roll solution before the feature to the slow-roll solution after the feature. Even though fast-roll lasts less than one e-fold, the terms in ϵ_2 and δ_1 are not negligible. This is a big difference with the canonical case where there is a convenient cancellation in the SR parameters. We don't know the form of the solution when the SR parameters cannot be neglected. We have tried different approaches to solve the perturbation equation.

The first and simplest approach consists in solving the two de Sitter perturbation equations before and after the feature and matching them. The sound speed at the feature is estimated as $c_s(\eta_1) \simeq (c_s(N_1 + 1) + c_s(N_1 - 1))/2$. When assuming c_s is constant and neglecting ϵ_2 and δ_1 , we find by a direct analogy with the canonical case that

$$v_k^-(\eta_1) = \frac{H_0}{\sqrt{2kc_s^-}} \alpha \left(-\eta_1 + \frac{i}{kc_s^-} \right) e^{-ikc_s^- \eta_1} \quad (8.77)$$

$$+ \frac{H_0}{\sqrt{2kc_s^-}} \beta \left(-\eta_1 - \frac{i}{kc_s^-} \right) e^{ikc_s^- \eta_1} \quad (8.78)$$

with the limit

$$v(k \rightarrow 0) = \frac{iH_0}{\sqrt{2(kc_s^-)^3}} \left[1 + \frac{A_+ - A_-}{3\gamma_1 H_0 \dot{\phi}_1} \left(1 - \frac{1}{2} \left(\frac{1}{\gamma_1^2} - 1 \right) \right) \right] \quad (8.79)$$

and that

$$\Delta_{\mathcal{R}}^2 = \frac{k^3}{2\pi^2} \frac{|v|^2}{|z|^2} = \frac{H_0^4}{4\pi^2 a^2 \dot{\phi}_-^2} |\alpha - \beta|^2 = \frac{H_0^4 f \gamma_-^2}{4\pi^2 a^2 (\gamma_-^2 - 1)} |\alpha - \beta|^2 \quad (8.80)$$

with

$$\begin{aligned} |\alpha - \beta|^2 &= 1 - \frac{A_+ - A_-}{\dot{\phi}_1 \gamma_1 H_1} \left(1 - \frac{1}{2} \left(\frac{1}{\gamma_1^2} - 1 \right) \right) \frac{1}{y} \left(\frac{2}{y} \cos(2y) + \left(1 - \frac{1}{y^2} \right) \sin(2y) \right) \\ &+ \frac{(A_+ - A_-)^2}{2\dot{\phi}_1^2 \gamma_1^2 H_1^2} \left(1 - \frac{1}{2} \left(\frac{1}{\gamma_1^2} - 1 \right) \right)^2 \frac{1}{y^2} \left(1 + \frac{1}{y^2} \right) \left(1 + \frac{1}{y^2} + \left(1 - \frac{1}{y^2} \right) \cos(2y) - \frac{2}{y} \sin(2y) \right) \end{aligned}$$

But this prediction does not fit with the numerical spectrum.

Since we observe that the γ factor evolves rapidly during the fast-roll regime, we can define a sound speed before the feature c_s^+ and a sound speed after the feature c_s^- . In this case the junction conditions bear some factors c_s^+/c_s^- . But this analysis would imply that the γ factor is discontinuous so what we rather do is consider a slowly varying sound speed in the pre-feature slow-roll regime,

a slowly varying sound speed in the post-feature slow-roll regime and a non-zero time derivative of the sound speed at the feature. Since c'_s is discontinuous, it is ill-defined at η_1 so we simply set

$$c'_s(\eta_1) \sim H_1 a_1 \frac{c_s^- - c_s^+}{\Delta N_{\text{FR}}} \quad (8.81)$$

Then

$$v_k^+(\eta_1) = \frac{H_1}{\sqrt{2kc_s^+}} \left(-\eta_1 + \frac{i}{kc_s^+} \right) e^{-ikc_s^+ \eta_1} \quad (8.82)$$

and

$$v_k^-(\eta_1) = \frac{H_1}{\sqrt{2kc_s^-}} \alpha \left(-\eta_1 + \frac{i}{kc_s^-} \right) e^{-ikc_s^- \eta_1} + \frac{H_1}{\sqrt{2kc_s^-}} \alpha \left(-\eta_1 - \frac{i}{kc_s^-} \right) e^{ikc_s^- \eta_1} \quad (8.83)$$

where we have defined a sound speed (right) before the feature c_s^+ and a sound speed (right) after the feature c_s^- . In this case, v'_k bears derivatives $c'_s(\eta_1)$. The Bogoliubov factors computed with this method lead to a spectrum much different from the numerical one.

We have even thought of assuming that the γ factor was not continuous and brought a derivative of a dirac δ' in the perturbation equation

$$v_k'' + (k^2 c_s^2 + u\delta + b\delta') v_k = 0 \quad (8.84)$$

But it is totally physically incoherent to consider that the γ factor is not continuous. As we have said in section 8.5, no δ' can come from the potential. All the same the phenomenological model of a perturbation equation with both a δ term and a δ' term (see appendix D) is conceivable but it is not successful in accounting for the shape of the numerical spectrum.

We have not found a solution which fits with the numerical results (e.g. figure 8.5). After many tests, we trust our code for the resolution of the background as well as the perturbations. We rather blame our analytical analysis.

The problem is that we cannot find any reasonable approximation to solve the perturbation equation with the abruptly varying sound speed, with the terms in ϵ_2 and δ_1 and with the dirac. The width of the fast roll regime jeopardizes the analytical analysis and ruins all simplicity.

We have also tried to phenomenologically find the dependence of the jump in the spectrum on the ratio A_-/A_+ but failed to bring out a pattern. The dependence is probably highly non trivial. We can only do some observations, for example with the plot 8.5 we notice that the jump is much smaller than what would be expected in the canonical case with the same ratio A_-/A_+ .

So there is still much work to do on the subject so as to understand how things work and how to treat analytically such a perturbation equation.

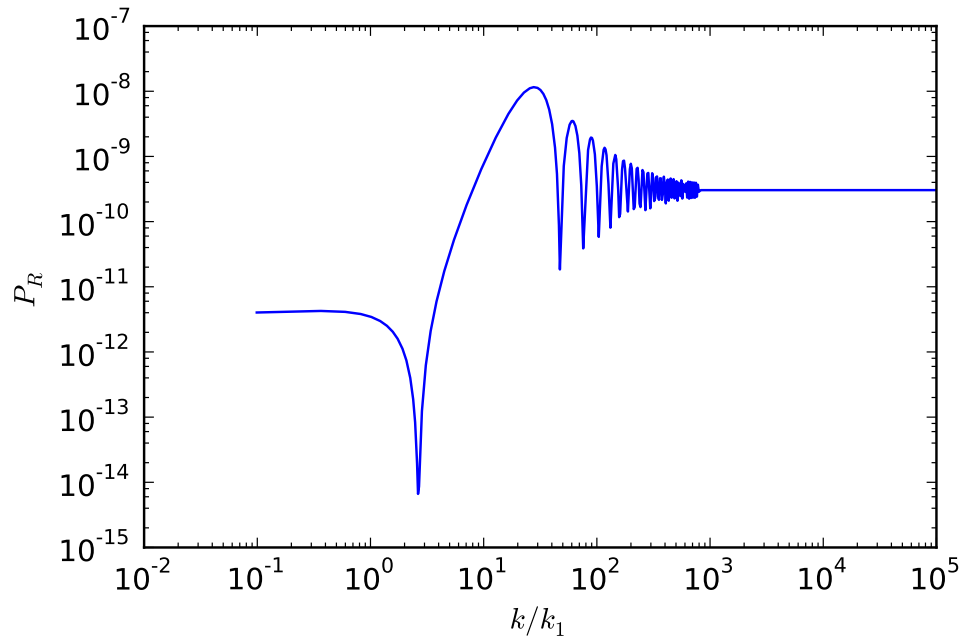


Figure 8.5: Numerical DBI scalar power spectrum for Starobinsky's potential with $A_-/A_+ = 10^{-2}$. k_1 can be chosen in the observable window.

8.8 Numerical analysis

We plot the theoretical power spectrum and compare it with the power spectrum obtained by integrating numerically the background and the perturbations with a Fortran 77 code. The code was first tested on Starobinsky's canonical case. The numerical results were a perfect match to the predictions. The code solves the background and the perturbations using a 4th order Runge-Kutta solver with adaptative time steps. For the background, we compute the evolution of the vector $\begin{pmatrix} \phi \\ \dot{\phi} \end{pmatrix} (N)$. This choice is extremely important for the code to run well. To compute the potential (8.1), we use a regularized expression with hyperbolic tangents. Extending V as a distribution, we may write

$$\frac{dV}{d\phi} = (A_+ - A_-)Y(\phi - \phi_0) + A_- \quad \text{where } Y \text{ is a Heaviside function.} \quad (8.85)$$

We must be careful with the normalization of each variable. For the perturbations, we must define the range of momenta over which to integrate. The largest

mode corresponds to the mode created at the beginning of inflation

$$k_{\text{phys}}^{\text{ini}} = CH^{\text{ini}}\gamma^{\text{ini}} \quad (8.86)$$

The constant C controls at which depth under the Hubble radius are chosen the initial conditions. The final mode corresponds to the mode which crosses the Hubble radius at the end of inflation. Since it is too small, we increase it phenomenologically, we choose a cut-off before the Hubble rate varies too much. The momenta range is logarithmically sampled. For each momentum, the initial conditions are different. They are determined with the first background integration and a spline interpolation of each function. Then the background and perturbations are integrated all together from $N_{\text{ini}}(k)$. We must check that the mode is indeed inside the Hubble radius at the beginning and check that $N_{\text{ini}}(k) < N_{\text{feature}}$. We define the real and imaginary parts of the Mukhanov-Sasaki variable v , the z variable and the curvature perturbation \mathcal{R} . We express z''/z in terms of the slow-roll parameters. The perturbation equation both for the real and imaginary parts is written in e-fold number

$$\frac{d^2v}{dN^2} + (1 - \epsilon_1) \frac{dv}{dN} + \left(\frac{k^2}{\gamma^2} - \frac{z''}{z} \right) \frac{v}{a^2 H^2} = 0 \quad (8.87)$$

For each momentum we store the value of the curvature perturbation at sound horizon crossing. In the end we can build the power spectrum.

8.9 About features

In [118]–[127], steps and features in the power spectra are studied and the CMB data is analyzed to search for features. In [117, 128, 129, 130], features are physically motivated by something else than a step-like potential. Their origin is a varying sound speed in k-inflation [130] or a varying warp factor [117] or brane annihilation [129] in DBI inflation, or a coupling with matter in canonical inflation [128]. In the next chapter, features from the coupling with matter fields will be studied in the context of k-inflation.

Coupling with matter

“Nothing will come of nothing”, W. Shakespeare

One salient characteristic of DBI inflation is that matter can be produced during inflation. Imagine that some trapped D3 branes are stuck at fixed points of orbifold symmetries. There are no direct interactions between parallel BPS branes but particles living on trapped branes can be coupled to the inflaton.

In *“Trapped Inflation”* [131], the authors consider a quartic coupling

$$\sum_i g^2 (\phi - \phi_i)^2 \chi_i^2 \tag{9.1}$$

between the inflaton and matter fields. The general idea is that inflation may occur even with a very steep potential in this context because particle production and backreaction slow down the inflaton. I have worked on this idea in the context of DBI inflation where the coupling with matter is indeed justified in the presence of trapped branes inside the throat ; and where inflation in the relativistic regime does not require a flat potential so that we do not need a spectacular slowing-down effect from backreaction to have a coherent model of inflation. I will consider every possible regime of particle creation and carefully justify my approximations.

9.1 WKB approximation

We study DBI inflation with a quadratic potential. Up to section 9.6, we will exclusively focus on the quadratic potential. We take into account the presence of one trapped brane. The trapped brane has an influence on the inflationary brane evolution. To determine its effect we need to study the quantum modes of the matter field χ . Let us expand the quantum field χ in terms of creation and

annihilation operators. For convenience sake we work in conformal time. The field reads

$$\chi(\eta) = \int \frac{d^3k}{(2\pi)^3} (a_k \chi_k(\eta) e^{ikx} + a_k^\dagger \chi_k^*(\eta) e^{-ikx}) \quad (9.2)$$

and each mode satisfies the Klein-Gordon equation

$$\chi_k'' + 2\mathcal{H}\chi_k' + k^2\chi_k + a^2g^2|\phi - \phi_1|^2\chi_k = 0 \quad (9.3)$$

We can put it in a Schrodinger form by defining

$$\Psi(\eta) = a\chi(\eta) \quad (9.4)$$

So Ψ obeys

$$\Psi_k'' + \omega_k^2\Psi_k = 0 \quad (9.5)$$

with a time dependent frequency

$$\omega_k(\eta) = \sqrt{k^2 + A(\eta)}, \quad A(\eta) = a^2g^2|\phi - \phi_1|^2 - \frac{a''}{a} \quad (9.6)$$

where ϕ is the unperturbed $\phi(\eta)$ corresponding to the unperturbed motion of the inflationary brane (see section 6.2). Here we have assumed ω_k^2 positive. When it is negative, the regime is tachyonic and the frequency will be written $\Omega_k = \pm i\omega_k = \pm i\sqrt{|k^2 + A(\eta)|}$, so that $\Omega_k^2 = -\omega_k^2 > 0$. The equation for the modes (9.5) can be approximately solved using the Wentzel-Kramers-Brillouin or WKB approximation. Far in the past, the solution is assumed to be in a Bunch-Davies vacuum where for $\eta \rightarrow -\infty$ we have

$$\Psi_k(\eta) = \frac{1}{\sqrt{2\omega_k(\eta)}} e^{-i\int^\eta \omega_k(\eta')d\eta'} \quad (9.7)$$

When the inflationary brane has passed through the trapped brane it is a mixture of two possible modes

$$\Psi_k(\eta) = \frac{\alpha_k(\eta)}{\sqrt{2\omega_k(\eta)}} e^{-i\int^\eta \omega_k(\eta')d\eta'} + \frac{\beta_k(\eta)}{\sqrt{2\omega_k(\eta)}} e^{i\int^\eta \omega_k(\eta')d\eta'} \quad (9.8)$$

where α_k and β_k are the Bogoliubov coefficients. The WKB approximation is valid when $|\frac{\omega'}{\omega^2}| \ll 1$. We define

$$R = \left| \frac{\omega'}{\omega^2} \right| \quad (9.9)$$

and find

$$R = \left| \frac{\mathcal{H}g^2a^2|\phi - \phi_1|^2 + \phi'g^2a^2|\phi - \phi_1| - \frac{1}{2}\left(\frac{a''}{a}\right)'}{(k^2 + a^2g^2|\phi - \phi_1|^2 - \frac{a''}{a})^{3/2}} \right| \quad (9.10)$$

Our goal is to determine under which conditions the WKB approximation is violated. There are two physically different situations where the analysis can be easily carried out. They depend on

$$\xi = \frac{H^2}{g|\dot{\phi}|} \quad (9.11)$$

which is a constant in DBI inflation with a quadratic potential as appears from equations (6.16, 6.18, 6.20)

$$\xi = \frac{1}{g\epsilon^2\sqrt{\lambda}} \approx \frac{\sqrt{\lambda}}{3g^3} \left(\frac{m}{M_P} \right)^2 \quad (9.12)$$

The creation of particles is very different for small or large ξ .

9.2 Small ξ regime

In this region of the parameter space, the creation of particles occurs when the DBI brane is close to the trapped brane which corresponds to the regime where

$$|\phi - \phi_1| \ll \frac{|\dot{\phi}|}{H} \quad (9.13)$$

In this case the R factor becomes

$$R \approx R_{\text{near}} = \frac{|\phi' g^2 a^2 |\phi - \phi_1| - \frac{1}{2} \left(\frac{a''}{a} \right)' |}{|k^2 + a^2 g^2 |\phi - \phi_1|^2 - \frac{a''}{a}|^{3/2}} \quad (9.14)$$

and non-adiabaticity is mainly present in the region where $g^2 a^2 |\phi - \phi_1|^2 \gg \frac{a''}{a}$ (or equivalently $g^2 |\phi - \phi_1|^2 \gg 2H^2$) for which we have

$$R \approx \left| \frac{\phi' g^2 a^2 |\phi - \phi_1|}{(k^2 + a^2 g^2 |\phi - \phi_1|^2)^{3/2}} \right| \quad (9.15)$$

From now on we define

$$\mathcal{K} = \frac{k}{a} \quad (9.16)$$

which corresponds to physical momenta. The creation of particles arises when $R > 1$ at its maximum. When deriving (9.15) with respect to $g|\phi - \phi_1|$ we find that this maximum is located at $g^2 |\phi - \phi_1|^2 = \frac{\mathcal{K}^2}{2}$ and is given by

$$R_{\text{max}} = \frac{2}{3^{3/2}} \frac{g|\dot{\phi}|}{\mathcal{K}^2} \quad (9.17)$$

implying that the creation of particles occurs when $\mathcal{K} \leq \frac{\sqrt{2}}{3^{3/4}} \sqrt{g|\dot{\phi}|}$. The maximal extension of the non-adiabatic region is

$$\Delta\phi = \frac{1}{3^{3/4}} \sqrt{\frac{|\dot{\phi}|}{g}} \quad (9.18)$$

Notice that $\Delta\phi \gg \frac{H}{g}$ as $\xi \ll 1$. Inside a region of size $|\phi - \phi_1| \leq H/g$ around the origin, there is a domain of non-adiabaticity when

$$R \approx \frac{\left| \left(\frac{a''}{a} \right)' \right|}{2|k^2 - \frac{a''}{a}|^{3/2}} > 1 \quad (9.19)$$

corresponding to

$$\sqrt{2 - 2^{2/3}}H \leq \mathcal{K} \leq \sqrt{2 + 2^{2/3}}H \quad (9.20)$$

Due to the very small width of this zone in momentum space, virtually no particles are created in this interval. Finally when $\mathcal{K} \leq \sqrt{2}H$, there is a tachyonic instability. The size of the tachyonic region is much smaller than the size of the non-adiabaticity region where most particles are created. In fact, the creation of particles in the tachyonic region is negligible as it scales like $\exp(H\Delta t_{\text{tachyon}}) \sim \exp(\xi) \sim 1$ where the time spent in the tachyonic region is $\Delta t_{\text{tachyon}} \sim \frac{H}{g|\dot{\phi}|}$. It is interesting to notice that the time spent by the brane in the interaction region is

$$\Delta t = \frac{1}{3^{3/4}} \frac{\sqrt{\xi}}{H} \quad (9.21)$$

implying that the interaction lasts less than a Hubble time and therefore the interaction time corresponds to a number of e-folds

$$\Delta N = \frac{\Delta a}{a} \approx \sqrt{\xi} \ll 1 \quad (9.22)$$

The interaction is almost instantaneous. So far we have used the fact that the Hubble rate is nearly constant in the interaction region. This can be ascertained as the variation of the Hubble rate in the interaction region is given by

$$\left| \frac{\Delta H}{H} \right| \approx \frac{1}{(g\sqrt{\lambda})^{1/2}} \quad (9.23)$$

Therefore we must impose that $g\sqrt{\lambda} \gg 1$. This is always the case in this regime when $\epsilon \ll 1$. The Hubble rate H being constant in the interaction region, the boundaries for the physical momentum in the interval (9.20) for instance are time-independent.

9.3 Large ξ regime

In this case, the ratio R can be simplified in two regions depending on whether the DBI brane has moved far from the trapped brane or not. If the inflationary brane is far from the trapped brane then $|\phi - \phi_1| \gg \dot{\phi}/H$ and

$$R \approx R_{\text{far}} = \frac{|\mathcal{H}g^2a^2|\phi - \phi_1|^2 - \frac{1}{2}\left(\frac{a''}{a}\right)'|}{|k^2 + a^2g^2|\phi - \phi_1|^2 - \frac{a''}{a}|^{3/2}} \quad (9.24)$$

On the contrary, if they are close, $|\phi - \phi_1| \ll \dot{\phi}/H$ so

$$R \approx R_{\text{near}} = \frac{|\phi' g^2 a^2 |\phi - \phi_1| - \frac{1}{2} \left(\frac{a''}{a}\right)'|}{|k^2 + a^2 g^2 |\phi - \phi_1|^2 - \frac{a''}{a}|^{3/2}} \approx \frac{\left|\left(\frac{a''}{a}\right)'\right|}{2|k^2 - \frac{a''}{a}|^{3/2}} \quad (9.25)$$

These two regimes capture all the physics of the χ -particle creation. First, we will study the case when the two branes are far from each other. The ratio R is maximal when $g^2|\phi - \phi_1|^2 = 2\mathcal{K}^2 + (2 - 7\epsilon)H^2$ and its value is simply

$$R_{\text{max}} = \frac{|2H\mathcal{K}^2 - 4\epsilon H^3|}{|3\mathcal{K}^2 - 6\epsilon H^2|^{3/2}} \quad (9.26)$$

We find that there is a pole for $\mathcal{K}_{\text{pole}} = \sqrt{2\epsilon}H$. The value at the origin is very large: $R_{\text{max}}(\mathcal{K} = 0) \approx \epsilon^{-1/2} \gg 1$ as $\epsilon \ll 1$. In all the interval between the origin and the pole, R_{max} is greater than one. We want to determine the physical momentum \mathcal{K}_{max} for which $R_{\text{max}} = 1$ and then becomes smaller than unity for larger momenta. Expanding around the pole

$$R_{\text{max}} = \frac{2}{3\sqrt{3}} \frac{H}{(\mathcal{K}^2 - \mathcal{K}_{\text{pole}}^2)^{1/2}} \quad (9.27)$$

implying that

$$\mathcal{K}_{\text{max}}^2 \approx \frac{4H^2}{27}. \quad (9.28)$$

Hence we find that for physical momenta $0 < \mathcal{K} < \mathcal{K}_{\text{max}} \approx \frac{2H}{3\sqrt{3}}$, the WKB approximation is violated around $g^2|\phi - \phi_1|^2 = 2(\mathcal{K}^2 + H^2)$. Therefore there are two non-adiabatic regions far from the trapped brane: regions I and II centered respectively around ϕ_A and ϕ_B . The approximation used here is valid as the maximal extension of the interaction zone is given by $\Delta\phi \approx \frac{H}{g}$ implying that $\Delta\phi \gg |\dot{\phi}|/H$ when $\xi \gg 1$.

We now consider when the inflationary brane and the trapped brane are close to each other. From (9.25), we find that $R > 1$ when

$$\sqrt{2 - 2^{2/3}}H < \mathcal{K} < \sqrt{2 + 2^{2/3}}H \quad (9.29)$$

The inequality (9.29) gives the range of physical momenta for which a non-adiabatic region appears in the immediate vicinity of the trapped brane. It is consistent with $g^2|\phi - \phi_1|^2 \ll 2H^2$ as $\xi \gg 1$. On top of the non-adiabatic instability detailed above, there is a tachyonic resonance when $\omega_k^2 < 0$ corresponding to

$$\mathcal{K}^2 + g^2|\phi - \phi_1|^2 - 2H^2 < 0 \quad (9.30)$$

So for physical momenta larger than $2H^2$, there is no tachyonic regime. We define η_- and η_+ as the two turning points such that $\omega_k^2(\eta_-) = \omega_k^2(\eta_+) = 0$.

There is a physical momentum \mathcal{K}^* for which the non-adiabatic and tachyonic regions intersect in just one point. For $0 < \mathcal{K} < \mathcal{K}^*$, the regions intersect and for $\mathcal{K}^* < \mathcal{K} < \mathcal{K}_{\max}$ the tachyonic region and the non-adiabatic region are disconnected. In the tachyonic regime, we also use the WKB approximation. It is valid when $\left| \frac{\Omega'_k}{\Omega_k^2} \right| < 1$ and the modes are

$$\Psi_k(\eta) = \frac{a_k(\eta)}{\sqrt{2\Omega_k(\eta)}} e^{-\int^\eta \Omega_k(\eta') d\eta'} + \frac{b_k(\eta)}{\sqrt{2\Omega_k(\eta)}} e^{\int^\eta \Omega_k(\eta') d\eta'} \quad (9.31)$$

The Bogoliubov coefficients change after going through a non-adiabatic region. The interaction time can be estimated and gives

$$H\Delta t \approx \xi \quad (9.32)$$

leading to

$$\Delta N = \frac{\Delta a}{a} \approx \xi \quad (9.33)$$

So the interaction region is spread out over a large number of efoldings. Moreover we must impose that the variation of the Hubble rate is small in the interaction region

$$\frac{\Delta H}{H} \approx \frac{1}{g\epsilon\sqrt{\lambda}} \quad (9.34)$$

hence we must have $g\epsilon\sqrt{\lambda} \gg 1$.

9.4 Creation of particles

We are interested in the particles created when the inflationary brane crosses the trapped brane. This happens when the WKB approximation breaks down. Let us first concentrate on the $\xi \gg 1$ regime. We have found different situations depending on the physical momentum \mathcal{K} . The configuration where $0 < \mathcal{K} < \mathcal{K}_{\max}$ is the most complex. There are two symmetric non-adiabatic regions far from ϕ_1 and a tachyonic region in the proximity of ϕ_1 . The tachyonic region intersect with the non-adiabatic regions for $0 < \mathcal{K} < \mathcal{K}^* < \mathcal{K}_{\max}$. For $\mathcal{K}_{\max} < \mathcal{K} < \sqrt{2 - 2^{2/3}}H$, the tachyonic region is still there but we no longer have any non-adiabatic region. For $\sqrt{2 - 2^{2/3}}H < \mathcal{K} < \sqrt{2}H$, there is a tachyonic region and inside of it a non-adiabatic zone. For $\sqrt{2}H < \mathcal{K} < \sqrt{2 + 2^{2/3}}H$, there is no tachyonic resonance but there is a non-adiabatic region around ϕ_1 . Finally for any $\mathcal{K} > \sqrt{2 + 2^{2/3}}H$, there is no tachyonic resonance and the regime is always adiabatic. Notice that all these intervals are easy to interpret using the physical wave number \mathcal{K} . The size of the physical intervals in \mathcal{K} is time-independent.

Let us first study the creation of particles for $0 < \mathcal{K}^* < \mathcal{K} < \mathcal{K}_{\max}$. This case is typical and will allow us to deduce the particle spectrum in the other intervals

too.

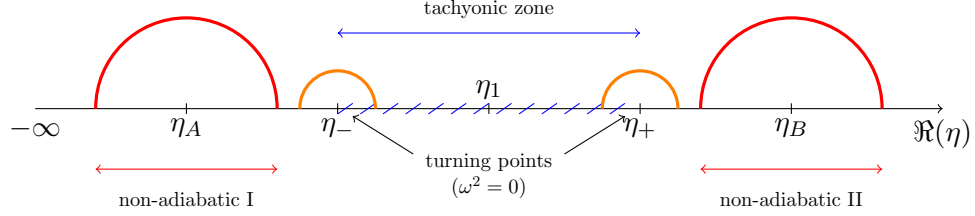


Figure 9.1: Configuration of the interaction zone in the complex plane for $\mathcal{K}^* < \mathcal{K} < \mathcal{K}_{\max}$

Initially, for $\eta \rightarrow -\infty$, the modes are in a Bunch-Davies vacuum. Then the WKB approximation breaks down in the non-adiabatic region I, far enough from it the modes become

$$\Psi_k(\eta) = \frac{\alpha_k(\eta)}{\sqrt{2\omega_k(\eta)}} e^{-i \int^\eta \omega_k(\eta') d\eta'} + \frac{\beta_k(\eta)}{\sqrt{2\omega_k(\eta)}} e^{i \int^\eta \omega_k(\eta') d\eta'} \quad (9.35)$$

We need to determine the two Bogoliubov coefficients.

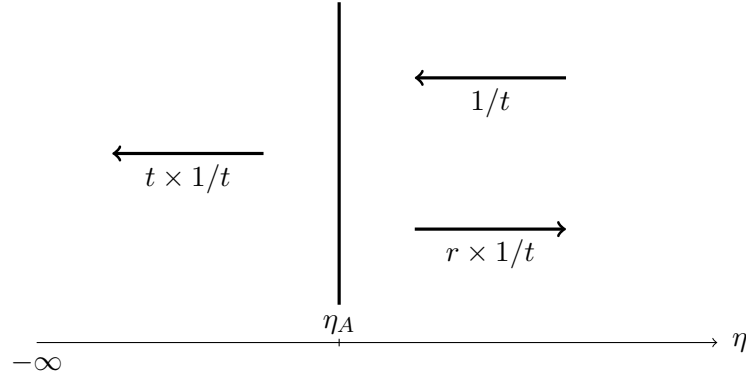


Figure 9.2: Computation of Bogoliubov coefficients around region I by analogy with wave propagation

In fact they can be expressed as transmission and reflection coefficients t and r (see [132])

$$\alpha_k(\eta < \eta_A) = t\alpha_k(\eta > \eta_A) \text{ and } \beta_k(\eta > \eta_A) = r\alpha_k(\eta > \eta_A) \quad (9.36)$$

where the conformal time η increases. So with the chosen initial condition $\alpha_k(-\infty) = 1$, this gives

$$\alpha_k(\eta > \eta_A) = 1/t, \quad \beta_k(\eta > \eta_A) = r/t \quad (9.37)$$

The solution before the non-adiabatic region I is linked to the solution on the other side of the non-adiabatic region by an analytic continuation in the complex plane. We consider that the time variable η is a complex variable. We draw a contour around $\eta = \eta_A$ in the complex plane (see figure 1). The radius of this semi-circle must be large enough for the WKB approximation to be valid before and after the non-adiabatic region. This is the case if

$$\omega_k(\eta_A)|\eta - \eta_A| \gtrsim R(\eta_A) = R_{\max} \quad (9.38)$$

and we trust the expansion of ω_k^{-1} around η_A

$$\frac{1}{\omega_k(\eta)} = \frac{1}{\omega_k(\eta_A)} - \left(\frac{\omega'_k}{\omega_k^2}\right)(\eta_A)(\eta - \eta_A) - \sum_{n=2}^{\infty} \frac{R_A^{(n-1)}}{n!}(\eta - \eta_A)^n \quad (9.39)$$

where $R_A^{(n)}$ is the n-th derivative of R at η_A . The condition on the size of the semi-circle implies that

$$\omega_k(\eta) \approx -\frac{1}{R_{\max}(\eta - \eta_A)} \quad (9.40)$$

Using the fact that in the non-adiabatic region $\omega_k(\eta_A) = \mathcal{O}(aH)$ and $R_A = \mathcal{O}(\frac{H}{\mathcal{K}}) = \mathcal{O}(1)$, the condition on the contour is equivalent to $\delta t \gtrsim 1/H$. Now the duration of the interaction region is $\frac{H}{g|\phi|}$ implying that the contour circling around the non-adiabatic region is much smaller than the interaction region. As a result we obtain that

$$\exp\left(\pm i \int \omega_k(\eta') d\eta'\right) \approx \exp\left(\mp i \int \frac{1}{R_{\max}(\eta' - \eta_A)} d\eta'\right) \quad (9.41)$$

Notice that $\eta - \eta_A$ is negative before the non-adiabatic region and positive later on. A positive-frequency mode is changed in a negative-frequency mode when going through the non-adiabatic region (and vice versa). With $(\eta - \eta_A) = \rho e^{i\theta}$ and $d\eta = i\rho e^{i\theta} d\theta$, the contour integral is given by the residue theorem. A factor of i also appears from $\eta - \eta_A \rightarrow e^{i\pi}(\eta_A - \eta)$ in $\frac{1}{\sqrt{2\omega_k}}$ so finally

$$\beta_k = -i \exp(-2i\theta^A) \exp\left(\frac{\pi}{R_{\max}}\right) = -i \exp(-2i\theta^A) \exp\left(\frac{3\sqrt{3}\pi \mathcal{K}_A}{2H}\right) \quad (9.42)$$

with $\mathcal{K}_A = k/a_A$ and the phase is

$$\theta^A = \int_{-\infty}^{\eta_A} \omega_k d\eta \quad (9.43)$$

Probability conservation imposes $|\alpha_k|^2 - |\beta_k|^2 = 1$, so we deduce

$$\alpha_k = e^{i\varphi} \sqrt{1 + \exp\left(3\sqrt{3}\pi \frac{\mathcal{K}_A}{H}\right)} \quad (9.44)$$

where φ is a random phase.

We now compute the Bogoliubov coefficient b_k of the non-vanishing wave in the tachyonic region [38]. We neglect the decaying mode in this region depending on the coefficient a_k . We draw a contour around the turning point η_- where $\omega_k^2(\eta_-) = 0$. We assume the radius of the semi-circle is large enough for the WKB approximation to be valid along the contour :

$$\omega_k^2 = \frac{d\omega_k^2}{d\eta}(\eta_-)(\eta - \eta_-) \quad (9.45)$$

After an analytic continuation we find

$$b_k = \alpha_k e^{-i(\theta^- + \frac{\pi}{4})} + \beta_k e^{i(\theta^- + \frac{\pi}{4})} \quad (9.46)$$

with the phase

$$\theta^- = \int_{-\infty}^{\eta_-} \omega_k d\eta \quad (9.47)$$

depending on the wave evolution before the turning point. Then passing around the second turning point at η_+ , we obtain a new contribution to the Bogoliubov coefficients.

$$\tilde{\beta}_k = e^{\int_{\eta_-}^{\eta_+} \Omega d\eta} e^{-i(\theta^- + \frac{\pi}{4})} b_k = e^{\int_{\eta_-}^{\eta_+} \Omega d\eta} \left(\beta_k + \alpha_k e^{-2i(\theta^- + \frac{\pi}{4})} \right) \quad (9.48)$$

$$\tilde{\alpha}_k = e^{\int_{\eta_-}^{\eta_+} \Omega d\eta} e^{i(\theta^- + \frac{\pi}{4})} b_k = e^{\int_{\eta_-}^{\eta_+} \Omega d\eta} \left(\alpha_k + \beta_k e^{2i(\theta^- + \frac{\pi}{4})} \right) \quad (9.49)$$

The final contribution comes from the non-adiabatic region II where the wave appears to break into reflected and transmitted ones

$$\tilde{\alpha}_k \chi_- \rightarrow R_- \chi_+ + T_- \chi_- \quad (9.50)$$

$$\tilde{\beta}_k \chi_+ \rightarrow R_+ \chi_- + T_+ \chi_+ \quad (9.51)$$

We are particularly interested in the final Bogoliubov coefficient

$$\beta_k^f = R_- + T_+ \quad (9.52)$$

The first situation (9.50) is the same as in (9.36) but with a phase θ^B .

$$R_- = \frac{r}{t} \tilde{\alpha}_k = -i \exp(-2i\theta^B) \exp\left(\frac{3\sqrt{3}\pi}{2} \frac{\mathcal{K}_B}{H}\right) \tilde{\alpha}_k \quad (9.53)$$

where $\mathcal{K}_B = k/a_B$

The second situation (9.51) is the dual configuration for Ψ^* as represented in figure 9.3, where we find

$$|T_+|^2 = |\tilde{\beta}_k|^2 \left(1 + \left| \frac{r^*}{t^*} \right|^2 \right) \quad (9.54)$$

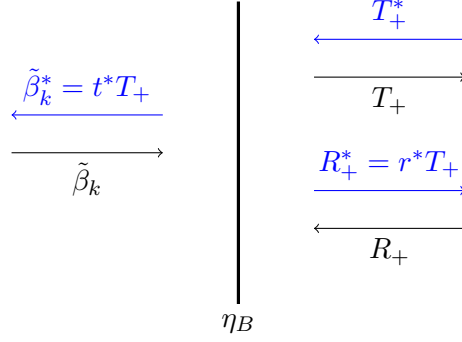


Figure 9.3: Computation of Bogoliubov coefficients around region II by analogy with wave propagation

via current conservation.

Therefore we can introduce another phase ϑ such that

$$T_+ = e^{i\vartheta} \tilde{\beta}_k \sqrt{1 + e^{3\sqrt{3}\pi \frac{\mathcal{K}_B}{H}}} \quad (9.55)$$

As a result we find the Bogoliubov coefficient

$$\begin{aligned} \beta_k^f = & -i \left(e^{2i(\theta^- - \theta^A - \theta^B)} e^{3\sqrt{3}\pi \frac{\mathcal{K}_A + \mathcal{K}_B}{2H}} + e^{i\varphi + i\vartheta - 2i\theta^-} \sqrt{(1 + e^{3\sqrt{3}\pi \frac{\mathcal{K}_A}{H}})(1 + e^{3\sqrt{3}\pi \frac{\mathcal{K}_B}{H}})} \right. \\ & \left. + e^{i\varphi - 2i\theta^B} e^{\frac{3\sqrt{3}\pi}{2} \frac{\mathcal{K}_B}{H}} \sqrt{1 + e^{3\sqrt{3}\pi \frac{\mathcal{K}_A}{H}}} + e^{i\vartheta - 2i\theta^A} e^{\frac{3\sqrt{3}\pi}{2} \frac{\mathcal{K}_A}{H}} \sqrt{1 + e^{3\sqrt{3}\pi \frac{\mathcal{K}_B}{H}}} \right) e^{\int_{\eta^-}^{\eta^+} \Omega_k d\eta} \quad (9.56) \end{aligned}$$

Let us now examine the other regions. For $\mathcal{K}_{\max}^2 < \mathcal{K}^2 < (2 - 2^{2/3})H^2$, there is a purely tachyonic contribution. For $\alpha_k(-\infty) = 1$, we know from (9.48) that

$$|\beta_k^f|^2 = e^{2 \int_{\eta^-}^{\eta^+} \Omega_k d\eta} \quad (9.57)$$

The same behavior is valid for $(2 - 2^{2/3})H^2 < \mathcal{K}^2 < 2H^2$ because the non-adiabatic region has no importance when it is included in the tachyonic regime. Indeed the passage through the non-adiabatic region in a tachyonic region only changes the phase of the Bogoliubov coefficients.

When $2H^2 < \mathcal{K}^2 < (2 + 2^{2/3})H^2$, there is a non-adiabatic region centered at ϕ_1 . In this region where \mathcal{K} is large, the duration of the interaction is less than $1/H$. We continue the wave function in the complex plane on a semi-circle of radius larger than $1/H$ such that

$$\frac{\omega_k}{a} \approx \sqrt{\mathcal{K}^2 - 2H^2 + g^2 \dot{\phi}_1^2 \delta t^2} \approx g \dot{\phi}_1 \delta t + \frac{\mathcal{K}^2 - 2H^2}{2g \dot{\phi}_1 \delta t} \quad (9.58)$$

Notice that the WKB approximation is valid along this circle. The integral $\int \frac{\omega_k}{a} dt$ picks up an imaginary value due to the residue at the origin. As in (9.42) positive and negative-frequency modes are exchanged. The coefficient β_k is computed with the residue theorem

$$|\beta_k^f|^2 = e^{\pi \frac{2H^2 - \kappa_1^2}{g|\phi_1|}} \quad (9.59)$$

Notice that this is a small number in the region where $\mathcal{K} \geq \mathcal{O}(\sqrt{2}H)$.

For $0 < \mathcal{K} < \mathcal{K}^*$, the method used for $\mathcal{K}^* < \mathcal{K} < \mathcal{K}_{\max}$ is not reproducible as the semi-circles drawn around the non-adiabatic regions I and II intersect the semi-circles drawn around the turning points. We will see that the low energy part of the spectrum is dominated by the tachyonic instability and therefore does not really depend on the non-adiabatic region. As a result we will extend our results to the whole momentum range $0 < \mathcal{K} < \mathcal{K}_{\max}$.

The computation of particle creation in the $\xi \ll 1$ regime is much simpler, it was done in [86]. The Bogoliubov coefficient is obtained by expanding

$$\frac{\omega_k}{a} \approx \sqrt{\mathcal{K}^2 + g^2|\phi - \phi_1|^2} \approx g|\dot{\phi}_1|\delta t \left(1 - \frac{\mathcal{K}^2}{2g^2\dot{\phi}_1^2(\delta t)^2} \right) \quad (9.60)$$

around ϕ_1 ($\delta t = t - t_1$) and integrating around a contour where the WKB approximation is still valid in the complex plane. Using the same technique as before we find that

$$|\beta_k^f|^2 = e^{-\pi \frac{\kappa_1^2}{g|\dot{\phi}_1|}} \quad (9.61)$$

where $\mathcal{K}_1 = k/a_1$. As a result, the spectrum is Gaussian with a width determined by the speed of the brane.

We have now obtained the Bogoliubov coefficients in both regimes for ξ . This is particularly important as one can define an adiabatic invariant for equation (9.5)

$$\mathcal{N}_k = \frac{\omega_k}{2} \left(\frac{|\Psi'_k|^2}{\omega_k^2} + |\Psi_k|^2 \right) - \frac{1}{2} = |\beta_k^f|^2 \quad (9.62)$$

As explained in [36], this is the comoving occupation number of particles with momentum k .

9.5 The modified potential

We will compute the energy density of the created particles. In fact this energy density appears to add a contribution to the potential of the inflaton. This effect corresponds to the slowing down of the inflationary brane by the trapped brane. The emitted energy density is

$$\rho_\chi = \int \frac{d^3\mathcal{K}}{(2\pi)^3} \tilde{\omega}_k \mathcal{N}_k \quad (9.63)$$

where the integration is done over the physical momenta. This brings an extra factor of $1/a^3$ corresponding to the dilution of the created particles. The frequency $\tilde{\omega}_k = \omega_k/a$ is the rescaled frequency coming from the energy in conformal time $\frac{1}{2}\tilde{\omega}_k^2|\chi|^2 = \frac{1}{2}\omega_k^2\frac{|\Psi|^2}{a^2}$. Far from the trapped brane, once particles have been created in the immediate vicinity of the brane,

$$\rho_\chi \approx \frac{g|\phi - \phi_1|}{a^3} \int |\beta_k^f|^2 \frac{d^3k}{(2\pi)^3} \quad (9.64)$$

This approximation is valid as long as $g|\phi - \phi_1| \gg \sqrt{|2H^2 - \mathcal{K}^2|}$. When $\xi \ll 1$, the right hand side is at most $\sqrt{2g|\dot{\phi}|}$, which implies that $|\phi - \phi_1| \gg \frac{|\dot{\phi}|}{g}$, i.e. outside of the interaction region. In the $\xi \gg 1$ regime, the same condition gives $|\phi - \phi_1| \gg \frac{H}{g}$ which is also the size of the interaction region. In the effective description of the inflationary brane motion, this energy density is equivalent to a linear potential and a constant force towards the trapped brane. In the absence of the inflationary potential, this force may pull the passing brane towards the trapped brane. We are in a position to determine the effective potential in both cases $\xi \ll 1$ and $\xi \gg 1$.

When $\xi \ll 1$ the potential can be easily calculated as the particle spectrum is gaussian

$$\rho_\chi \approx \frac{1}{(2\pi)^3} \frac{a_S^3}{a^3} (g|\dot{\phi}_1|)^{3/2} g|\phi - \phi_1| \quad (9.65)$$

where $a_S \equiv a_1$ and the energy density is diluted before finally tending to zero rapidly.

In the $\xi \gg 1$ regime, the creation of particles is largely dominated by the tachyonic instability in the vicinity of the trapped brane and depends on $\int_{t_-}^{t^+} \frac{\Omega_k}{a} dt$. The behavior of this integral is dominated by the region of small momenta. Let us concentrate on the low frequency part of the spectrum. In this case the integration region is maximal and the turning points are located at

$$\delta t_\pm \approx \pm \sqrt{2} \frac{H}{g|\dot{\phi}_1|} \quad (9.66)$$

whose norm is always less than t_1 . When K is small, we can expand Ω_k

$$\frac{\Omega_k}{a} \approx \sqrt{2H^2 - g^2\dot{\phi}_1^2\delta t^2} - \frac{1}{2\sqrt{2H^2 - g^2\dot{\phi}_1^2\delta t^2}} \frac{k^2}{a^2} \quad (9.67)$$

Integrating between the two turning points we find

$$\int_{t_-}^{t^+} \frac{\Omega_k}{a} dt \approx \frac{\pi}{2} \frac{2H^2 - \mathcal{K}_S^2}{g|\dot{\phi}_1|} \quad (9.68)$$

where $\mathcal{K}_S = k/a_S$ and we have defined

$$\frac{1}{a_S^2} = \frac{1}{a_1^2} \frac{1}{\pi} \int_{-1}^1 \frac{du}{\sqrt{1-u^2}} \frac{1}{\left(1 + \frac{\sqrt{2}}{g\epsilon\sqrt{\lambda}}u\right)^{2/\epsilon}} \quad (9.69)$$

where we recall that $g\epsilon\sqrt{\lambda} \gg 1$. This result is very important as it shows that the spectrum is approximately Gaussian with a width $\sqrt{g|\dot{\phi}_1|}$ which is much smaller than the band of integration $\Delta\mathcal{K} = \sqrt{2}H$. Moreover the amplitude of the number of particles depends on $e^{2\pi H^2/g|\dot{\phi}_1|}$ which is an exponentially large number. Notice that the same factor is negligible in the $\xi \ll 1$ regime. Now that we know that the spectrum is dominated by the tachyonic instability, we can evaluate the energy density

$$\rho_\chi \approx \frac{9}{(2\pi)^3} \frac{a_S^3}{a^3} e^{2\pi H^2/g|\dot{\phi}_1|} (g|\dot{\phi}_1|)^{3/2} g|\phi - \phi_1| \quad (9.70)$$

Notice that the main difference with the $\xi \ll 1$ is the presence of a large exponential factor coming from the tachyonic instability close to the trapped brane. Here also, the energy is diluted after going out of the interaction region. The scale factor a_S takes into account the fact that momenta are red-shifted in the integration region. In both cases the effective potential after the interaction region becomes

$$V_{\text{eff}} \approx m^2\phi^2 + \frac{1}{(2\pi)^3} y(\xi) \frac{a_S^3}{a^3} H^3 g|\phi - \phi_1| \quad (9.71)$$

where the coupling function depends on ξ and reads

$$y(\xi) \approx \xi^{-3/2} \quad (9.72)$$

when $\xi \ll 1$ and

$$y(\xi) \approx 9\xi^{-3/2} e^{2\pi\xi} \quad (9.73)$$

when $\xi \gg 1$. This potential is similar to the ones used in chameleon models [112] (see also chapter 7). It has a moving minimum where

$$\phi_{\text{min}} = \frac{1}{(2\pi)^3} y(\xi) g \frac{a_S^3}{a^3} \frac{H^3}{2m^2} \quad (9.74)$$

This minimum approaches the origin as the scale factor increases. This implies that the effect of the trapped brane is only relevant for a few e-foldings after the passage through the interaction region. Immediately after the passage, the minimum is located at

$$\frac{\phi_{\text{ini}}}{\phi_1} \approx \frac{1}{16\pi^3} \frac{y(\xi)\epsilon\sqrt{\lambda}}{3g} \frac{H^2}{M_p^2} \quad (9.75)$$

This gives a criterion for the influence of the trapped brane on the motion of the inflationary brane. If $\phi_{\text{ini}} \ll \phi_1$, the trapped brane has no influence as the

inflaton feels the $m^2\phi^2$ branch of the potential. On the other hand, if H is large enough and $\phi_{\text{ini}} \geq \phi_1$, the inflationary brane feels the steep potential due to the trapped brane. In this case, the motion of the inflationary brane is affected for a few e-foldings.

Let us evaluate the jump in the potential at the end of the interaction zone

$$\Delta V \approx \frac{9}{(2\pi)^3} \xi^{-3/2} e^{2\pi\xi} H^4 \quad (9.76)$$

when $\xi \gg 1$ and

$$\Delta V \approx \frac{1}{(2\pi)^3} \frac{H^4}{\xi^2} \quad (9.77)$$

when $\xi \ll 1$. In both case it depends only on H^4 and ξ . For large enough H , this jump in V can also change the Hubble rate due to the release of energy in the form of radiated particles.

As we have considered that H is nearly constant and we have neglected any backreaction on the dynamics of the inflaton while the brane particles are created, we must impose that $\Delta V/V \leq 1$, which gives for $\xi \ll 1$

$$\frac{H^2}{M_p^2} \leq 3 \cdot (2\pi)^3 g^2 \xi^2 \quad (9.78)$$

and for $\xi \gg 1$,

$$\frac{H^2}{M_p^2} \leq 3 \cdot (2\pi)^3 g^2 \xi^{3/2} e^{-2\pi\xi} \quad (9.79)$$

This condition gives an upper limit on ξ . In fact, if we require that the Hubble rate H should be at least of order 1 GeV, ξ must be at most equal to $\xi_{\text{lim}} \approx 14$ for $g \sim 10^{-1}$. For larger values of ξ , the tachyonic instability implies that there is a strong backreaction due to the explosive creation of particles. In this case, the inflaton loses all its energy very quickly and transfers it into radiated particles.

9.6 Discussion on the parameters

Let us now make explicit some of the constraints on the parameters of the model. Using the condition $\epsilon \ll 1$, we get a lower bound on the inflaton mass

$$m \gg \frac{g}{\sqrt{\lambda}} M_p \quad (9.80)$$

This implies that

$$\xi \gg \frac{1}{g\sqrt{\lambda}} \quad (9.81)$$

guaranteeing the constancy of H in the $\xi \ll 1$ region. Using this inequality we obtain that

$$m \gg \frac{g^2}{\xi} M_p \quad (9.82)$$

For a fixed string coupling g_s , we see that ξ determines the range of masses leading to inflation. When ξ is large, the mass m can be smaller than the Planck scale. In the large ξ regime we have

$$g^2 \gg \frac{m}{M_p} \quad (9.83)$$

and

$$\lambda \gg \frac{M_p}{m} \quad (9.84)$$

This regime tends to favor small masses and a large compactification radius.

So far we have not tried to connect DBI inflation to observations. Let us now assume that the DBI inflation regime we have analyzed is responsible for the phase of inflation resulting in the quantum fluctuations leading to the CMB spectrum. In this case, the COBE normalization determines the curvature perturbation

$$\Delta_{\mathcal{R}}^2 \sim \frac{H_{\text{inf}}^2 \gamma}{M_p^2 \epsilon} \sim g^4 \xi^2 \sim \zeta^2 \sim 10^{-10} \quad (9.85)$$

So $\zeta \approx g^2 \xi \sim 10^{-5}$. For a reasonable value of the string coupling $g_s \sim 10^{-2}$, we find that inflationary branes whose quantum fluctuations lead to the CMB anisotropies must be in the $\xi \ll 1$ regime. We have another observational constraint, the ratio $r = \frac{\mathcal{P}_t}{\mathcal{P}_s}$ must be small. The tensor perturbations spectrum being

$$\Delta_T^2 = \frac{4H_{\text{inf}}^2}{\pi M_p^2} \quad (9.86)$$

We deduce

$$r = \frac{16\epsilon}{\gamma} \leq 0.3 \quad (9.87)$$

With both (9.85) and (9.87), we find

$$\frac{H}{M_p} \leq 10^{-5} \quad (9.88)$$

We note that this upper bound for the Hubble rate is smaller than the bound given by (9.78) and therefore the backreaction is always negligible in the $\xi \ll 1$ regime. We have seen that in this regime the slowing down by a trapped brane can be effective if

$$\frac{H^2}{M_p^2} \geq \frac{3.16\pi^3 g \xi^{3/2}}{\epsilon \sqrt{\lambda}} \quad (9.89)$$

or equivalently

$$\frac{H^2}{M_p^2} \geq 16\sqrt{3}\pi^3 \xi^{3/2} \frac{m}{M_p} \quad (9.90)$$

Using (9.82), we find

$$\frac{H^2}{M_p^2} \geq 16\sqrt{3}\pi^3 g \xi^{1/2} \quad (9.91)$$

This is not compatible with (9.88). So it is not possible to slow the motion of the inflationary brane drastically after hitting a single trapped brane. If we assume that there exists a stack of N closely packed branes in the interaction region, then equation (9.75) becomes

$$\frac{\phi_{\text{ini}}}{\phi_1} \approx \frac{1}{16\pi^3} \frac{y(\xi)\epsilon\sqrt{\lambda}}{3g} N \frac{H^2}{M_p^2} \quad (9.92)$$

and condition (9.91) becomes :

$$\frac{H^2}{M_p^2} \geq \frac{1}{N} 16\sqrt{3}\pi^3 g \zeta^{1/2} \quad (9.93)$$

Unless we have at least $N \sim 10^9$ branes in the stack, the slowing effect of the stack is not drastic. The motion of an inflationary brane leading to the CMB spectrum is hardly affected by trapped branes. On the contrary, branes in a regime $\xi \gg 1$ are efficiently slowed down because of radiated particles, this is what we have called brane bremsstrahlung. This gives a selection mechanism for the branes. Only the small ξ regime is physically relevant for the CMB observations so now on we will focus on this regime. We have shown that the motion of the probe brane is not affected by the presence of matter, nor are the other background quantities. But we have no clues about the effect of a trapped brane or a stack of trapped branes on the linear perturbations. The presence of matter and its pull-back force might affect the density perturbations and thus might lead to interesting features in the CMB spectrum. The mass of the particles at the end of the interaction zone at ϕ_s is

$$m_\chi \approx \frac{H}{\xi} \gg H \quad (9.94)$$

so that the trapped particles behave like a fluid of cold dark matter. This corroborates the fact that ρ_χ decays like a^{-3} and is proportional to the mass of the χ -particles in $|\phi - \phi_1|$. We will consider that the interaction between the inflaton and the trapped brane is almost instantaneous. Details on the physics inside the region of particle creation are given farther in section 9.14.

9.7 K-inflation coupled to matter

In the following, we will build an effective theory based on a k-inflation action coupled to non-relativistic matter with an inflaton potential similar to (9.71). We will study the perturbations in these k-inflation models coupled to matter and analyse conditions for the existence of features which generalize Starobinsky's results when abrupt changes in the coupling to matter are present. The models we will consider are scalar-tensor theories (see chapter 7) where the inflaton field couples to matter. In such scalar-tensor theories, the action is a sum of

the k-inflation action for the inflaton, the matter term and the Einstein-Hilbert action.

$$S = \int d^4x \sqrt{-g} \frac{M_{\text{P}}^2}{2} R + \int d^4x \sqrt{-g} \mathcal{P}(\phi, X) + \int d^4x \mathcal{L}_m(\psi, \tilde{g}_{\mu\nu}) \quad (9.95)$$

in the Einstein frame, here ψ is a matter field. We have defined $X = \frac{1}{2} g_{\mu\nu} \partial^\mu \phi \partial^\nu \phi$ and the conformally ϕ -dependent metric $\tilde{g}_{\mu\nu} = A^2(\phi) g_{\mu\nu}$.

Let us study some general properties of the dynamics of k-inflation models coupled to matter. First of all, the Einstein equations are not modified and read

$$R_{\mu\nu} - \frac{g_{\mu\nu}}{2} R = \kappa (T_{\mu\nu}^\phi + T_{\mu\nu}^m) \quad (9.96)$$

This a consequence of the non-modification of the Einstein-Hilbert term. The energy momentum tensors are defined by

$$T_{\mu\nu}^{m,\phi} = -\frac{2}{\sqrt{-g}} \frac{\delta S_{m,\phi}}{\delta g^{\mu\nu}} \quad (9.97)$$

where we have identified

$$S_\phi = \int d^4x \sqrt{-g} \mathcal{P}(\phi, X) \quad (9.98)$$

and

$$S_m = \int d^4x \mathcal{L}_m(\psi, \tilde{g}_{\mu\nu}) \quad (9.99)$$

In terms of the non-linear function $\mathcal{P}(\phi, X)$, the inflaton energy momentum tensor is given by:

$$T_{\mu\nu}^\phi = g_{\mu\nu} \mathcal{P} - \frac{\partial \mathcal{P}}{\partial X} \partial_\mu \phi \partial_\nu \phi \quad (9.100)$$

The dynamics of the inflaton are governed by the Klein-Gordon equation

$$D_\mu \frac{\partial \mathcal{P}}{\partial_\mu \phi} - \frac{\partial \mathcal{P}}{\partial \phi} = \beta_\phi T^m \quad (9.101)$$

where $T^m = g^{\mu\nu} T_{\mu\nu}^m$ is the trace of the matter energy momentum tensor and

$$\beta_\phi = \frac{d \ln A(\phi)}{d\phi} \quad (9.102)$$

is the coupling constant of the inflaton to matter as defined in (7.7). The Klein-Gordon equation is also equivalent to

$$D_\mu \left(\partial^\mu \phi \frac{\partial \mathcal{P}}{\partial X} \right) - \frac{\partial \mathcal{P}}{\partial \phi} = \beta_\phi T^m \quad (9.103)$$

Notice that due to the coupling to matter there is a new matter term in the Klein-Gordon equation. The Bianchi identity implies that the total energy momentum is conserved as seen in (7.7)

$$D^\mu(T_{\mu\nu}^m + T_{\mu\nu}^\phi) = 0 \quad (9.104)$$

but it also implies that matter is not conserved due to the energy exchange between matter and the inflaton

$$D^\mu T_{\mu\nu}^m = \beta_\phi T^m \partial_\nu \phi \quad (9.105)$$

It is of particular interest to focus on the case where the matter fluid is pressureless

$$T_{\mu\nu}^m = \rho_E u_\mu u_\nu \quad (9.106)$$

where the velocity field $u^\mu = \frac{dx^\mu}{d\tau}$ is normalized $u^2 = -1$ and τ is the proper time along the trajectories of the matter particles. Up to linear order $u_\mu = (-1 + \delta u_0, v_i)$ and $g^{00} = -1 + 2\varphi_N$ so that $\delta u_0 = -\varphi_N$. From this, the local expansion rate can be derived up to first order

$$\begin{aligned} 3h &= D_\mu u^\mu & (9.107) \\ &= \partial_\mu u^\mu + \Gamma_{\mu\nu}^\mu u^\nu \\ &= \partial_0 u^0 + \partial_i u^i + \Gamma_{00}^0 u^0 + \Gamma_{i0}^i u^0 + \Gamma_{0i}^0 u^i \\ &= -\dot{\varphi}_N + \frac{1}{a^2} \partial_i v^i + \dot{\varphi}_N + 3(H - \dot{\varphi}_N)(1 - \varphi_N) + \partial_i \varphi_N \frac{v^i}{a^2} \\ &= 3H - 3\dot{\varphi}_N - 3H\varphi_N + \frac{1}{a^2} \partial_i v^i & (9.108) \end{aligned}$$

The matter density ρ_E is the Einstein frame density. It is not conserved as follows from the (non-)conservation equation (equation 7.9 with $p = 0$)

$$\dot{\rho}_E + 3h\rho_E = \beta_\phi \rho_E \dot{\phi} \quad (9.109)$$

where the time derivative along the trajectory is given by $\dot{\rho}_E = u^\mu D_\mu \rho_E$. Defining

$$\rho_E = A(\phi) \rho_m \quad (9.110)$$

we find that ρ_m is conserved

$$\dot{\rho}_m + 3h\rho_m = 0 \quad (9.111)$$

In a cosmological context with the local Hubble rate $h = H$ being equal to the global one, we have that $\rho_m = \rho_0/a^3$. Finally, the effect of the inflaton on the matter particles is to induce a scalar force as

$$\dot{u}_\mu = -\beta_\phi \dot{\phi} u_\mu - \beta_\phi \partial_\mu \phi \quad (9.112)$$

This modifies the geodesics of the matter particles.

Coming back to the Klein-Gordon equation, we find that the dynamics are governed by an effective Lagrangian

$$\mathcal{P}_{\text{eff}}(\phi, X) = \mathcal{P}(\phi, X) - \rho_m(A(\phi) - 1). \quad (9.113)$$

When the coupling is trivial $A(\phi) = 1$, the effective Lagrangian is unchanged. It is only modified for non-trivial coupling functions.

9.8 Abrupt change in the coupling function

When $\mathcal{P}(\phi, X) = P(\phi, X) - V(\phi)$, the effective potential seen by the inflaton is

$$V_{\text{eff}}(\phi) = V(\phi) + \rho_m(A(\phi) - 1) \quad (9.114)$$

where $\rho_m = \rho_0/a^3$ is the conserved energy density of the matter fluid. This potential is similar to the ones used in chameleon models [112]. We will consider the coupling function to be linear

$$A(\phi) = 1 + \frac{|\phi - \phi_1|}{\phi_1} Y_\delta(\phi_1 - \phi) \quad (9.115)$$

where the function Y_δ varies abruptly from 0 to 1 over a neighborhood of the origin of size δ and is such that for $(\phi_1 - \phi) > \delta$ we have $Y_\delta(\phi_1 - \phi) = 1$. Before the threshold value ϕ_1 , the coupling is identically $A(\phi) = 1$ which implies that matter and the inflaton are effectively decoupled. After the threshold crossing, the effective potential becomes

$$V_{\text{eff}}(\phi) = V(\phi) + \rho_m \frac{|\phi - \phi_1|}{\phi_1} \quad (9.116)$$

Now this is the same type of behavior for the inflaton potential as the one in the trapped brane case (9.71) when identifying $P(\phi, X) = P_{\text{DBI}}(\phi, X)$. In the following, we will study the consequences of such a change in the effective potential on the perturbation spectrum.

A simplified situation occurs when $\rho_m \ll V(\phi)$ implying that the matter density has no effect on the inflationary dynamics before the crossing of the threshold ϕ_1 . After the threshold, the effective potential has a matter dependent minimum where

$$\partial_\phi V|_{\phi_{\text{min}}} = -\rho_m \partial_\phi A(\phi)|_{\phi_{\text{min}}} \quad (9.117)$$

Assuming that the potential $V(\phi)$ is a smooth function with a minimum at the origin, like $\frac{1}{2}m_0^2\phi^2$, the position of the minimum is determined by

$$\phi_{\text{min}} = \frac{\rho_m}{m_0^2\phi_1} \quad (9.118)$$

where m_0 is the mass at the origin. As long as $\rho_m \ll m_0^2 \phi_1^2$, which amounts to neglecting the matter density compared to the inflaton energy density, we have $\phi_{\min} \ll \phi_1$ and the background dynamics of the inflaton are not influenced by the coupling to matter.

9.9 Perturbations

The inflaton dynamics are governed by (3.34, 3.35). The Klein-Gordon equation is given by (3.38)

$$\frac{\partial \mathcal{P}_{\text{eff}}}{\partial \phi} + \frac{\partial \mathcal{P}_{\text{eff}}}{\partial X} (\ddot{\phi} + 3H\dot{\phi}) + \dot{\phi} \frac{d}{dt} \left(\frac{\partial \mathcal{P}_{\text{eff}}}{\partial X} \right) = 0 \quad (9.119)$$

expressed as a function of the effective Lagrangian \mathcal{P}_{eff} . In the following we will assume that the solutions to the Klein-Gordon equation lead to an inflationary behavior and study cosmological perturbations of this inflationary background.

Due to the absence of anisotropic stress in the Einstein frame, we describe the metric perturbations using the Newton gauge, leading to the perturbed FLRW line element

$$ds^2 = -(1 + 2\varphi_N)dt^2 + a^2(t)(1 - 2\varphi_N)\delta_{ij}dx^i dx^j \quad (9.120)$$

where φ_N is the Newtonian potential. The velocity field can be expanded as in (4.6, 4.7, 4.8, 4.9)

$$u_\mu = (-1 - \varphi_N, v_i) \quad (9.121)$$

Being interested in the scalar modes only we define

$$v_i = \partial_i \psi \quad (9.122)$$

The Euler equation is

$$\dot{\psi} = -\varphi_N - \beta_\phi \dot{\phi} \psi - \beta_\phi \delta\phi \quad (9.123)$$

Similarly the conservation equation reads

$$\dot{\delta}_m + \frac{\Delta\psi}{a^2} = 3\dot{\varphi}_N \quad (9.124)$$

These equations have to be complemented with the perturbed Einstein equations.

Following [133] we define

$$\delta T_i^0 \equiv \partial_i q \quad (9.125)$$

with

$$q = -(\rho_\phi + p_\phi) \frac{\delta\phi}{\dot{\phi}} + A\rho_m \psi \quad (9.126)$$

This implies that the 0i component of the perturbed Einstein equation leads to

$$\dot{\varphi}_N + H\varphi_N = 4\pi G_N [(\rho_\phi + p_\phi) \frac{\delta\phi}{\dot{\phi}} - A\rho_m \psi] \quad (9.127)$$

We also derive the energy density perturbation (see equation 4.39)

$$\delta T_0^0 = -\delta\rho \quad (9.128)$$

where $\rho = \rho_\phi + \rho_E$ is the total energy density. Using

$$\delta\rho = \frac{\partial\rho}{\partial\phi}\delta\phi + \frac{\partial\rho}{\partial X}\delta X + A\delta\rho_m \quad (9.129)$$

where $\delta\rho_m$ is the intrinsic matter perturbation and using the conservation equation (4.42) for the total energy density

$$\frac{d\rho}{dt} = -3H(\rho + p) = \frac{\partial\rho}{\partial\phi}\dot{\phi} + \frac{\partial\rho}{\partial X}\dot{X} + A\dot{\rho}_M \quad (9.130)$$

we find that

$$\delta\rho = -3H(\rho_\phi + p_\phi)\frac{\delta\phi}{\dot{\phi}} + \frac{\rho_\phi + p_\phi}{2c_s^2 X} \left(\delta X - \dot{X}\frac{\delta\phi}{\dot{\phi}} \right) + A\delta\rho_m \quad (9.131)$$

and finally

$$\delta\rho = -3H(\rho_\phi + p_\phi)\frac{\delta\phi}{\dot{\phi}} + \frac{\rho_\phi + p_\phi}{c_s^2} \left(\frac{d}{dt}\frac{\delta\phi}{\dot{\phi}} - \phi_N \right) + A\delta\rho_m \quad (9.132)$$

We have defined the speed of sound as in (3.37), it only depends on the inflaton. With the metric (9.120), the perturbed Einstein tensor is given by (4.36)

$$-\frac{1}{2}\delta G_0^0 = \frac{1}{a^2}\Delta\varphi_N - 3H(\dot{\varphi}_N + H\varphi_N) \quad (9.133)$$

which leads to the perturbed 00 Einstein equation

$$\frac{d}{dt} \left(\frac{\delta\phi}{\dot{\phi}} \right) = \varphi_N + \frac{c_s^2}{4\pi G_N a^2 (\rho_\phi + p_\phi)} \Delta\varphi_N + U_m \quad (9.134)$$

where the source term from the matter perturbations is

$$U_m = 3H \frac{c_s^2}{\rho_\phi + p_\phi} A\rho_m \psi - \frac{c_s^2}{\rho_\phi + p_\phi} A\delta\rho_m \quad (9.135)$$

The two Einstein equations are a generalization of those obtained in section 4.2 when a non-dynamical matter field is present. Together with the conservation and the Euler equations, these Einstein equations describe the system of perturbations. They are valid for any k-inflation model coupled to matter.

It is convenient to introduce gauge invariant quantities and study their dynamical evolution. The comoving curvature perturbation \mathcal{R}_T is such a gauge invariant quantity:

$$\mathcal{R}_T = \varphi_N - \frac{H}{\rho + p} q \quad (9.136)$$

This can be written as

$$\mathcal{R}_T = \varphi_N + H \frac{\rho_\phi + p_\phi}{\rho + p} \frac{\delta\phi}{\dot{\phi}} + \mathcal{R}_\psi \quad (9.137)$$

where

$$\mathcal{R}_\psi = -\frac{A\rho_m H}{\rho + p} \left(\psi - \frac{\delta\phi}{\dot{\phi}} \right) \quad (9.138)$$

We define

$$\mathcal{R} = \mathcal{R}_T + \frac{A\rho_m H}{\rho + p} \psi \quad (9.139)$$

which coincides with the comoving curvature perturbation in the absence of matter

$$\mathcal{R} = \varphi_N + H \frac{\delta\phi}{\dot{\phi}} \quad (9.140)$$

The effect of matter on \mathcal{R} can be seen when analyzing its time evolution

$$\begin{aligned} \dot{\mathcal{R}} &= H \frac{\Delta\varphi_N}{a^2} \frac{c_s^2}{4\pi G_N(\rho_\phi + p_\phi)} - 4\pi G_N A\rho_m \frac{\delta\phi}{\dot{\phi}} \\ &+ A\rho_m \left(-4\pi G_N + \frac{3H^2 c_s^2}{\rho_\phi + p_\phi} \right) \psi - \frac{c_s^2 H}{\rho_\phi + p_\phi} A\delta\rho_m \end{aligned} \quad (9.141)$$

It is convenient to rewrite

$$\dot{\mathcal{R}} = C \frac{\delta\phi}{\dot{\phi}} + DR + T_\psi \quad (9.142)$$

where we have identified

$$C = \frac{k^2 H^2}{a^2} \frac{c_s^2}{4\pi G_N(\rho_\phi + p_\phi)} (1 + W), \quad D = -\frac{k^2 H c_s^2}{a^2 4\pi G_N(\rho_\phi + p_\phi)} \quad (9.143)$$

and

$$W = -\frac{k_c^2}{k^2} \quad (9.144)$$

The characteristic momentum k_c is given by

$$k_c^2 = A\rho_m \frac{a^2 (4\pi G_N)^2 (\rho_\phi + p_\phi)}{H^2 c_s^2} \quad (9.145)$$

When matter is absent we have $W = 0$. We have also introduced

$$T_\psi = \left(-4\pi G_N + \frac{3H^2 c_s^2}{\rho_\phi + p_\phi} \right) A\rho_m \psi - \frac{H c_s^2}{\rho_\phi + p_\phi} A\delta\rho_m \quad (9.146)$$

This allows one to obtain a second order differential equation for \mathcal{R}

$$\ddot{\mathcal{R}} + \left(H - \frac{\dot{C}}{C} \right) \dot{\mathcal{R}} + \left(\frac{k^2 c_s^2}{a^2} + 4\pi G_N A\rho_m \right) \mathcal{R} = \Delta_\psi \quad (9.147)$$

or equivalently in conformal time with $' = d/d\eta$.

$$\mathcal{R}'' - \frac{C'}{C}\mathcal{R}' + (k^2\tilde{c}_s^2 + a^2 4\pi G_N A\rho_m)\mathcal{R} = a^2\Delta_\psi \quad (9.148)$$

where we have identified the effective speed of sound

$$\tilde{c}_s^2 = c_s^2 \left(1 - \frac{W'}{\mathcal{H}(1+W)} \frac{2}{3(1+w_\phi)} \right) \quad (9.149)$$

and we have used the inflaton equation of state $w_\phi = p_\phi/\rho_\phi$. The source term reads

$$\Delta_\psi = \dot{T}_\psi + \left(H - \frac{k^2 c_s^2}{4\pi G_N a^2 (\rho_\phi + p_\phi)} \right) T_\psi - \frac{\dot{C}}{C} T_\psi + C U_m \quad (9.150)$$

Let us define

$$z_A = z|1+W|^{-1/2} \quad (9.151)$$

where

$$z = \frac{a(\rho_\phi + p_\phi)^{1/2}}{H c_s} \quad (9.152)$$

and the modified Mukhanov-Sasaki variable

$$v_A = z_A \mathcal{R}, \quad (9.153)$$

we then find the perturbation equation

$$v_A'' + \left(k^2 \tilde{c}_s^2 + a^2 4\pi G_N A\rho_m - \frac{z_A''}{z_A} \right) v_A = a^2 z_A \Delta_\psi \quad (9.154)$$

When matter is absent, this reduces to the usual Mukhanov-Sasaki equation generalized to k-inflation by Garriga and Mukhanov [75] and recalled in section 4.2. In our case the Mukhanov-Sasaki variable is k-dependent.

The full perturbation equations are very complex. Here we will simply emphasize some salient points which differ from the case with no matter. First of all, the perturbation equations depend crucially on the scale k_c which is time dependent. When $k \gg k_c$, the speed of sound is not altered $\tilde{c}_s = c_s$. On larger scales when $k \ll k_c$, the speed of sound \tilde{c}_s is largely modified by the presence of matter. Similarly, z_A differs greatly from z when $k \ll k_c$. Moreover, as matter perturbations enter as sources in the v -equation, we expect new modes which would affect the \mathcal{R}_T power spectrum.

During an acceleration era such as the late time acceleration of the universe where ρ_m and ρ_ϕ are of the same order, the equations are difficult to tackle analytically. On the other hand, during primordial inflation when the number of inflationary efoldings is large, the influence of ρ_m is limited to a few efoldings before being red-shifted away. In this case, modes of interest will always satisfy $k \gg k_c$. Moreover we can concentrate on the efoldings when $\rho_m \ll \rho_\phi$. Despite being negligible at the background level, the matter energy density can play a significant role when the matter coupling $A(\phi)$ varies abruptly along the inflationary trajectory. We will focus on this possibility in section 9.11.

9.10 Reminder of the resolution of a perturbation equation with a dirac function

In conformal time, we consider the perturbation equation for the Mukhanov-Sasaki variable v in a quasi de Sitter phase with a delta function feature at time η_1

$$v'' + \left(c_s^2 k^2 - \frac{z''}{z} + u\delta(\eta - \eta_1) \right) v = 0 \quad (9.155)$$

In the following we will analyze the solutions when c_s is constant. Thus it will be very similar to the resolution for the canonical Starobinsky's model. A slightly better approximation amounts to changing adiabatically $c_s \rightarrow c_s(\eta)$ in the solutions as long as $c_s(\eta)$ is a slowly varying function. Such an approximation is acceptable at first order [97]. To leading order in the slow roll parameters, the de Sitter term $\frac{z''}{z} \approx \frac{a''}{a}$ is a good approximation for the potential term in the perturbation equation.

It is convenient to define $x = kc_s\eta$ then

$$\frac{d^2v}{dx^2} + \left(1 - \frac{2}{x^2} + \hat{u}\delta(x - x_1) \right) v = 0 \quad (9.156)$$

whose solutions are

$$(\pm i + \frac{1}{x})e^{\mp ix} \quad (9.157)$$

with $\hat{u} = \frac{u}{kc_s}$. Notice that \hat{u} is dimensionless. Before the feature we have a Bunch-Davies vacuum [116] with

$$v = C \left(i + \frac{1}{x} \right) e^{-ix} \quad (9.158)$$

where $C \propto \frac{1}{\sqrt{2k}}$ and after the passage

$$v = \alpha \left(i + \frac{1}{x} \right) e^{-ix} + \beta \left(-i + \frac{1}{x} \right) e^{ix} \quad (9.159)$$

with the junction condition

$$\left[\frac{dv}{dx} \right]_{x_1} = -\hat{u}v(x_1) \quad (9.160)$$

The Bogoliubov coefficients are

$$\alpha = C \left(1 + \frac{\hat{u}}{2i} \left(1 + \frac{1}{x_1^2} \right) \right) \quad (9.161)$$

and

$$\beta = \frac{ix_1 + 1}{ix_1 - 1} \left(1 + \frac{1}{x_1^2} \right) \frac{\hat{u}C}{2i} e^{-2ix_1} \quad (9.162)$$

We are interested in the long time behaviour of the modes evaluated at $\eta_* \rightarrow 0$ implying that

$$v \approx \frac{\alpha + \beta}{x_*} \quad (9.163)$$

We find that

$$v \approx \frac{C}{x_*} \left(1 + \hat{u} \frac{1 + \frac{1}{x_1^2}}{i - \frac{1}{x_1}} \left(\cos x_1 - \frac{\sin x_1}{x_1} \right) e^{-ix_1} \right) \quad (9.164)$$

Now defining $x_1 = -\frac{k}{k_1}$ where $k_1 = -\frac{1}{c_s \eta_1}$, we can study the limits $k \gg k_1$ and $k \ll k_1$. When k is large, \hat{u} goes to zero implying that

$$v(k \rightarrow \infty) = \frac{C}{x_*} \quad (9.165)$$

in an oscillatory manner. This correspond to a scale invariant spectrum $k^3 |v|^2$. On the contrary we find that as $x_1 \rightarrow 0$

$$v(k \rightarrow 0) = \frac{C}{x_*} \left(1 + \frac{\hat{u} x_1}{3} \right) = \frac{C}{x_*} \left(1 - \frac{u}{3c_s k_1} \right) \quad (9.166)$$

This implies that the power spectrum jumps from small to large k . This result will be used in the next sections applications.

9.11 Scalar-tensor features

We are interested in deriving analytical properties of the power spectrum for \mathcal{R} when $\rho_m \ll \rho_\phi$ and $|W| \ll 1$. In this case we find that the source term Δ_ψ is regular and negligible. Moreover the speed of sound is not perturbed $\tilde{c}_s = c_s$. The effect of the coupling function $A(\phi)$ appears at the level of its second derivative which is singular and behaves like a δ function. This leads to the following perturbation equation

$$v_k'' + \left(c_s^2 k^2 - \frac{z_A''}{z_A} \right) v_k = 0 \quad (9.167)$$

with

$$z_A^2 = \frac{a^2}{H^2} \frac{1}{|1+W|} \tilde{z}^2 \quad (9.168)$$

where

$$\tilde{z}^2 \equiv 2X \left(\frac{\partial \mathcal{P}}{\partial X} + 2X \frac{\partial^2 \mathcal{P}}{\partial X^2} \right) = 2X \left(\frac{\partial \mathcal{P}_{\text{eff}}}{\partial X} + 2X \frac{\partial^2 \mathcal{P}_{\text{eff}}}{\partial X^2} \right) \quad (9.169)$$

We have

$$\begin{aligned} \frac{z_A''}{z_A} &= \frac{a''}{a} + \frac{\tilde{z}''}{\tilde{z}} + 2 \frac{a'}{a} \frac{\tilde{z}'}{\tilde{z}} - W' \frac{\tilde{z}'}{\tilde{z}} - \frac{1}{2} W'' - W' \frac{a'}{a} + \frac{3}{4} W'^2 \\ &\quad - 2 \frac{H'}{H} \frac{a'}{a} - 2 \frac{H'}{H} \frac{\tilde{z}'}{\tilde{z}} + \frac{H'}{H} W' - \frac{H''}{H} + 2 \frac{H'^2}{H^2} \end{aligned} \quad (9.170)$$

where we find that

$$W'' \supset \frac{\phi'_1 k_c^2(\eta_1)}{\phi_1 k^2} \delta(\eta - \eta_1) \quad (9.171)$$

where all the time dependent factors are evaluated at η_1 . This allows one to identify

$$u_I(k) = \frac{\phi'_1 k_c^2(\eta_1)}{\phi_1 2k^2} \quad (9.172)$$

This is the first source of feature for scalar-tensor theories and it is due to the change of normalization of the variable z to the variable z_A . We notice that the coefficient of the Dirac function is scale-dependent. Another feature will also come from the coupling with matter through the matter coupling term in the effective potential (9.114).

$$\begin{aligned} \frac{z''_A}{z_A} &= \frac{a''}{a} + \frac{1}{2} a^2 \frac{1}{\tilde{z}^2} \frac{d^2 \tilde{z}^2}{dt^2} + \frac{1}{2} a \mathcal{H} \frac{1}{\tilde{z}^2} \frac{d\tilde{z}^2}{dt} - \frac{1}{4} a^2 \left(\frac{1}{\tilde{z}^2} \frac{d\tilde{z}^2}{dt} \right)^2 + a \left(\mathcal{H} - \frac{\mathcal{H}'}{\mathcal{H}} - \frac{W'}{2} \right) \frac{1}{\tilde{z}^2} \frac{d\tilde{z}^2}{dt} \\ &\quad - \frac{1}{2} W'' + \frac{3}{4} W'^2 + W' \left(\frac{\mathcal{H}'}{\mathcal{H}} - 2\mathcal{H} \right) + 3\mathcal{H}^2 - 3\mathcal{H}' + 2 \left(\frac{\mathcal{H}'}{\mathcal{H}} \right)^2 - \frac{\mathcal{H}''}{\mathcal{H}} \quad (9.173) \end{aligned}$$

The last four terms sum up to zero in pure de Sitter case. We are interested in the terms containing \tilde{z} and its derivatives :

$$\frac{z''_A}{z_A} = \frac{a''}{a} + \frac{1}{2} \frac{(\tilde{z}^2)''}{\tilde{z}^2} - \frac{1}{2} W'' + \text{regular negligible terms} \quad (9.174)$$

Using

$$\frac{(\tilde{z}^2)''}{\tilde{z}^2} = a \mathcal{H} \frac{1}{\tilde{z}^2} \frac{d\tilde{z}^2}{dt} + a^2 \frac{1}{\tilde{z}^2} \frac{d^2 \tilde{z}^2}{dt^2} \quad (9.175)$$

and

$$\begin{aligned} \frac{d\tilde{z}^2}{dt} &= -2\ddot{\phi}\dot{\phi} \left(\frac{\partial \mathcal{P}_{\text{eff}}}{\partial X} + 5X \frac{\partial^2 \mathcal{P}_{\text{eff}}}{\partial X^2} + 2X^2 \frac{\partial^3 \mathcal{P}_{\text{eff}}}{\partial X^3} \right) \\ &\quad + 2X\dot{\phi} \left(\frac{\partial^2 \mathcal{P}_{\text{eff}}}{\partial \phi \partial X} + 2X \frac{\partial^3 \mathcal{P}_{\text{eff}}}{\partial \phi \partial X^2} \right) \quad (9.176) \end{aligned}$$

together with the Klein-Gordon equation (9.119), we can utilize

$$\ddot{\phi} \left(\frac{\partial \mathcal{P}_{\text{eff}}}{\partial X} + 2X \frac{\partial^2 \mathcal{P}_{\text{eff}}}{\partial X^2} \right) = - \left(\frac{\partial \mathcal{P}_{\text{eff}}}{\partial \phi} - 2X \frac{\partial^2 \mathcal{P}_{\text{eff}}}{\partial \phi \partial X} + 3H\dot{\phi} \frac{\partial \mathcal{P}_{\text{eff}}}{\partial X} \right) \quad (9.177)$$

to replace $\ddot{\phi}$ in the previous equation (9.176). We find that a term in $\frac{\partial \mathcal{P}_{\text{eff}}}{\partial \phi}$ appears

$$\begin{aligned} \frac{1}{\tilde{z}^2} \frac{d\tilde{z}^2}{dt} &= \frac{\dot{\phi} \left(\frac{\partial \mathcal{P}_{\text{eff}}}{\partial \phi} - 2X \frac{\partial^2 \mathcal{P}_{\text{eff}}}{\partial \phi \partial X} + 3H\dot{\phi} \frac{\partial \mathcal{P}_{\text{eff}}}{\partial X} \right) \left(\frac{\partial \mathcal{P}_{\text{eff}}}{\partial X} + 5X \frac{\partial^2 \mathcal{P}_{\text{eff}}}{\partial X^2} + 2X^2 \frac{\partial^3 \mathcal{P}_{\text{eff}}}{\partial X^3} \right)}{X \left(\frac{\partial \mathcal{P}_{\text{eff}}}{\partial X} + 2X \frac{\partial^2 \mathcal{P}_{\text{eff}}}{\partial X^2} \right)^2} \\ &\quad + \frac{\dot{\phi} \left(\frac{\partial^2 \mathcal{P}_{\text{eff}}}{\partial \phi \partial X} + 2X \frac{\partial^3 \mathcal{P}_{\text{eff}}}{\partial \phi \partial X^2} \right)}{\frac{\partial \mathcal{P}_{\text{eff}}}{\partial X} + 2X \frac{\partial^2 \mathcal{P}_{\text{eff}}}{\partial X^2}} \quad (9.178) \end{aligned}$$

For simplicity and conciseness, we define :

$$M = \left(\frac{\partial \mathcal{P}_{\text{eff}}}{\partial \phi} - 2X \frac{\partial^2 \mathcal{P}_{\text{eff}}}{\partial \phi \partial X} + 3H \dot{\phi} \frac{\partial \mathcal{P}_{\text{eff}}}{\partial X} \right) = \tilde{M} + 3H \dot{\phi} \frac{\partial \mathcal{P}_{\text{eff}}}{\partial X} \quad (9.179)$$

$$N = \left(\frac{\partial \mathcal{P}_{\text{eff}}}{\partial X} + 5X \frac{\partial^2 \mathcal{P}_{\text{eff}}}{\partial X^2} + 2X^2 \frac{\partial^3 \mathcal{P}_{\text{eff}}}{\partial X^3} \right) \quad (9.180)$$

$$Q = \left(\frac{\partial \mathcal{P}_{\text{eff}}}{\partial X} + 2X \frac{\partial^2 \mathcal{P}_{\text{eff}}}{\partial X^2} \right) \quad (9.181)$$

If we derive a second time to compute $\frac{d^2 \tilde{z}^2}{dt^2}$, we obtain

$$\begin{aligned} \frac{1}{\tilde{z}^2} \frac{d^2 \tilde{z}^2}{dt^2} &= 3\ddot{\phi} \left(\frac{\partial^2 \mathcal{P}_{\text{eff}}}{\partial \phi \partial X} + \frac{\partial^3 \mathcal{P}_{\text{eff}}}{\partial \phi \partial X^2} \right) \frac{1}{Q} + \dot{\phi} \dot{X} \left(3 \frac{\partial^3 \mathcal{P}_{\text{eff}}}{\partial \phi \partial X^2} + 2X \frac{\partial^4 \mathcal{P}_{\text{eff}}}{\partial \phi \partial X^3} \right) \frac{1}{Q} \\ &- 2X \left(\frac{\partial^3 \mathcal{P}_{\text{eff}}}{\partial \phi^2 \partial X} + 2X \frac{\partial^4 \mathcal{P}_{\text{eff}}}{\partial \phi^2 \partial X^2} \right) \frac{1}{Q} - 2 \left(\frac{\partial_\phi \tilde{M}}{M} + \frac{\partial_\phi N}{N} - \frac{\partial_\phi Q}{Q} \right) \frac{M \cdot N}{Q^2} \\ &+ \frac{\dot{\phi}}{X} \left(3\dot{H} \dot{\phi} \frac{\partial \mathcal{P}_{\text{eff}}}{\partial X} + 3H \ddot{\phi} \frac{\partial \mathcal{P}_{\text{eff}}}{\partial X} + 3H \dot{\phi}^2 \frac{\partial^2 \mathcal{P}_{\text{eff}}}{\partial \phi \partial X} + 3H \dot{\phi} \dot{X} \frac{\partial^2 \mathcal{P}_{\text{eff}}}{\partial X^2} \right) \frac{N}{Q^2} \\ &+ 2\ddot{\phi} \left(\frac{\partial_X \tilde{M}}{M} + \frac{\partial_X N}{N} - \frac{\partial_X Q}{Q} \right) \frac{M \cdot N}{Q^2} + \frac{\ddot{\phi}}{X} \frac{M \cdot N}{Q^2} \end{aligned} \quad (9.182)$$

with

$$\begin{aligned} \partial_\phi \tilde{M} &= \frac{\partial^2 \mathcal{P}_{\text{eff}}}{\partial \phi^2} - 2X \frac{\partial^3 \mathcal{P}_{\text{eff}}}{\partial \phi^2 \partial X} \\ \partial_X \tilde{M} &= -\frac{\partial^2 \mathcal{P}_{\text{eff}}}{\partial \phi \partial X} - 2X \frac{\partial^3 \mathcal{P}_{\text{eff}}}{\partial \phi \partial X^2} \\ \partial_\phi N &= \frac{\partial^2 \mathcal{P}_{\text{eff}}}{\partial \phi \partial X} + 5X \frac{\partial^3 \mathcal{P}_{\text{eff}}}{\partial \phi \partial X^2} + 2X^2 \frac{\partial^4 \mathcal{P}_{\text{eff}}}{\partial \phi \partial X^3} \\ \partial_X N &= 6 \frac{\partial^2 \mathcal{P}_{\text{eff}}}{\partial X^2} + 9X \frac{\partial^3 \mathcal{P}_{\text{eff}}}{\partial X^3} + 2X^2 \frac{\partial^4 \mathcal{P}_{\text{eff}}}{\partial X^4} \\ \partial_\phi Q &= \frac{\partial^2 \mathcal{P}_{\text{eff}}}{\partial \phi \partial X} + 2X \frac{\partial^3 \mathcal{P}_{\text{eff}}}{\partial \phi \partial X^2} \\ \partial_X Q &= \frac{3\partial^2 \mathcal{P}_{\text{eff}}}{\partial X^2} + 2X \frac{\partial^3 \mathcal{P}_{\text{eff}}}{\partial X^3} \end{aligned}$$

In equation (9.182), we can replace again $\ddot{\phi}$ using the Klein-Gordon equation (9.177), we can use the Friedmann equation (9.183) to replace H and we can use the Hamilton-Jacobi equation (9.184) to replace \dot{H} where

$$H^2 = \frac{8\pi G_N}{3} \left(-\mathcal{P}_{\text{eff}} + 2X \frac{\partial \mathcal{P}_{\text{eff}}}{\partial X} \right) \quad (9.183)$$

The Hamilton-Jacobi equation is obtained by combining the Klein-Gordon equation and the derivative of the Friedmann equation

$$\dot{\phi} \frac{\partial \mathcal{P}_{\text{eff}}}{\partial X} = \frac{1}{4\pi G_N} \frac{dH}{d\phi} \quad (9.184)$$

If we use this equation to derive \mathcal{H}'' , we can check that no $\frac{\partial^2 \mathcal{P}_{\text{eff}}}{\partial \phi^2}$ term appears, so that the term $-\mathcal{H}''/\mathcal{H}$ in (9.173) contains no singularity.

Finally, equation (9.182) depends only on X , derivatives of \mathcal{P}_{eff} with respect to X up to the fourth order, mixed derivatives in X and ϕ , first derivatives of \mathcal{P}_{eff} with respect to ϕ and only one second-order derivative $\frac{\partial^2 \mathcal{P}_{\text{eff}}}{\partial \phi^2}$. This is the only term where $\frac{d^2 V_{\text{eff}}}{d\phi^2}$ is present, hence the only term where a singular second-derivative of the abruptly-evolving coupling with matter $\frac{d^2 A}{d\phi^2}$ appears. We find then that

$$\frac{d^2 \tilde{z}^2}{dt^2} \supset -4X \frac{\partial^2 \mathcal{P}_{\text{eff}}}{\partial \phi^2} \frac{\frac{\partial \mathcal{P}_{\text{eff}}}{\partial X} + 5X \frac{\partial^2 \mathcal{P}_{\text{eff}}}{\partial X^2} + 2X^2 \frac{\partial^3 \mathcal{P}_{\text{eff}}}{\partial X^3}}{\left(\frac{\partial \mathcal{P}_{\text{eff}}}{\partial X} + 2X \frac{\partial^2 \mathcal{P}_{\text{eff}}}{\partial X^2}\right)^2} \quad (9.185)$$

so

$$\frac{z_A''}{z_A} \supset a^2 \frac{d^2 V_{\text{eff}}}{d\phi^2} \frac{\frac{\partial \mathcal{P}_{\text{eff}}}{\partial X} + 5X \frac{\partial^2 \mathcal{P}_{\text{eff}}}{\partial X^2} + 2X^2 \frac{\partial^3 \mathcal{P}_{\text{eff}}}{\partial X^3}}{\left(\frac{\partial \mathcal{P}_{\text{eff}}}{\partial X} + 2X \frac{\partial^2 \mathcal{P}_{\text{eff}}}{\partial X^2}\right)^2} \quad (9.186)$$

This formula can be used to evaluate the Dirac term in the perturbation equation for any potential with discontinuous derivatives. If for example we have a canonical kinetic term $\mathcal{P}_{\text{eff}}(\phi, X) = -X - V(\phi)$, we find that $u = a^2 \frac{d^2 V_{\text{eff}}}{d\phi^2}$ and it is straightforward to recover Starobinsky's result from previous chapter. From (9.114, 9.115) we find that

$$\frac{d^2 V_{\text{eff}}}{d\phi^2} \supset \frac{\rho_m}{\phi_1} \delta(\phi - \phi_1) \quad (9.187)$$

so that

$$u_{II} = -\frac{\rho_m a_1}{\phi_1 \dot{\phi}_1} \delta(\eta - \eta_1) \frac{\frac{\partial \mathcal{P}_{\text{eff}}}{\partial X} + 5X \frac{\partial^2 \mathcal{P}_{\text{eff}}}{\partial X^2} + 2X^2 \frac{\partial^3 \mathcal{P}_{\text{eff}}}{\partial X^3}}{\left(\frac{\partial \mathcal{P}_{\text{eff}}}{\partial X} + 2X \frac{\partial^2 \mathcal{P}_{\text{eff}}}{\partial X^2}\right)^2} \quad (9.188)$$

This is the second kind of feature which is present in scalar-tensor extensions of k-inflation coupled to matter. It is completely scale independent. The jump in the power spectrum due to this Dirac term will be dominant compared to the effect of the other Dirac term (9.171).

If we now consider a non trivial effective Lagrangian, such as the one inspired from the trapped brane case (9.113, 9.114)

$$\mathcal{P}_{\text{eff}}(\phi, X) = \frac{1}{f(\phi)} \left(1 - \sqrt{1 + 2Xf(\phi)}\right) - V_{\text{eff}}(\phi) \quad (9.189)$$

we obtain

$$u_{II} = \frac{\rho_m a_1}{\gamma_1 \phi_1 \dot{\phi}_1} \left(\frac{3}{2} - \frac{1}{2\gamma_1^2} \right) \delta(\eta - \eta_1) \quad (9.190)$$

As a result, solving the perturbation equation in a quasi de Sitter phase (9.165, 9.166) we find that the jump in the power spectrum is determined by

$$\frac{v(k_c \ll k \ll k_1)}{v(k \rightarrow \infty)} \approx 1 + \frac{\eta_1 \phi_1'}{6\phi_1} \frac{k_c^2(\eta_1)}{k^2} + \frac{\rho_m a_1 \eta_1}{3\gamma_1 \phi_1 \dot{\phi}_1} \left(\frac{3}{2} - \frac{1}{2\gamma_1^2} \right) \quad (9.191)$$

9.12 Application

We want to evaluate the impact of the feature for an effective model whose parameters coincide with the ones of the trapped brane case. We use these values as a realistic example for a set of plausible parameters. We have

$$-\frac{u_{II}}{3c_s k_1} \sim -\frac{\rho_m a_1}{2\gamma_1 \phi_1 \dot{\phi}_1 k_1 / \gamma_1} \quad (9.192)$$

from (9.65) which we can express as

$$-\frac{u_{II}}{3c_s k_1} \sim \frac{1}{2} \frac{1}{(2\pi)^3} \xi^{-1/2} g^2 \frac{1}{\gamma_1} \quad (9.193)$$

Recalling from (6.16, 6.18, 6.21) that

$$H \approx \frac{1}{\epsilon t} \quad \text{and} \quad \gamma \approx \frac{2M_P^2}{\lambda} \frac{1}{\epsilon} t^2 \quad (9.194)$$

where

$$f(\phi) = \frac{\lambda}{\phi^4}, \quad (9.195)$$

we deduce that

$$\gamma_1 \approx \frac{2M_P^2}{\lambda \epsilon^3 H_1^2} \quad (9.196)$$

and we obtain that

$$\gamma_1 \sim \lambda \epsilon^3 \frac{k_1^2 / a_1^2}{2M_P^2}. \quad (9.197)$$

Therefore we find

$$-\frac{u_{II}}{3c_s k_1} \sim \frac{1}{2} \frac{1}{(2\pi)^3} \epsilon^{-2} g^{5/2} \lambda^{-3/4} \frac{2M_P^2}{k_1^2 / a_1^2} \quad (9.198)$$

and typically for k_1 in the observable window, $\frac{2M_P^2}{k_1^2 / a_1^2}$ varies from 10^{-6} to 10^5 . To satisfy the COBE normalization, we can choose $\epsilon = 10^{-1}$, $g = 10^{-2}$ and $\lambda = 10^9$. Therefore,

$$-\frac{u_{II}}{3c_s k_1} \sim 10^{-18} - 10^{-7} \quad (9.199)$$

This induces a jump which is relatively small if $N = 1$. For a choice of $N = 10^6$, the background evolution is not affected and we can expect a noticeable effect in the power spectrum with an appropriate choice of k_1 .

$$-\frac{u_{II}}{3c_s k_1} \sim \frac{1}{2} \frac{1}{(2\pi)^3} N \epsilon^{-2} g^{5/2} \lambda^{-3/4} \frac{2M_P^2}{k_1^2/a_1^2} \quad (9.200)$$

In figure 9.4, we have plotted the power spectrum of the Mukhanov-Sasaki

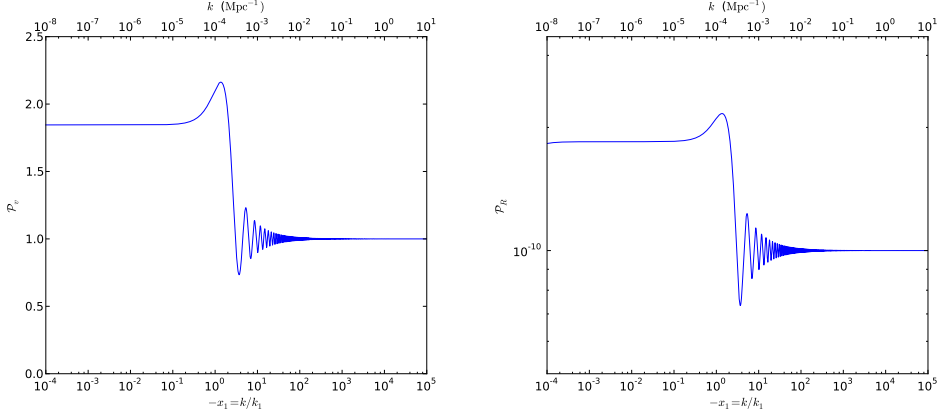


Figure 9.4: Left : Power spectra for Mukhanov-Sasaki variable. Right : Power spectra for the curvature perturbation, for a feature in DBI inflation, with $\epsilon = 10^{-1}$, $g = 10^{-2}$ and $\lambda = 10^9$ satisfying the COBE normalization.

variable and of the curvature perturbation \mathcal{R} for $k_1 = 10^{-4} \text{Mpc}^{-1}$, $\epsilon = 10^{-1}$, $g = 10^{-2}$, $\lambda = 10^9$ and $N = 10^6$. We have chosen k_1 in the observable window of the Planck experiment [81] (roughly $10^{-4} \text{Mpc}^{-1} - 10^{-1} \text{Mpc}^{-1}$). From (9.145), we can compute $k_c^2(\eta_1)/k_1^2$:

$$\frac{k_c^2(\eta_1)}{k_1^2} = 2^{-19/4} \pi^{-13/2} g^6 \lambda^{-2} \epsilon^{-6} \zeta^{-7/2} \frac{\sqrt{2} M_P}{k_1/a_1} \frac{\phi_1}{\sqrt{2} M_P} \approx 10^{-10} \ll 1 \quad (9.201)$$

implying that k_c is tiny compared to k_1 and (9.191) is valid.

For such a small k_c , the curvature power spectrum is not much different from the power spectrum for v . For both spectra we observe a step in the spectrum which depends on the parameters of the model and some additional oscillations. This should be put in perspective with actual observations of features in the CMB spectrum. Of course, such a feature is quite similar to those obtained in the previous section and is thus not particularly discriminating. Still, correlated data could favor one or another model. Other mechanisms of particle production during inflation exist and also lead to features in the observables [128, 134, 135].

9.13 On other scales

It is worth considering what happens for large scales such that $k \ll k_c$ i.e. $|W| \gg 1$ when the energy density of matter is still negligible compared to the inflaton energy density $\rho_m \ll \rho_\phi$. In this case the perturbation equation reads

$$v_A'' + \left(k^2 \tilde{c}_s^2 - \frac{z_A''}{z_A} \right) v_A = 0 \quad (9.202)$$

with

$$\tilde{c}_s^2 \approx c_s^2 \left(1 - \frac{W'}{\mathcal{H}W} \frac{2}{3(1+w_\phi)} \right) \quad (9.203)$$

and

$$\frac{z_A''}{z_A} \approx \frac{9}{4} \mathcal{H}^2 + \frac{3}{2} \mathcal{H}' - \frac{1}{2} \frac{A''}{A} + \frac{3}{4} \frac{A'^2}{A^2} - \frac{3}{2} \mathcal{H} \frac{A'}{A} \quad (9.204)$$

The main contribution is $\frac{15}{4} \mathcal{H}^2$ much different from the usual $2\mathcal{H}^2$ in the de Sitter universe. Moreover the speed of sound is greatly modified. This situation is too far from the de Sitter case to be of any phenomenological relevance.

9.14 Inside the interaction region

In the interaction region, we must consider rescattering effects of the ψ modes with the ϕ modes since they are expected to modify the inflaton perturbations. The results of this section are preliminary results of a work which is still in progress. Up to now, we have only investigated the effects of particle production and backreaction assuming it was an instantaneous process. But it is interesting to check that the contribution of the physics inside the interaction region is negligible. To do so, we will use the ADM formalism and compute the second-order action. We will use the results of [103] for $\mathcal{P}(\phi, X, \psi, Y)$ which now contains both the matter Lagrangian and the inflaton Lagrangian. Since the background for the matter field is zero, all expressions get a lot simpler in our case. We have two fields, ϕ which has DBI dynamics and ψ which has canonical dynamics. The action is

$$S = \int d^4x \sqrt{-g} \frac{M_p^2}{2} R^{(4)} + \int d^4x \sqrt{-g} \mathcal{P}(\phi, X, \psi, Y) \quad (9.205)$$

We write

$$X = \frac{1}{2} g_{\mu\nu} \partial^\mu \phi \partial^\nu \phi = -\frac{1}{2} \dot{\phi}^2 \quad (9.206)$$

$$\psi = 0, \quad \dot{\psi} = 0 \quad \text{and} \quad Y = \frac{1}{2} g_{\mu\nu} \partial^\mu \psi \partial^\nu \psi = 0 \quad (9.207)$$

here we do not write zero indices for the background quantities out of simplicity. In the formalism of [103] for inflation with multiple fields $\{\phi^K\}$, the Lagrangian is written with the general form

$$\mathcal{P}(X^{IJ}, \phi^K) \quad (9.208)$$

with

$$X^{IJ} = \frac{1}{2}g^{\mu\nu}\partial_\mu\phi^I\partial_\nu\phi^J \quad (9.209)$$

In the ADM formalism, the metric in the uniform curvature slicing gauge is

$$ds^2 = -N^2dt^2 + h_{ij}(dx^i + N^i dt)(dx^j + N^j dt) \quad (9.210)$$

where the lapse N and the shift N^i are Lagrange multipliers. This formalism is particularly useful (e.g.[136]) because of the metric perturbations computation. The action now becomes

$$S = \frac{1}{2} \int dt dx^3 \sqrt{h} N (R^{(3)} + 2\mathcal{P}) + \frac{1}{2} \int dt dx^3 \frac{\sqrt{h}}{N} (E_{ij}E^{ij} - E^2) \quad (9.211)$$

with $E_{ij} = \frac{1}{2}\dot{h}_{ij} - D_{(i}N_{j)}$, D_i the spatial covariant derivative associated with the spatial metric h_{ij} , $R^{(3)}$ the scalar curvature and h the determinant of the spatial metric. When varying the action with respect to the Lagrange multipliers we obtain the energy or Hamiltonian constraint

$$2(N^2\mathcal{P} - \mathcal{P}_{\langle IJ \rangle})(\dot{\phi}^I - N^i\partial_i\phi^I)(\dot{\phi}^J - N^i\partial_i\phi^J) + E^2 - E_{ij}E^{ij} = 0 \quad (9.212)$$

and the momentum constraint

$$D_j \left(\frac{1}{N}(E_i^j - E\delta_i^j) \right) = \frac{1}{N}\mathcal{P}_{\langle IJ \rangle}(\dot{\phi}^I - N^k\partial_k\phi^I)\partial_i\phi^J \quad (9.213)$$

with $\mathcal{P}_{\langle IJ \rangle}$ defined as in (3.44). In our framework where the two fields ϕ and ψ are to be considered, those two equations are :

$$2(N^2\mathcal{P} - \frac{\partial\mathcal{P}}{\partial X}(\dot{\phi} - N^i\partial_i\phi)^2) + E^2 - E_{ij}E^{ij} = 0 \quad (9.214)$$

and

$$D_j \left(\frac{1}{N}(E_i^j - E\delta_i^j) \right) = \frac{1}{N}\frac{\partial\mathcal{P}}{\partial X}(\dot{\phi} - N^k\partial_k\phi)\partial_i\phi \quad (9.215)$$

Perturbing each field

$$\phi \rightarrow \phi + \delta\phi \quad (9.216)$$

$$\delta\psi \neq 0 \quad (9.217)$$

$$N = 1 + \delta N \text{ and } N_i = \partial_i U \quad (9.218)$$

δN and U are obtained by the linearization of the constraint equations :

$$\delta N = \frac{1}{2H}\frac{\partial\mathcal{P}}{\partial X}\dot{\phi}\delta\phi \quad (9.219)$$

and

$$-2H \left(\frac{\partial^2 U}{a^2} \right) = 2A\delta N + B\dot{\phi}\delta\phi + C_1\delta\phi + C_2\delta\psi \quad (9.220)$$

with

$$A = \frac{\partial \mathcal{P}}{\partial X} X - 2X^2 \frac{\partial^2 \mathcal{P}}{\partial X^2} - \mathcal{P} \quad (9.221)$$

$$B = \frac{\partial \mathcal{P}}{\partial X} + 2X \frac{\partial^2 \mathcal{P}}{\partial X^2} \quad (9.222)$$

$$C_1 = -\frac{\partial \mathcal{P}}{\partial \phi} + 2X \frac{\partial^2 \mathcal{P}}{\partial X \partial \phi} \quad (9.223)$$

$$C_2 = -\frac{\partial \mathcal{P}}{\partial \psi} \quad (9.224)$$

In the general case it is :

$$\delta N = \frac{1}{2H} \mathcal{P}_{\langle IJ \rangle} \dot{\phi}^I \dot{Q}^J \quad (9.225)$$

and

$$-2H \left(\frac{\partial^2 U}{a^2} \right) = 2A \delta N + B_{IJ} \dot{\phi}^J \dot{Q}^I + C_I \dot{Q}^I \quad (9.226)$$

with

$$A = \mathcal{P}_{\langle IJ \rangle} X^{IJ} - 2X^{IJ} X^{KL} \mathcal{P}_{\langle IJ \rangle, \langle KL \rangle} - \mathcal{P} \quad (9.227)$$

$$B_{IJ} = \mathcal{P}_{\langle IJ \rangle} + 2X^{KL} \mathcal{P}_{\langle IJ \rangle, \langle KL \rangle} \quad (9.228)$$

$$C_I = -\mathcal{P}_{,I} + 2X^{KL} \mathcal{P}_{\langle KL \rangle, I} \quad (9.229)$$

The second order action obtained in [103] in the context of “general multi-field inflation” is

$$S^{(2)} = \frac{1}{2} \int dt dx^3 a^3 \left((\mathcal{P}_{\langle IJ \rangle} + 2\mathcal{P}_{\langle MJ \rangle, \langle IK \rangle} X^{MK}) \dot{Q}^I \dot{Q}^J - \mathcal{P}_{\langle IJ \rangle} h^{ij} \partial_i Q^I \partial_j Q^J - M_{KL} Q^K Q^L + 2\Omega_{KI} Q^K \dot{Q}^I \right) \quad (9.230)$$

where the Q^I are the linear perturbation of the ϕ^I fields. The correspondence with my notations is

$$\phi^1 = \phi \quad (9.231)$$

$$\phi^2 = \psi = 0 \quad (9.232)$$

$$Q^1 = \delta \phi \quad (9.233)$$

$$Q^2 = \delta \psi \quad (9.234)$$

$$X^{11} = X \quad (9.235)$$

$$X^{22} = Y = 0 \quad (9.236)$$

$$X^{12} = X^{21} = 0 \quad (9.237)$$

$$\mathcal{P}_{,1} = \frac{\partial \mathcal{P}}{\partial \phi} \quad (9.238)$$

$$\mathcal{P}_{,2} = \frac{\partial \mathcal{P}}{\partial \psi} = -\frac{\partial V}{\partial \psi} \quad (9.239)$$

$$\mathcal{P}_{\langle 11 \rangle} = \frac{\partial \mathcal{P}}{\partial X} \quad (9.240)$$

$$\mathcal{P}_{\langle 22 \rangle} = -1 \quad (9.241)$$

$$\mathcal{P}_{\langle 12 \rangle} = \mathcal{P}_{\langle 21 \rangle} = 0 \quad (9.242)$$

$$\mathcal{P}_{\langle 11 \rangle, \langle 11 \rangle} = \frac{\partial^2 \mathcal{P}}{\partial X^2} \quad (9.243)$$

and all the other second derivatives are zero. Many simplifications arise, especially in the mass matrix M_{KL} and in the mixing matrix Ω_{KL} .

$$S^{(2)} = \frac{1}{2} \int dt dx^3 a^3 \left(\left(\frac{\partial \mathcal{P}}{\partial X} + 2X \frac{\partial^2 \mathcal{P}}{\partial X^2} \right) \delta \dot{\phi}^2 - \frac{\partial \mathcal{P}}{\partial X} h^{ij} \partial_i \phi \partial_j \dot{\phi} \right. \\ \left. - M_{11} \delta \phi^2 - M_{22} \delta \psi^2 - 2M_{12} \delta \phi \delta \psi + 2\Omega_{11} \delta \phi \delta \dot{\phi} \right) \quad (9.244)$$

with

$$\Omega_{11} = \dot{\phi} \frac{\partial^2 \mathcal{P}}{\partial X \partial \phi} - \frac{2}{H} \frac{\partial \mathcal{P}}{\partial X} \frac{\partial^2 \mathcal{P}}{\partial X^2} X^2 \quad (9.245)$$

After some long but straightforward computations, we obtain the equation of motion for the inflaton perturbation

$$\ddot{\delta \phi} + 3H \dot{\delta \phi} + \frac{c_s^2}{\frac{\partial \mathcal{P}}{\partial X}} \left(3\dot{X} \frac{\partial^2 \mathcal{P}}{\partial X^2} + \dot{\phi} \frac{\partial^2 \mathcal{P}}{\partial X \partial \phi} + 2X \dot{X} \frac{\partial^3 \mathcal{P}}{\partial X^3} + 2X \dot{\phi} \frac{\partial^3 \mathcal{P}}{\partial X^2 \partial \phi} \right) \delta \dot{\phi} \\ + \frac{k^2 c_s^2}{a^2} \delta \phi + M_{11} \frac{c_s^2}{\frac{\partial \mathcal{P}}{\partial X}} \delta \phi + 3H \frac{c_s^2}{\frac{\partial \mathcal{P}}{\partial X}} \left(\dot{\phi} \frac{\partial^2 \mathcal{P}}{\partial X \partial \phi} - \frac{2X^2}{H} \frac{\partial \mathcal{P}}{\partial X} \frac{\partial^2 \mathcal{P}}{\partial X^2} \right) \delta \phi \\ + \frac{c_s^2}{\frac{\partial \mathcal{P}}{\partial X}} \frac{d}{dt} \left(\dot{\phi} \frac{\partial^2 \mathcal{P}}{\partial X \partial \phi} - \frac{2X^2}{H} \frac{\partial \mathcal{P}}{\partial X} \frac{\partial^2 \mathcal{P}}{\partial X^2} \right) \delta \phi = -M_{12} \frac{c_s^2}{\frac{\partial \mathcal{P}}{\partial X}} \delta \psi = \Delta_\psi \quad (9.246)$$

There is a coupling with the perturbation of the matter field $\delta \psi$, with

$$M_{11} = -\frac{\partial^2 \mathcal{P}}{\partial \phi^2} + 3X \left(\frac{\partial \mathcal{P}}{\partial X} \right)^2 + \frac{\dot{\phi}}{H} \frac{\partial \mathcal{P}}{\partial X} \left(2X \frac{\partial^2 \mathcal{P}}{\partial X \partial \phi} - \frac{\partial \mathcal{P}}{\partial \phi} \right) \\ - \frac{1}{a^3} \frac{d}{dt} \left(\frac{a^3}{H} X \left(\frac{\partial \mathcal{P}}{\partial X} \right)^2 \right) - \frac{1}{H^2} \left(\frac{\partial \mathcal{P}}{\partial X} \right)^2 X^2 \left(\frac{\partial \mathcal{P}}{\partial X} + 2X \frac{\partial^2 \mathcal{P}}{\partial X^2} \right) \quad (9.247)$$

and

$$M_{12} = M_{21} = -\frac{\partial^2 \mathcal{P}}{\partial \phi \partial \psi} \quad (9.248)$$

We also have

$$M_{22} = -\frac{\partial^2 \mathcal{P}}{\partial \psi^2} = \frac{\partial^2 V}{\partial \psi^2} \quad (9.249)$$

We may write the equation of motion for $\delta\psi$, which is quite simple :

$$\delta\ddot{\psi} + 3H\delta\dot{\psi} + \left(\frac{k^2}{a^2} + \frac{\partial^2 V}{\partial\psi^2}\right)\delta\psi = -M_{21}\delta\phi \quad (9.250)$$

it is sourced by the inflaton potential and it carries a second derivative of the potential.

Equation (9.246) reduces to the usual DBI perturbation equation when the coupling with matter tends to zero. It can be solved inside the interaction region with a Green function. The solution before the feature that is to say the solution with no source, is known, let's call it $\tilde{\delta\phi}_k(t)$. We define the retarded Green function

$$G_k(t-t') = i\Theta(t-t')(\tilde{\delta\phi}_k(t)\tilde{\delta\phi}_k^*(t') - \tilde{\delta\phi}_k^*(t)\tilde{\delta\phi}_k(t')) \quad (9.251)$$

where Θ is the Heaviside function. The solution $\delta\phi_k$ inside the interaction region is the convolution of the Green function with the source

$$\delta\phi_k(t) = \int G_k(t-t')\Delta_\psi(t')dt' \quad (9.252)$$

We only keep the retarded Green function because the advanced Green function has no physical meaning. The solution before the interaction region is known and the solution after is also known, it is the sum of two modes. We need to write the junction conditions and match the solutions. Then it is possible to prove that the first order inflaton perturbation is not affected by rescattering effects and that entropy perturbations can be neglected. But this work has not been properly put into form up to now. It has to be done so as to prove without ambiguity that reducing the interaction region to a point like particle creation process does not change the power spectrum.

9.15 Non-Gaussianities from particle production

Here the framework is the same as in the previous section but computations have now to be carried out up to the next order and the third-order action must be derived. It is still possible to adapt results from [103] directly to our particular situation. This project was inspired by Niel Barnaby who has already investigated the dynamics of particle production, rescattering and IR cascading during inflation and has studied non-Gaussianities from particle production [128]. Inflaton fluctuations generated by rescattering are expected to be significantly non-gaussian. The investigation method is to write the Klein Gordon equation for $\delta^2\phi$. It is sourced by $\delta\phi$ on the one part and $\delta\psi$ on the other part. The contribution in $\delta\phi^2$ is the usual non-gaussian minor correction coming from self-interaction. The other contribution to the bispectrum is the one of interest. The shape of the non-gaussianities is expected to be very specific. Thus non-gaussianities from particle production could be identified easily. However nothing can be said about the original mechanism of particle production.

Prospects and conclusion

“Science is a wonderful thing if one does not have to earn one’s living at it.”,
A. Einstein

10.1 Conclusion

In this thesis, we have reviewed the physics of the phase of cosmic inflation and we have emphasized the uncertainty about what drove inflation. We have investigated a well-motivated alternative to slow-roll inflation : Dirac-Born-Infeld inflation. We have studied in particular a natural extension of the DBI inflation scenario where matter is present during inflation. This occurs when spectator branes are trapped along the inflationary valley. When the inflationary brane hits a trapped brane, particles are suddenly created. We have proved that the backreaction of the particles was not efficient to slow the motion of the brane but did modify the inflaton perturbations leading to features in the spectrum at the scales which left the sound horizon at the time of the particle burst. Our motivation was to determine whether such features were in accordance with some of the localized anomalies in the observed spectrum. Distortions up to 10% of the usual scale invariant vacuum fluctuations are compatible with current data. In the case of several trapped branes along the inflationary valley, there are several bursts of particle production and possibly several glitches in the spectrum, some of which could overlap. Features from the coupling with matter are not the only features studied in this thesis. We have also analyzed the consequences of potentials with steps, both in canonical and DBI inflation. Features generated by the inflaton potential are very similar to features from a suddenly varying coupling with matter. Nevertheless, the context is completely different. Another novelty which appears in the study of scalar-tensor features is the scale dependence of the z variable relating the curvature perturbation to the Mukhanov-Sasaki variable. Typically there is a jump in the infrared and some additional oscillations in the spectrum. The value of the jump is constrained by the theory parameters

and can thus be constrained by the CMB data and putative observed features if the exotic physics which source the feature occur in the last twenty e-folds of inflation. Examples of features in this manuscript are not exhaustive. They are meant to point out the observational effects of physics beyond the simplest slow-roll scenario. Signatures are left in the spectrum as well as the bispectrum. Those signatures may be within the detectability of the Planck satellite. But we understand that it is difficult for example to differentiate between k-inflation and canonical models or between stringy and non-stringy models just from a feature in the spectrum. Only the cross-comparison of different data could help us discriminate among all the models. This is why information on non-gaussianities are very valuable and any other new piece of information we can extract from the observation and measurement of the CMB is priceless. Though we must be careful to distinguish statistical effects from original physical effects. We also understand that it is sometimes very difficult to have a purely analytical approach of exotic inflationary models and to make trustworthy predictions.

10.2 Open problems

We have left some unfinished work in the project about rescattering effects. The study of the bispectrum is highly important and is worth the tedious computations. A point which was brought to my attention during my research is the importance to study in detail the phenomenology of the featureful power spectra obtained and the constraints on parameter space. We could compare all “exotic” models of inflation, compare their features and anticipate on how to distinguish them. It would be an ambitious project to catalog them but it would be very useful. We should consider other theoretical sources of features cited before. We could improve our own model, for example by taking in account angular coordinates of the brane, or by considering other inflaton potentials. On the analytical point of view, I think it could be worth trying to derive non-Gaussianities in scalar-tensor theories using the Langlois-Vernizzi geometrical approach.

Appendix A :

Matter radiation equality

This computation is adapted from [137].

At equality $\rho_m = \rho_r = \rho_\gamma + \rho_\nu$

$$\rho_\gamma = 2 \int \frac{d^3p}{(2\pi)^3} \frac{p}{e^{p/T} - 1} = \frac{8\pi T^4}{(2\pi)^3} \int_0^\infty \frac{x^3 dx}{e^x - 1} = \frac{8\pi T^4}{(2\pi)^3} 6\zeta(4) = \frac{8\pi T^4}{(2\pi)^3} \frac{\pi^4}{15} = \frac{\pi^2 T^4}{15}$$

The coefficient 2 accounts for the spin 2. The zeta function is the Riemann function.

So today :

$$\frac{\rho_\gamma}{\rho_{cr}} = \frac{\pi^2}{15} \left(\frac{2.725K}{a} \right)^4 \frac{1}{8.098 \cdot 10^{-11} h^2 eV^4} = \frac{2.47 \cdot 10^{-5}}{h^2 a^4}$$

Before the annihilation of electrons and positrons, all particles are at equilibrium, the entropy is

$$s_- = \frac{2\pi^2 T_{\text{annih}}^3}{45} \left(2 + \frac{7}{8} (2 + 2 + 3 + 3) \right)$$

where we have accounted for photons and then electrons, positrons, neutrinos and anti-neutrinos. After annihilation, the electrons and positrons have disappeared and photons and neutrinos are no longer at the same temperature.

$$s_+ = \frac{2\pi^2}{45} \left(2T_\gamma^3 + \frac{7}{8} (3 + 3) T_\nu^3 \right)$$

For relativistic particles, the cooling is such that $T(t_2) = T(t_1) \frac{a_1}{a_2}$ so right after annihilation $T_\nu^+ = T_{\text{annih}}$ (~ 1 MeV) so we find that

$$\frac{T_\nu}{T_\gamma} = \left(\frac{4}{11} \right)^{1/3}$$

so finally

$$\rho_\nu = 3 \frac{7}{8} \left(\frac{4}{11} \right)^{4/3} \rho_\gamma$$

Solving $\rho_r^{\text{eq}} = \rho_m^{\text{eq}}$ leads to 1.29.

Appendix B :

Perturbation computations in DBI Starobinsky model

Here are given the ingredients for the calculation of z''/z in DBI inflation. Our motivation is to reexpress ϵ_3 and δ_2 in terms of smaller-order SR parameters and of the second derivative of the potential and the warp factor. In Starobinsky's model, the second derivative of the potential is of special interest since it is equivalent to a dirac function.

Let's first derive Friedmann equation, we obtain

$$\frac{dH}{d\phi} = \frac{\kappa}{2H} \frac{V'}{3 - \frac{2\epsilon_1\gamma}{\gamma+1}} + \frac{\kappa}{2H} \frac{\kappa V}{\left(3 - \frac{2\epsilon_1\gamma}{\gamma+1}\right)^2} \left(-\kappa \frac{\gamma^2}{\gamma+1} \frac{H}{dH/d\phi} \epsilon_1 \epsilon_2 + \frac{2\epsilon_1}{(\gamma+1)^2} \frac{d\gamma}{d\phi} \right)$$

We derive this a second time

$$\begin{aligned} \left(3 - \frac{2\epsilon_1\gamma}{\gamma+1} - \frac{\gamma\epsilon_2}{\gamma+1}\right) \frac{d^2H}{d\phi^2} &= \frac{\kappa V''}{2H} + \frac{H\epsilon_1}{(\gamma+1)^2} \frac{d^2\gamma}{d\phi^2} - \frac{2H\epsilon_1}{(\gamma+1)^3} \left(\frac{d\gamma}{d\phi}\right)^2 \\ -\frac{\kappa H\gamma^2}{2(\gamma+1)} \left(\frac{3(\gamma+1)}{\gamma} \epsilon_1 - 2\epsilon_1^2 + 5\epsilon_1\epsilon_2 + \frac{4}{\gamma+1} \epsilon_1\delta_1 - \epsilon_2^2 - \epsilon_2\epsilon_3 + \frac{\gamma+3}{\gamma+1} \epsilon_2\delta_1\right) \end{aligned}$$

with

$$\left(\frac{d\gamma}{d\phi}\right)^2 = \frac{\kappa\gamma^3}{2} \frac{\delta_1^2}{\epsilon_1}$$

and

$$-\delta_2 - \frac{3}{2}\delta_1 + \frac{1}{2}\epsilon_2 = \frac{2}{\kappa\gamma H} \frac{dH/d\phi}{d\gamma/d\phi} \frac{d^2\gamma}{d\phi^2} = \frac{2}{\kappa\gamma^2} \frac{\epsilon_1}{\delta_1} \frac{d^2\gamma}{d\phi^2}$$

and

$$\frac{4}{\kappa\gamma H} \frac{d^2H}{d\phi^2} = 2\epsilon_1 - \epsilon_2\delta_1$$

comes equation (8.34). We use the same procedure to obtain equation (8.35). When replacing this expression in z''/z it leads to equation (8.36).

We also want to give some hints on how to get the limit (8.76). An expansion of (8.71) in $y = k/k_1 \rightarrow 0$ must be carried out thoroughly.

$$|\alpha - \beta|^2 \sim 1 + \frac{u}{k} \left(\frac{2}{y} (1 - 2y^2) + \left(1 - \frac{1}{y^2}\right) \left(2y - \frac{4y^3}{3}\right) \right) + \frac{u^2}{2k^2} \frac{1}{y^2} \left(1 + \frac{1}{y^2} + \left(1 - \frac{1}{y^2}\right) \left(1 - 2y^2 + \frac{2}{3}y^4 - \frac{4}{45}y^6\right) - \frac{2}{y} \left(2y - \frac{4}{3}y^3 + \frac{4}{15}y^5\right) \right)$$

$$|\alpha - \beta|^2 \sim 1 - \frac{2}{3} \frac{u}{k_1} + \frac{1}{9} \frac{u^2}{k_1^2}$$

For Starobinsky's model

$$u = 3a_1 H_0 \left(1 - \frac{A_-}{A_+}\right) = 3k_1 \left(1 - \frac{A_-}{A_+}\right)$$

$$|\alpha - \beta|^2 \sim \left(\frac{A_-}{A_+}\right)^2$$

Appendix C :

Perturbation equations with δ -singularities

Let us consider a simple case such as a massive field with a linear potential for field values larger than a given ϕ_1 . The background Klein-Gordon equation reads in a fixed cosmological background

$$\ddot{\phi} + 3H\dot{\phi} + m^2\phi + \Lambda^3 Y(\phi - \phi_1) = 0$$

where Λ is a given scale. Let us denote by $\phi(t)$ the solution to this equation. Imagine now that we are interested in linear perturbations $\delta\phi$ around this time dependent solution $\phi(t)$. The perturbation equation reads

$$\delta\ddot{\phi} + 3H\delta\dot{\phi} + \left(m^2 + \frac{k^2}{a^2}\right)\delta\phi + \Lambda^3[Y(\phi + \delta\phi - \phi_1) - Y(\phi - \phi_1)] = 0$$

To make sense of the last term, one should understand this equation in the sense of distribution theory. Integrating this equation after multiplication by a test function ψ , i.e. \mathcal{C}^∞ with compact support, we obtain

$$\int dt \left(\delta\ddot{\phi} + 3H\delta\dot{\phi} + \left(m^2 + \frac{k^2}{a^2}\right)\delta\phi \right) \psi + \Lambda^3 \int_{t_\delta}^{t_1} \psi dt = 0$$

where t_1 is the instant when $\phi(t_1) = \phi_1$ (assumed to be unique) and t_δ is the instant when $\phi(t_\delta) + \delta\phi(t_\delta) = \phi_1$. In linear perturbation theory, we obtain that

$$t_\delta = t_1 - \frac{\delta\phi(t_1)}{\dot{\phi}(t_1)}$$

Hence in the linear perturbation theory, the perturbation equation in the distributional sense becomes

$$\int dt \left(\delta\ddot{\phi} + 3H\delta\dot{\phi} + \left(m^2 + \frac{k^2}{a^2}\right)\delta\phi \right) \psi + \Lambda^3 \frac{\delta\phi(t_1)}{\dot{\phi}(t_1)} \psi(t_1) = 0$$

The last term can be equally written as

$$\frac{\delta\phi(t_1)}{\dot{\phi}(t_1)}\psi(t_1) = \int \frac{\delta\phi(t)}{\dot{\phi}(t)}\psi(t)\delta(t-t_1)dt = \int \delta\phi(t)\delta(\phi(t)-\phi_1)\psi(t)dt$$

This proves that the linear perturbation equation in the sense of distributions reads

$$\delta\ddot{\phi} + 3H\delta\dot{\phi} + \left(m^2 + \frac{k^2}{a^2}\right)\delta\phi + \Lambda^3\delta(\phi-\phi_1)\delta\phi = 0$$

where the δ -function is nothing but the second derivative of the piece-wise linear potential in the sense of distributions.

Appendix D : Perturbation equation with a δ and a δ' term

We study the following perturbation equation

$$v_k'' + \left(k^2 c_s^2 - \frac{2}{\eta^2} + u\delta(\eta_1 - \eta) + b\delta'(\eta_1 - \eta_1) \right) v_k = 0$$

We define the reduced variable $x = c_s k \eta$ and assume that the sound speed is either one either nearly constant.

$$\frac{d^2 v_k}{dx^2} + \left(1 - \frac{2}{x^2} + \hat{u}\delta(x - x_1) + b\delta'(x - x_1) \right) v_k = 0$$

with $\hat{u} = \frac{u}{kc_s} = \frac{u_0}{x_1}$. Before the feature the solution reads

$$v_k^- = C \left(i + \frac{1}{x} \right) e^{-ix}$$

while after the feature we obtain

$$v_k^+ = \alpha \left(i + \frac{1}{x} \right) e^{-ix} + \beta \left(-i + \frac{1}{x} \right) e^{+ix}$$

The solution is continuous across the feature at brane crossing

$$[v_k]_{x_1} = 0$$

implying that

$$\beta = (\alpha - C) e^{-2ix_1} \frac{i + \frac{1}{x_1}}{i - \frac{1}{x_1}}$$

The presence of singularities in the perturbation equation implies that the first derivative is not continuous but jumps

$$[v_k']_{x_1} = -\hat{u}v_1 + \frac{b}{2}(v_{x_1}^+ + v_{x_1}^-)$$

leading to

$$\begin{aligned} \alpha & \left(1 - \frac{i}{x_1} - \frac{1}{x_1^2}\right) \left(1 - \frac{b}{2}\right) + \beta e^{2ix_1} \left(1 + \frac{i}{x_1} - \frac{1}{x_1^2}\right) \left(1 - \frac{b}{2}\right) \\ & = C \left(1 - \frac{i}{x_1} - \frac{1}{x_1^2} - \hat{u} \left(i + \frac{1}{x_1}\right) + \frac{b}{2} \left(1 - \frac{i}{x_1} - \frac{1}{x_1^2}\right)\right) \end{aligned}$$

So we find the two Bogoliubov coefficients

$$\alpha = \frac{C}{(2-b)i} \left(2i + \frac{b}{x_1^3} + \hat{u} \left(1 + \frac{1}{x_1^2}\right)\right)$$

and

$$\beta = -C e^{-2ix_1} \frac{i + \frac{1}{x_1}}{i - \frac{1}{x_1}} \left(1 - \frac{1}{(2-b)i} \left(2i + \frac{b}{x_1^3} + \hat{u} \left(1 + \frac{1}{x_1^2}\right)\right)\right)$$

The spectrum is evaluated for $\eta_* \rightarrow 0$,

$$v_k \approx \frac{\alpha + \beta}{x_*}$$

We can now distinguish the behavior of v_k for $k \ll k_1$ and $k \gg k_1$. When k is very large, we find that v_k converges to C in an oscillatory manner

$$(\alpha + \beta) (k \rightarrow \infty) = C$$

As $C \propto 1/\sqrt{k}$ we find that the spectrum is scale invariant with a normalization given by C . On the contrary, when k is very small we find that

$$(\alpha + \beta) \sim C \left[1 - \frac{2}{2-b} \left(\frac{b}{x_1^3} + \frac{\hat{u}}{x_1^2}\right) \frac{1}{i - \frac{1}{x_1}} e^{-ix_1} \left(-\cos(x_1) + \frac{\sin(x_1)}{x_1}\right)\right]$$

With $\hat{u} = u_0/x_1$

$$(\alpha + \beta) \rightarrow C \left[1 + \frac{2(b_0 + u_0)}{3(2-b_0)}\right]$$

which depends on $b_0 = b(k \rightarrow 0)$ and u_0 . Hence the spectrum of v has a constant jump across the feature.

Publications

- *Brane Bremsstrahlung in DBI Inflation*, P. Brax and E. Cluzel, arXiv:0912.0806, JCAP 03 (2010) 016

Abstract : We consider the effect of trapped branes on the evolution of a test brane whose motion generates DBI inflation along a warped throat. The coupling between the inflationary brane and a trapped brane leads to the radiation of non-thermal particles on the trapped brane. We calculate the Gaussian spectrum of the radiated particles and their backreaction on the DBI motion of the inflationary brane. Radiation occurs for momenta lower than the speed of the test brane when crossing the trapped brane. The slowing down effect is either due to a parametric resonance when the interaction time is small compared to the Hubble time or a tachyonic resonance when the interaction time is large. In both cases the motion of the inflationary brane after the interaction is governed by a chameleonic potential, which tends to slow it down. We find that a single trapped brane can hardly slow down a DBI inflaton whose fluctuations lead to the Cosmic Microwave Background spectrum. A more drastic effect is obtained when the DBI brane encounters a tightly spaced stack of trapped branes.

- *Trapped Brane Features in DBI Inflation*, P. Brax and E. Cluzel, arXiv:1010.4462

Abstract : We consider DBI inflation with a quadratic potential and the effect of trapped branes on the inflationary fluctuations. When going through a trapped brane the effective potential of the inflaton receives a contribution whose effect is to induce a jump in the power spectrum of the inflaton perturbations. This feature appears in the power spectrum at a scale corresponding to the size of the sound horizon when the two branes cross each other.

This paper has been replaced by the following one which generalizes the results to any k-inflation model coupled to matter.

- *Perturbation Theory in k-Inflation Coupled to Matter*, P. Brax and E. Cluzel, arXiv: 1102.1917, JCAP 04 (2011) 014

Abstract : We consider k-inflation models where the action is a non-linear function of both the inflaton and the inflaton kinetic term. We focus on a scalar-tensor extension of k-inflation coupled to matter for which we derive a modified Mukhanov-Sasaki equation for the curvature perturbation. Significant corrections to the power spectrum may appear when the coupling function changes abruptly along the inflationary trajectory. This gives rise to a modification of Starobinsky's model of perturbation features. We analyse the way the power spectrum may be altered in the infrared when such features are present.

Bibliography

- [1] P. Peter, JP Uzan, “Primordial Cosmology,” Oxford Graduate Texts
- [2] N. Jackson, “The Hubble Constant,” Living Rev. Rel. **10**, 4 (2007). [arXiv:0709.3924 [astro-ph]].
- [3] E. Komatsu *et al.* [WMAP Collaboration], “Five-Year Wilkinson Microwave Anisotropy Probe (WMAP) Observations: Cosmological Interpretation,” Astrophys. J. Suppl. **180**, 330-376 (2009). [arXiv:0803.0547 [astro-ph]].
- [4] F. Zwicky, “Spectral displacement of extra galactic nebulae,” Helv. Phys. Acta **6**, 110-127 (1933).
- [5] V. C. Rubin, N. Thonnard and W. K.W. K.Ford, “Extended rotation curves of high-luminosity spiral galaxies. IV - Systematic dynamical properties, SA through SC,” Astrophys. J. **225** (1978) 107-111
- [6] V. Springel, C. S. Frenk, S. D. M. White, “The large-scale structure of the Universe,” Nature **440** 2006. [astro-ph/0604561].
- [7] M. Milgrom, “A Modification of the Newtonian dynamics as a possible alternative to the hidden mass hypothesis,” Astrophys. J. **270** (1983) 365-370.
- [8] D. Clowe, A. Gonzalez and M. Markevitch, “Weak lensing mass reconstruction of the interacting cluster 1E0657-558: Direct evidence for the existence of dark matter,” Astrophys. J. **604** (2004) 596 [arXiv:astro-ph/0312273].
- [9] S. Perlmutter *et al.* [Supernova Cosmology Project Collaboration], “Measurements of Omega and Lambda from 42 high redshift supernovae,” Astrophys. J. **517**, 565-586 (1999). [astro-ph/9812133].
- [10] A. G. Riess *et al.* [Supernova Search Team Collaboration], “Observational evidence from supernovae for an accelerating universe and a cosmological constant,” Astron. J. **116**, 1009-1038 (1998). [astro-ph/9805201].
- [11] E. Hubble, “A relation between distance and radial velocity among extragalactic nebulae,” Proc. Nat. Acad. Sci. **15**, 168-173 (1929).
- [12] Particle Data Group, “Review of particle physics,” J. Phys **G33** (2006) 1-1232

- [13] I. Zlatev, L. -M. Wang, P. J. Steinhardt, “Quintessence, cosmic coincidence, and the cosmological constant,” *Phys. Rev. Lett.* **82**, 896-899 (1999). [astro-ph/9807002].
- [14] P. J. Steinhardt, L. -M. Wang, I. Zlatev, “Cosmological tracking solutions,” *Phys. Rev.* **D59**, 123504 (1999). [astro-ph/9812313].
- [15] J. Polchinski, “String theory. Vol. 1: An introduction to the bosonic string,” and “String theory. Vol. 2: Superstring theory and beyond,” Cambridge, UK: Univ. Pr. (1998).
- [16] E. Kiritsis, “String theory in a nutshell,” Princeton, USA: Univ. Pr. (2007) 588 p.
- [17] K. Becker, M. Becker, J. H. Schwarz, “String theory and M-theory: A modern introduction,” Cambridge, UK: Cambridge Univ. Pr. (2007) 739 p.
- [18] J. Polchinski, “Tasi lectures on D-branes,” [hep-th/9611050].
- [19] I. R. Klebanov and M. J. Strassler, “Supergravity and a confining gauge theory: Duality cascades and chiSB-resolution of naked singularities,” *JHEP* **0008** (2000) 052 [arXiv:hep-th/0007191].
- [20] R. Kallosh and A. D. Linde, “Testing String Theory with CMB,” *JCAP* **0704** (2007) 017 [arXiv:0704.0647 [hep-th]].
- [21] J. -P. Uzan, F. Bernardeau, “Cosmic strings lens phenomenology: General properties of distortion fields,” *Phys. Rev.* **D63**, 023004 (2001). [astro-ph/0004105].
- [22] K. J. Mack, D. H. Wesley, L. J. King, “Observing cosmic string loops with gravitational lensing surveys,” *Phys. Rev.* **D76**, 123515 (2007). [astro-ph/0702648 [ASTRO-PH]].
- [23] D. F. Chernoff, S. H. H. Tye, “Cosmic String Detection via Microlensing of Stars,” [arXiv:0709.1139 [astro-ph]].
- [24] S. Dyda, R. H. Brandenberger, “Cosmic Strings and Weak Gravitational Lensing,” [arXiv:0710.1903 [astro-ph]].
- [25] J. E. Lidsey and I. Huston, “Gravitational wave constraints on Dirac-Born-Infeld inflation,” *JCAP* **0707** (2007) 002 [arXiv:hep-th/0705.0240].
- [26] D. Baumann, “TASI Lectures on Inflation,” arXiv:0907.5424 [hep-th].
- [27] D. Langlois, “Lectures on inflation and cosmological perturbations,” *Lect. Notes Phys.* **800** (2010) 1-57. [arXiv:1001.5259 [astro-ph.CO]].
- [28] J. L. Lehners, “Ekpyrotic and Cyclic Cosmology,” *Phys. Rept.* **465** (2008) 223 [arXiv:0806.1245 [astro-ph]].
- [29] A. D. Linde, “Nonsingular Regenerating Inflationary Universe,”

- [30] A. Vilenkin, “The Birth of Inflationary Universes,” *Phys. Rev.* **D27** (1983) 2848.
- [31] A. D. Linde, “Eternally Existing Selfreproducing Chaotic Inflationary Universe,” *Phys. Lett.* **B175** (1986) 395-400.
- [32] T. Battefeld, S. Watson, “String gas cosmology,” *Rev. Mod. Phys.* **78** (2006) 435-454. [hep-th/0510022].
- [33] R. H. Brandenberger, “String Gas Cosmology,” [arXiv:0808.0746 [hep-th]].
- [34] A. H. Guth *Phys. Rev. D* **23**, 347 (1981)
- [35] A. D. Linde *Phys. Rev. Lett. B* **108**, 389 (1982), A. Albrecht and P. J. Steinhardt *Phys. Rev. Lett* **48**, 1220 (1982)
- [36] L. Kofman, A. D. Linde and A. A. Starobinsky, “Towards the theory of reheating after inflation,” *Phys. Rev. D* **56** (1997) 3258 [arXiv:hep-ph/9704452].
- [37] G. N. Felder, L. Kofman and A. D. Linde, “Instant preheating,” *Phys. Rev. D* **59** (1999) 123523 [arXiv:hep-ph/9812289].
- [38] J. F. Dufaux, G. N. Felder, L. Kofman, M. Peloso and D. Podolsky, “Preheating with Trilinear Interactions: Tachyonic Resonance,” *JCAP* **0607** (2006) 006 [arXiv:hep-ph/0602144].
- [39] N. Barnaby, J. R. Bond, Z. Huang and L. Kofman, “Preheating After Modular Inflation,” arXiv:0909.0503 [hep-th].
- [40] D. Wands, “Local non-Gaussianity from inflation,” *Class. Quant. Grav.* **27**, 124002 (2010). [arXiv:1004.0818 [astro-ph.CO]].
- [41] K. Ichikawa, T. Suyama, T. Takahashi, M. Yamaguchi, “Primordial Curvature Fluctuation and Its Non-Gaussianity in Models with Modulated Reheating,” *Phys. Rev.* **D78**, 063545 (2008). [arXiv:0807.3988 [astro-ph]].
- [42] J. Garcia-Bellido, D. G. Figueroa, “A stochastic background of gravitational waves from hybrid preheating,” *Phys. Rev. Lett.* **98**, 061302 (2007). [astro-ph/0701014].
- [43] J. F. Dufaux, A. Bergman, G. N. Felder, L. Kofman, J. -P. Uzan, “Theory and Numerics of Gravitational Waves from Preheating after Inflation,” *Phys. Rev.* **D76**, 123517 (2007). [arXiv:0707.0875 [astro-ph]].
- [44] K. Jedamzik, M. Lemoine, J. Martin, “Generation of gravitational waves during early structure formation between cosmic inflation and reheating,” *JCAP* **1004**, 021 (2010). [arXiv:1002.3278 [astro-ph.CO]].
- [45] D. H. Lyth, “What would we learn by detecting a gravitational wave signal in the cosmic microwave background anisotropy?,” *Phys. Rev. Lett.* **78** (1997) 1861 [arXiv:hep-ph/9606387].

- [46] A. D. Linde, “Hybrid inflation,” *Phys. Rev. D* **49** (1994) 748 [arXiv:astro-ph/9307002].
- [47] E. J. Copeland, A. R. Liddle, D. H. Lyth, E. D. Stewart and D. Wands, “False vacuum inflation with Einstein gravity,” *Phys. Rev. D* **49** (1994) 6410 [arXiv:astro-ph/9401011].
- [48] S. Clesse, “Hybrid inflation along waterfall trajectories,” *Phys. Rev. D* **83** (2011) 063518 [arXiv:1006.4522 [gr-qc]].
- [49] V. Demozzi, A. Linde and V. Mukhanov, “Supercurvaton,” *JCAP* **1104** (2011) 013 [arXiv:1012.0549 [hep-th]].
- [50] C. Armendariz-Picon, T. Damour and V. F. Mukhanov, “k - inflation,” *Phys. Lett. B* **458** (1999) 209 [arXiv:hep-th/9904075].
- [51] L. Lorenz, J. Martin and C. Ringeval, “Constraints on Kinetically Modified Inflation from WMAP5,” *Phys. Rev. D* **78** (2008) 063543 [arXiv:0807.2414 [astro-ph]].
- [52] R. Kallosh, “On Inflation in String Theory,” *Lect. Notes Phys.* **738** (2008) 119 [arXiv:hep-th/07020].
- [53] G. R. Dvali and S. H. Tye, “Brane inflation,” *Phys. Lett. B* **450** (1999) 72 [arXiv:hep-ph/9812483].
- [54] G. R. Dvali, Q. Shafi and S. Solganik, “D-brane inflation,” arXiv:hep-th/0105203.
- [55] C. P. Burgess, M. Majumdar, D. Nolte, F. Quevedo, G. Rajesh and R. J. Zhang, “The Inflationary Brane-Antibrane Universe,” *JHEP* **0107** (2001) 047 [arXiv:hep-th/0105204].
- [56] S. H. S. Alexander, “Inflation from D - anti-D brane annihilation,” *Phys. Rev. D* **65** (2002) 023507 [arXiv:hep-th/0105032].
- [57] J. H. Brodie and D. A. Easson, “Brane inflation and reheating,” *JCAP* **0312** (2003) 004 [arXiv:hep-th/0301138].
- [58] S. Kachru, R. Kallosh, A. D. Linde, J. M. Maldacena, L. P. McAllister and S. P. Trivedi, “Towards inflation in string theory,” *JCAP* **0310** (2003) 013 [arXiv:hep-th/0308055].
- [59] S. Kachru, R. Kallosh, A. D. Linde and S. P. Trivedi, “De Sitter vacua in string theory,” *Phys. Rev. D* **68** (2003) 046005 [arXiv:hep-th/0301240].
- [60] S. S. Gubser, “Einstein manifolds and conformal field theories,” *Phys. Rev. D* **59**, 025006 (1999). [hep-th/9807164].
- [61] M. Bastero-Gil, A. Berera and J. G. Rosa, “Warming up brane-antibrane inflation,” arXiv:1103.5623 [hep-th].

- [62] J. P. Conlon and F. Quevedo, “Kahler moduli inflation,” *JHEP* **0601** (2006) 146 [arXiv:hep-th/0509012].
- [63] J. J. Blanco-Pillado *et al.*, “Racetrack inflation,” *JHEP* **0411** (2004) 063 [arXiv:hep-th/0406230].
- [64] J. J. Blanco-Pillado *et al.*, “Inflating in a better racetrack,” *JHEP* **0609** (2006) 002 [arXiv:hep-th/0603129].
- [65] P. Brax, A. C. Davis, S. C. Davis, R. Jeannerot and M. Postma, “D-term Uplifted Racetrack Inflation,” *JCAP* **0801** (2008) 008 [arXiv:0710.4876 [hep-th]].
- [66] J. J. Blanco-Pillado, D. Buck, E. J. Copeland, M. Gomez-Reino and N. J. Nunes, “Kahler Moduli Inflation Revisited,” arXiv:0906.3711 [hep-th].
- [67] C. Deffayet, G. Esposito-Farese and A. Vikman, “Covariant Galileon,” *Phys. Rev. D* **79** (2009) 084003 [arXiv:0901.1314 [hep-th]].
- [68] P. Creminelli, A. Nicolis and E. Trincherini, “Galilean Genesis: An Alternative to inflation,” *JCAP* **1011** (2010) 021 [arXiv:1007.0027 [hep-th]].
- [69] T. Kobayashi, M. Yamaguchi and J. Yokoyama, “G-inflation: Inflation driven by the Galileon field,” *Phys. Rev. Lett.* **105** (2010) 231302 [arXiv:1008.0603 [hep-th]].
- [70] C. Burrage, C. de Rham, D. Seery and A. J. Tolley, “Galileon inflation,” *JCAP* **1101** (2011) 014 [arXiv:1009.2497 [hep-th]].
- [71] M. Trodden and K. Hinterbichler, “Generalizing Galileons,” arXiv:1104.2088 [hep-th].
- [72] M. Zaldarriaga, U. Seljak, “An all sky analysis of polarization in the microwave background,” *Phys. Rev.* **D55**, 1830-1840 (1997). [astro-ph/9609170].
- [73] K. A. Malik and D. Wands, “Cosmological perturbations,” *Phys. Rept.* **475** (2009) 1 [arXiv:0809.4944 [astro-ph]].
- [74] C. Gordon, D. Wands, B. A. Bassett, R. Maartens, “Adiabatic and entropy perturbations from inflation,” *Phys. Rev.* **D63**, 023506 (2001). [astro-ph/0009131].
- [75] J. Garriga and V. F. Mukhanov, “Perturbations in k-inflation,” *Phys. Lett. B* **458** (1999) 219 [arXiv:hep-th/9904176].
- [76] J. R. Fergusson and E. P. S. Shellard, “The shape of primordial non-Gaussianity and the CMB bispectrum,” *Phys. Rev. D* **80** (2009) 043510 [arXiv:0812.3413 [astro-ph]].
- [77] L. Senatore, K. M. Smith, M. Zaldarriaga, “Non-Gaussianities in Single Field Inflation and their Optimal Limits from the WMAP 5-year Data,” *JCAP* **1001**, 028 (2010). [arXiv:0905.3746 [astro-ph.CO]].

- [78] K. M. Smith, L. Senatore, M. Zaldarriaga, “Optimal limits on f_{NL}^{local} from WMAP 5-year data,” JCAP **0909**, 006 (2009). [arXiv:0901.2572 [astro-ph]].
- [79] E. Komatsu *et al.* [WMAP Collaboration], “Seven-Year Wilkinson Microwave Anisotropy Probe (WMAP) Observations: Cosmological Interpretation,” Astrophys. J. Suppl. **192** (2011) 18 [arXiv:1001.4538 [astro-ph.CO]].
- [80] R. Durrer, “The Cosmic Microwave Background,” Cambridge, UK: Univ. Pr. (2008) 424 p.
- [81] [Planck Collaboration], “Planck: The scientific programme,” arXiv:astro-ph/0604069
- [82] Planck Collaboration, arXiv:1101.2022-2047
- [83] H. V. Peiris *et al.* [WMAP Collaboration], “First year Wilkinson Microwave Anisotropy Probe (WMAP) observations: Implications for inflation,” Astrophys. J. Suppl. **148** (2003) 213. [astro-ph/0302225].
- [84] E. Silverstein and D. Tong “Scalar Speed Limits and Cosmology: Acceleration from D-cceleration,” Phys. Rev. D **70** (2004) 103505 [arXiv:hep-th/0310221].
- [85] M. Alishahiha, E. Silverstein and D. Tong, “DBI in the sky,” Phys. Rev. D **70** (2004) 123505 [arXiv:hep-th/0404084].
- [86] L. Kofman, A. D. Linde, X. Liu, A. Maloney, L. McAllister and E. Silverstein, “Beauty is attractive: Moduli trapping at enhanced symmetry points,” JHEP **0405** (2004) 030 [arXiv:hep-th/0403001].
- [87] D. Baumann, A. Dymarsky, I. R. Klebanov, J. M. Maldacena, L. P. McAllister and A. Murugan, “On D3-brane potentials in compactifications with fluxes and wrapped D-branes,” JHEP **0611** (2006) 031 [arXiv:hep-th/0607050].
- [88] D. Baumann, A. Dymarsky, S. Kachru, I. R. Klebanov and L. McAllister, “Holographic Systematics of D-brane Inflation,” JHEP **0903** (2009) 093 [arXiv:0808.2811 [hep-th]].
- [89] D. Baumann and L. McAllister, “Advances in Inflation in String Theory,” arXiv:0901.0265 [hep-th].
- [90] D. Baumann, A. Dymarsky, S. Kachru, I. R. Klebanov, L. McAllister, “D3-brane Potentials from Fluxes in AdS/CFT,” JHEP **1006**, 072 (2010). [arXiv:1001.5028 [hep-th]].
- [91] X. Chen, “Inflation from warped space,” JHEP **0508** (2005) 045 [arXiv:hep-th/0501184].
- [92] S. Kecskemeti, J. Maiden, G. Shiu and B. Underwood, “DBI inflation in the tip region of a warped throat,” JHEP **0609** (2006) 076 [arXiv:hep-th/0605189].

- [93] D. Baumann, A. Dymarsky, I. R. Klebanov, L. McAllister and P. J. Steinhardt, “A Delicate Universe,” *Phys. Rev. Lett.* **99** (2007) 141601 [arXiv:0705.3837 [hep-th]].
- [94] B. Underwood, “Brane Inflation is Attractive,” *Phys. Rev. D* **78** (2008) 023509 [arXiv:0802.2117 [hep-th]].
- [95] S. Bird, H. V. Peiris and D. Baumann, “Brane Inflation and the Overshoot Problem,” *Phys. Rev. D* **80** (2009) 023534 [arXiv:0905.2412 [hep-th]].
- [96] D. A. Easson and R. Gregory, “Circumventing the eta problem,” arXiv:0902.1798 [hep-th].
- [97] L. Lorenz, J. Martin and C. Ringeval, “K-inflationary Power Spectra in the Uniform Approximation,” *Phys. Rev. D* **78** (2008) 083513 [arXiv:0807.3037 [astro-ph]].
- [98] R. Bean, X. Chen, H. Peiris and J. Xu, “Comparing Infrared Dirac-Born-Infeld Brane Inflation to Observations,” *Phys. Rev. D* **77** (2008) 023527 [arXiv:0710.1812 [hep-th]].
- [99] L. Lorenz, J. Martin and C. Ringeval, “Brane inflation and the WMAP data: a Bayesian analysis,” *JCAP* **0804** (2008) 001 [arXiv:0709.3758 [hep-th]].
- [100] J. Lachapelle and R. H. Brandenberger, “Preheating with Non-Standard Kinetic Term,” *JCAP* **0904** (2009) 020 [arXiv:0808.0936 [hep-th]].
- [101] A. C. Davis and R. H. Ribeiro, “Enhanced (p)reheating in DBI Inflation,” arXiv:0908.4217 [hep-th].
- [102] D. Langlois, S. Renaux-Petel, “Perturbations in generalized multi-field inflation,” *JCAP* **0804** (2008) 017. [arXiv:0801.1085 [hep-th]].
- [103] D. Langlois, S. Renaux-Petel, D. A. Steer and T. Tanaka, “Primordial perturbations and non-Gaussianities in DBI and general multi-field inflation,” *Phys. Rev. D* **78** (2008) 063523 [arXiv:0806.0336 [hep-th]].
- [104] P. Brax, C. van de Bruck, A. C. Davis, J. Khoury, A. Weltman, *AIP Conf. Proc.* **736** (2005) 105-110. [astro-ph/0410103]
- [105] T. Damour, K. Nordtvedt, “Tensor - scalar cosmological models and their relaxation toward general relativity,” *Phys. Rev.* **D48** (1993) 3436-3450.
- [106] A. Serna, J. M. Alimi, “Scalar - tensor cosmological models,” *Phys. Rev.* **D53** (1996) 3074-3086. [astro-ph/9510139].
- [107] B. Boisseau, G. Esposito-Farese, D. Polarski and A. A. Starobinsky, “Reconstruction of a scalar tensor theory of gravity in an accelerating universe,” *Phys. Rev. Lett.* **85** (2000) 2236 [arXiv:gr-qc/0001066].

- [108] E. Elizalde, S. Nojiri and S. D. Odintsov, “Late-time cosmology in (phantom) scalar-tensor theory: Dark energy and the cosmic speed-up,” *Phys. Rev. D* **70** (2004) 043539 [arXiv:hep-th/0405034].
- [109] G. Esposito-Farese, “Tests of scalar-tensor gravity,” *AIP Conf. Proc.* **736** (2004) 35 [arXiv:gr-qc/0409081].
- [110] P. Brax, C. van de Bruck, A. C. Davis and D. J. Shaw, “f(R) Gravity and Chameleon Theories,” *Phys. Rev. D* **78** (2008) 104021 [arXiv:0806.3415 [astro-ph]].
- [111] H. Motohashi, A. A. Starobinsky, J. i. Yokoyama, “f(R) Gravity and its Cosmological Implications,” [arXiv:1101.0716 [astro-ph.CO]].
- [112] P. Brax, C. van de Bruck, A. C. Davis, J. Khoury and A. Weltman, “Detecting dark energy in orbit: The cosmological chameleon,” *Phys. Rev. D* **70** (2004) 123518 [arXiv:astro-ph/0408415].
- [113] C. van de Bruck, D. F. Mota, J. M. Weller, “Embedding DBI inflation in scalar-tensor theory,” *JCAP* **1103** (2011) 034. [arXiv:1012.1567 [astro-ph.CO]].
- [114] A. A. Starobinsky, “Spectrum Of Adiabatic Perturbations In The Universe When There Are Singularities In The Inflation Potential,” *JETP Lett.* **55** (1992) 489 [*Pisma Zh. Eksp. Teor. Fiz.* **55** (1992) 477].
- [115] S. M. Leach, M. Sasaki, D. Wands and A. R. Liddle, “Enhancement of superhorizon scale inflationary curvature perturbations,” *Phys. Rev. D* **64** (2001) 023512 [arXiv:astro-ph/0101406].
- [116] W. H. Kinney, K. Tzirakis, “Quantum modes in DBI inflation: exact solutions and constraints from vacuum selection,” *Phys. Rev. D* **77** (2008) 103517. [arXiv:0712.2043 [astro-ph]].
- [117] R. Bean, X. Chen, G. Hailu, S. H. Tye and J. Xu, “Duality Cascade in Brane Inflation,” *JCAP* **0803** (2008) 026 [arXiv:0802.0491 [hep-th]].
- [118] J. A. Adams, B. Cresswell and R. Easther, “Inflationary perturbations from a potential with a step,” *Phys. Rev. D* **64** (2001) 123514 [arXiv:astro-ph/0102236].
- [119] L. Covi, J. Hamann, A. Melchiorri, A. Slosar and I. Sorbera, “Inflation and WMAP three year data: Features have a future!,” *Phys. Rev. D* **74** (2006) 083509 [arXiv:astro-ph/0606452].
- [120] J. Hamann, L. Covi, A. Melchiorri and A. Slosar, “New constraints on oscillations in the primordial spectrum of inflationary perturbations,” *Phys. Rev. D* **76** (2007) 023503 [arXiv:astro-ph/0701380].

- [121] M. Joy, V. Sahni and A. A. Starobinsky, “A New Universal Local Feature in the Inflationary Perturbation Spectrum,” *Phys. Rev. D* **77** (2008) 023514 [arXiv:0711.1585 [astro-ph]].
- [122] P. Hunt and S. Sarkar, “Multiple inflation and the WMAP ‘glitches’ II. Data analysis and cosmological parameter extraction,” *Phys. Rev. D* **76** (2007) 123504 [arXiv:0706.2443 [astro-ph]].
- [123] M. Joy, A. Shafieloo, V. Sahni and A. A. Starobinsky, “Is a step in the primordial spectral index favored by CMB data ?,” *JCAP* **0906** (2009) 028 [arXiv:0807.3334 [astro-ph]].
- [124] M. J. Mortonson, C. Dvorkin, H. V. Peiris and W. Hu, “CMB polarization features from inflation versus reionization,” *Phys. Rev. D* **79** (2009) 103519 [arXiv:0903.4920 [astro-ph.CO]].
- [125] C. Dvorkin and W. Hu, “Generalized Slow Roll for Large Power Spectrum Features,” *Phys. Rev. D* **81**, 023518 (2010) [arXiv:0910.2237 [astro-ph.CO]].
- [126] D. K. Hazra, M. Aich, R. K. Jain, L. Sriramkumar and T. Souradeep, “Primordial features due to a step in the inflaton potential,” arXiv:1005.2175 [astro-ph.CO].
- [127] R. Bean, S. E. Shandera, S. H. Henry Tye and J. Xu, “Comparing Brane Inflation to WMAP,” *JCAP* **0705** (2007) 004 [arXiv:hep-th/0702107].
- [128] N. Barnaby, “On Features and Nongaussianity from Inflationary Particle Production,” arXiv:1006.4615 [astro-ph.CO] ; N. Barnaby and Z. Huang, “Particle Production During Inflation: Observational Constraints and Signatures,” *Phys. Rev. D* **80**, 126018 (2009) [arXiv:0909.0751 [astro-ph.CO]] ; N. Barnaby, Z. Huang, L. Kofman and D. Pogosyan “Cosmological Fluctuations from Infra-Red Cascading During Inflation,” *Phys. Rev. D* **80**, 043501 (2009) [arXiv:0902.0615].
- [129] D. Battefeld, T. Battefeld, H. Firouzjahi and N. Khosravi, “Brane Annihilations during Inflation,” *JCAP* **1007** (2010) 009 [arXiv:1004.1417 [hep-th]].
- [130] M. Nakashima, R. Saito, Y. -i. Takamizu, J. 'i. Yokoyama, “The effect of varying sound velocity on primordial curvature perturbations,” [arXiv:1009.4394 [astro-ph.CO]].
- [131] D. Green, B. Horn, L. Senatore and E. Silverstein, “Trapped Inflation,” *Phys. Rev. D* **80** (2009) 063533 [arXiv:0902.1006 [hep-th]].
- [132] V. Mukhanov, “Physical foundations of cosmology,” Cambridge, UK: Univ. Pr. (2005) 421 p.
- [133] B. A. Bassett, S. Tsujikawa and D. Wands, “Inflation dynamics and reheating,” *Rev. Mod. Phys.* **78** (2006) 537 [arXiv:astro-ph/0507632].

- [134] H. Firouzjahi, S. Khoeini-Moghaddam, “Fields Annihilation and Particles Creation in DBI inflation,” *JCAP* **1102** (2011) 012. [arXiv:1011.4500 [hep-th]].
- [135] D. Battefeld, T. Battefeld, C. Byrnes and D. Langlois, “Beauty is Distractive: Particle production during multifield inflation,” arXiv:1106.1891 [astro-ph.CO].
- [136] D. Seery, J. E. Lidsey, “Primordial non-Gaussianities from multiple-field inflation,” *JCAP* **0509** (2005) 011. [astro-ph/0506056].
- [137] S. Dodelson, “Modern cosmology,” Amsterdam, Netherlands: Academic Pr. (2003) 440 p.